MODELING REACTIVE FLOW AND TRANSPORT IN NATURAL SYSTEMS

Peter C. Lichtner

Los Alamos National Laboratory (lichtner@lanl.gov)

Università degli Studi di Genova
Dipartimento di Scienze della Terra
Cattedra di Geochimica

Proceedings of the Rome Seminar on Environmental Geochemistry

Castelnuovo di Porto – May 22-26, 1996

PACINI EDITORE

TABLE OF CONTENTS

LIST OF TABLES

LIST OF FIGURES

INTRODUCTION

Numerical models describing flow and transport of chemically reacting species in porous media can provide a powerful tool for analyzing a wide variety of problems. For example, reactive transport models can be used to predict the rate of migration of a contaminant plume resulting from acid mine drainage and heavy metal mobilization. Quantitative models can also help design remedial strategies to clean up toxic waste sites, such as removal of volatile hydrocarbons by steam injection. Industrial applications include *in situ* leaching of copper and uranium. Finally, such models can be applied to understanding fundamental geochemical processes such as chemical weathering, hydrothermal mineral alteration, ore deposition, sediment diagenesis, and others involving the flow of fluids through the Earth's subsurface.

With the introduction of ever faster computers, problems which only a decade ago appeared hopeless are now becoming common place. This is true for computer models describing flow and transport of chemically reacting species in porous media. It is now possible to model the evolution of complex, multiphase-multicomponent geochemical systems in both time and space using workstations and personal computers. Reactive transport models are able to attain the same level of chemical sophistication commonly found in geochemical speciation and reaction path models.

Nevertheless, there remain many challenges for an accurate or even semi-quantitative description of natural systems. A reactive transport model is *not* a panacea for understanding complex geochemical phenomena. Geochemical processes and associated reaction mechanisms need to be understood first before they can be successfully incorporated into a reactive flow and transport model. A problem of fundamental importance is accounting for micro-scale processes taking place at the pore level, at the macro or continuum scale at which most reactive transport models are applicable. For example, fast reactions can result in concentration gradients within pore spaces in which the bulk fluid composition is no longer representative of the fluid in contact with mineral surfaces which determines the rate of reaction. Future models will need to incorporate multiple interacting continua corresponding to different scales of observation. Finally, in engineering problems it will always be necessary to first calibrate a model description to pertinent field data, if predictions are to be believable. Such quantities as reacting surface area, field scale heterogeneities, and other variables will never be know *a priori*, necessitating close collaboration between modeling, experiments and field observations.

This chapter begins with a discussion of the continuum hypothesis on which the classical conservation equations of mass and energy describing flow and transport in porous media are founded. A general conservation law is developed from which reactive mass conservation equations can be derived. It is shown that by transforming the chemical reactions to canonical form, the number of unknowns in the mass transport equations can be greatly reduced by eliminating of rates corresponding to local equilibrium reactions. An analytical solution for a single component system derived from the quasi-stationary state approximation is presented. The concept of equilibration length is illustrated. Fracture-matrix interaction is analyzed for the single component system. Parallel linearly dependent reactions are introduced for describing different kinetic rate mechanisms for mineral reactions. The approach is applied to microbiological processes. Finally two examples are presented using the computer code MULTIFLO, a multicomponent–multiphase reactive transport model (Lichtner, 1996; Lichtner and Seth, 1997). These are leaching of copper from a five-spot well pattern and acid mine drainage considering two parallel reactions for the oxidation of pyrite.

MASS CONSERVATION

Continuum Hypothesis

A rock mass consisting of aggregates of mineral grains and pore spaces or voids is referred to as a porous medium. A porous medium is a highly heterogeneous structure because of the irregular shaped grains and pore spaces which make up the medium. Although it is possible, in principle at least, to describe such a system at the microscale of a pore, this rapidly becomes a hopeless task as the size of the system is increased and many pore volumes become involved. It is therefore necessary to approximate the system by a more manageable one. The classical approach to describing quantitatively fluid flow through porous media is based on the continuum representation of a porous medium. In this approach the actual discrete physical system, consisting of aggregates of mineral grains, interstitial pore spaces, and fractures, is replaced by a continuous system in which physical variables describing the system vary continuously in space. Spatial variations are described through a grid of control volumes. A control volume is referred to as a representative elemental volume, abbreviated as REV. System properties may vary from one control volume to the next, but are presumed homogeneous within a control volume. The size of the control volume, therefore, must be small compared to average spatial variations in system properties, but large compared to individual pore and grain sizes. Allowance is made for the possibility of a discrete set of surfaces across which discontinuous changes in physical properties may occur. In this fictitious representation of the real physical system, solids and fluids coexist simultaneously at each point in space.

It may at first appear very strange to represent a real rock composed of mineral grains and pore spaces as a continuous medium. Perhaps even stranger is the concept that all phases—minerals, gases and an aqueous solution—simultaneously coexist at each point in space. It should not be forgotten that replacing a porous structure by a continuum involves significant simplifications of the real physical system which are not always valid. It is therefore important to appreciate the approximations made and to be on the lookout for situations in which a continuum description may not apply. For example, characteristic of a continuum description is a simple bulk fluid composition associated with each control volume. The bulk fluid is assumed to also represent the fluid composition in contact with mineral surfaces. Concentration gradients within a pore are not possible to describe within the framework of a single continuum. Future generation models can be expected to employ multiple interacting continua which remove this restriction.

A continuum formulation is at the basis of describing flow of fluid, gas or liquid, through a porous medium. The fluid flow velocity obeys Darcy's law first formulated by Darcy in 1856. Darcy's law is remarkably simple. It states that the volumetric flow rate $\boldsymbol{q}$ through a porous medium is proportional to the difference in hydraulic head h across the system, and inversely proportional to the fluid viscosity (Bear, 1972; Marsily, 1986). In symbols

$$\boldsymbol{q} \;=\; -\frac{\kappa}{\mu}\boldsymbol{\nabla} h, \tag{1}$$

where

$$h \;=\; p - \rho g z, \tag{2}$$

and where μ denotes the viscosity, p represent the fluid pressure, g denotes the acceleration of gravity, z denotes the vertical height of the datum, and the proportionality factor κ is a property of the porous medium referred to as its permeability. For steady-state conditions the volumetric flow rate is independent of the porosity of the porous medium. The average

fluid velocity within the pore spaces of the medium is inversely proportional to the porosity. Flow through a capillary tube obeys Darcy's law sufficiently far from the inlet to the tube.

It should be clear from the definition of a porous medium that one-dimensional porous media are really mathematical idealizations since fluid must follow circuitous pathways through the medium. In many instances two or three spatial dimensions are needed to adequately describe flow and transport in a porous medium. The number of spatial dimensions can have profound consequences on the types of solutions obtained to the mass transport equations as evidenced by fingering phenomena caused by reaction instabilities.

Mass Conservation Equations

The mathematical equations which describe transport of solute species and their chemical interaction are based on the principal of conservation of mass. These equations can be derived by considering the overall balance of some quantity over a representative elemental volume $V_{\rm REV}$. The balance law for a solute species indexed by i can be expressed as

$$\left[\begin{array}{c}\text{rate of accumulation}\\ \text{of species } i \text{ in } V_{\rm REV}\end{array}\right] = \left[\begin{array}{c}\text{net flux of } i \text{ across}\\ \text{boundary of } V_{\rm REV}\end{array}\right] + \left[\begin{array}{c}\text{supply or removal}\\ \text{of } i \text{ within } V_{\rm REV}\end{array}\right]. \tag{3}$$

Supply and removal of the species may occur through chemical reactions or other source or sink processes. In symbols the conservation relation can be expressed as

$$\frac{d}{dt}\int_{V_{\rm REV}} Z\,dV \;=\; -\int_{\partial V_{\rm REV}} \boldsymbol{J}_Z \cdot \boldsymbol{dS} + \int_{V_{\rm REV}} \mathcal{R}_Z\,dV, \tag{4}$$

where Z represents some quantity of interest. The term on the left-hand side gives the rate of change of the amount of the quantity Z contained in the volume $V_{\rm REV}$, equal to the time derivative of the integral of the quantity over the volume. The flux of the quantity Z across the surface enclosing the volume is equal to $\int_{\partial V_{\rm REV}} \boldsymbol{J}_Z \cdot \boldsymbol{dS}$, where $\boldsymbol{J}_Z$ is the flux across the surface $\partial V_{\rm REV}$ of the volume $V_{\rm REV}$, and $\boldsymbol{dS}$ points in a direction normal to the surface. The minus sign appears because the flux is taken to be positive if it is directed along the outward normal $\boldsymbol{dS}$ to the surface $\partial V_{\rm REV}$. The total amount of Z consumed or produced at the rate $\mathcal{R}_Z$ by chemical reactions taking place within the volume or from other sources, is equal to $\int_V \mathcal{R}_Z dV$.

The conservation equation, Eqn.(4), can put in the differential form

$$\frac{\partial Z}{\partial t} + \boldsymbol{\nabla}\cdot\boldsymbol{J}_Z \;=\; \mathcal{R}_Z. \tag{5}$$

This result is obtained by first transforming the surface integral in Eqn.(4) using Gauss's law to yield

$$\int_{\partial V_{\rm REV}} \boldsymbol{J}_Z \cdot \boldsymbol{dS} \;=\; \int_{V_{\rm REV}} \boldsymbol{\nabla}\cdot\boldsymbol{J}_Z\,dV. \tag{6}$$

This mathematical identity is known as the divergence theorem. It applies to any vector field and states that the vector field integrated over a closed surface is equal to the divergence of the vector field integrated over the volume enclosed by the surface. Physically the divergence of a vector field represents the escaping tendency of the field from an enclosed

volume. Putting this relation into the conservation relation, Eqn.(4), yields an equation in which all terms involve integrals over the volume $V_{\rm REV}$:

$$\frac{d}{dt}\int_{V_{\rm REV}} Z\,dV \;=\; -\int_{V_{\rm REV}} \boldsymbol{\nabla}\cdot\boldsymbol{J}_Z\,dV + \int_{V_{\rm REV}} \mathcal{R}_Z\,dV. \tag{7}$$

Rearranging this equation by placing the time derivative inside the integral, noting that

$$\frac{d}{dt}\int_{V_{\rm REV}} ZdV = \int_{V_{\rm REV}} \frac{\partial Z}{\partial t}dV, \tag{8}$$

and bringing all terms to the left hand side inside the volume integral results in the equation

$$\int_{V_{\rm REV}} \left\{ \frac{\partial Z}{\partial t} + \boldsymbol{\nabla}\cdot\boldsymbol{J}_Z - \mathcal{R}_Z \right\} dV \;=\; 0. \tag{9}$$

Because the volume $V_{\rm REV}$ is arbitrary the integrand itself must vanish leading to the differential equation, Eqn.(5). This equation holds at each point within the volume V and expresses the desired conservation law for the quantity Z. The quantity Z is said to be conserved if the source/sink term $\mathcal{R}_Z$ appearing on the right hand side vanishes and the flux only involves derivatives of Z and no other quantities. The main difficulty in applying the general conservation equation to any particular process is determining the appropriate form for the flux $\boldsymbol{J}_Z$, the source/sink term $\mathcal{R}_Z$, and any constitutive relations that are needed to define various material properties. By associating the quantity Z with mass, concentration of some species, and energy, the transport equations for these quantities follow.

Mass conservation equations for a multicomponent system can be developed in a general fashion for any number of aqueous, gaseous and mineral species. In this chapter the discussion is restricted to aqueous species and minerals and their interaction. The interested reader is referred to Lichtner (1996) for a very general formulation applicable to a multicomponent system including transport of both aqueous and gaseous species.

CHEMICAL REACTIONS

As pointed out by Aris and Mah (1963), the stoichiometry of chemical reactions is akin to kinematics, the branch of mechanics that deals with aspects of motion apart from considerations of mass and force. The stoichiometry of reactions allows one to analyze the possible changes in concentrations that can take place in a system. However, stoichiometric considerations alone do not say which reactions actually take place. For this one needs to solve the governing mass conservation equations along with kinetic rate laws and appropriate initial and boundary conditions for the particular system. The solution to the governing equations provides all the information possible within the confines of the model description. This includes the form of the overall reactions taking place in the system which lead to the predicted changes in concentrations of aqueous, gaseous and mineral species. Often just knowing the species concentrations as functions of time and space is sufficient, and there is no need or interest to back out the mechanistic processes which produced these changes. Indeed, the actual reactions which take place are usually some complicated linear combination, with space- and time-dependent reaction coefficients, of the stoichiometric reactions used as the basis for the calculation.

The first step in defining and setting up a reactive transport problem is to determine which chemical reactions are important in the system being investigated. A number of different chemical reactions take place in a geochemical system involving aqueous species, minerals and gases. The reactions may be classified into two distinct types: homogeneous reactions in which all chemical constituents in the reaction belong to a single phase; and heterogeneous reactions in which the constituents belong to two or more phases. Provided one can distinguish the different phases to which the constituents belong, it is easy to distinguish between homogeneous and heterogeneous reactions. Homogeneous reactions taking place within an aqueous phase include dissociation of water, ion pairing, complexation, and redox reactions. Examples of heterogeneous reactions include mineral precipitation/dissolution reactions, ion-exchange, surface complexation, and redox reactions involving species in different phases. Generally, heterogeneous reactions are much more difficult to describe mathematically compared to homogeneous reactions. This is because a heterogeneous reaction takes place at the interface separating the various phases which are involved in the reaction. Quantifying the interfacial area can be a difficult if not impossible task. Homogeneous reactions, by contrast, take place within a finite volume involving a single phase.

The chemical reactions taking place in a geochemical system may be written in the compact and general form

$$\varnothing \rightleftharpoons \sum_{i=1}^{N} \nu_{ir} \mathcal{A}_i, \quad (r = 1, \ldots, N_R), \tag{10}$$

for a set of N_R reactions involving N reacting constituents $\mathcal{A}_i$. In this form, all species have been brought to the right-hand side of the reaction. Here $\varnothing$ represents the null species, and ν_{ir} refers to the stoichiometric coefficient of the reaction giving the number of moles of the ith species involved in the rth reaction. The sign of the stoichiometric coefficient is defined to be positive for products and negative for reactants.

Canonical Form

Chemical reactions as written in Eqn.(10), while general, are not in a very useful form for distinguishing between intrinsically "fast" reactions which can be assumed locally to be in chemical equilibrium, and intrinsically "slow" reactions which require a kinetic description. The classification of reactions into kinetic and equilibrium reactions is assumed to be independent of time and space, which may not always be the case. Local equilibrium reactions can be described by adding algebraic mass action equations representing conditions of equilibrium to the governing transport equations. The rates of such reactions are controlled by transport including advection and diffusion, and hence such reactions are also referred to as being transport controlled. It is also possible to use a kinetic rate law to describe local equilibrium by taking the rate constant large enough so that for all practical purposes the reaction is close to local equilibrium. This approach is useful for mineral reactions; however, one must be aware that very fast reaction rates can lead to localized concentration gradients at the mineral surface. In such cases use of the bulk fluid composition to describe the solution at the mineral surface may not be valid.

It is possible to rewrite reactions (10) in "canonical" form which distinguishes between a set of N_c basis or primary species and the remaining N_{sec} secondary species (Lichtner, 1985). The sum of the primary and secondary species is equal to the total number of species

$$N_c + N_{\text{sec}} = N. \tag{11}$$

For a system in thermodynamic equilibrium the primary species are usually referred to as components. Components are the minimum number of species required to describe the equilibrium configuration of a system. Generally, however, most geochemical systems are in a state of partial equilibrium and a larger number of species may be needed to characterize the system compared to a system in equilibrium. The canonical form can be derived by noting that for a linearly independent set of reactions it is always possible to select a subset of N_R species indexed by $i{=}N_c{+}1, \ldots, N_c{+}N_R{=}N$, equal to the number of reactions, such that the square submatrix ν_{ir} is nonsingular. Rearranging the chemical reactions with these species on the left-hand side and the remaining species on the right-hand side leads to the reactions

$$\sum_{i=N_c+1}^{N} \nu_{ir}\mathcal{A}_i \;\rightleftharpoons\; -\sum_{j=1}^{N_c} \nu_{jr}\mathcal{A}_j. \tag{12}$$

The set of species $\{\mathcal{A}_j\}$ represent primary species, and the set $\{\mathcal{A}_i\}$ secondary species. It is now possible to "solve" these reactions for the secondary species $\mathcal{A}_i$ by multiplying through by the inverse matrix ν_{ri}^{-1} and summing over all reactions to give the new set of reactions

$$\sum_{j=1}^{N_c} \nu_{ji}\mathcal{A}_j \;\rightleftharpoons\; \mathcal{A}_i, \quad (i = N_c + 1, \ldots, N), \tag{13}$$

where

$$\nu_{ji} \;=\; -\sum_{r=1}^{N_R} \nu_{jr}\nu_{ri}^{-1}. \tag{14}$$

Reactions written in the form of Eqn.(13) are referred to as being in canonical form. The distinctive feature of expressing chemical reactions in this fashion is that each secondary species appears in only one reaction with unit stoichiometric coefficient. The primary species are not unique; however it is desirable to chose them from the set of aqueous species (Lichtner, 1996). Minerals are generally not suitable for primary species because they may not always be present over the entire spatial domain, and their spatial distribution may change with time. This would require using different sets of primary species in different regions of space. More convenient is to chose one set fixed once and for all which may be accomplished most easily by chosing the primary species from the set of aqueous species.

Examples of Geochemical Reactions

Homogeneous Reactions. Homogeneous reactions can be represented in canonical form as

$$\sum_{j=1}^{N_c} \nu_{ji}\mathcal{A}_j \;\rightleftharpoons\; \mathcal{A}_i, \tag{15}$$

where all species involved in the reaction belong to a single phase. Examples of homogeneous reactions include dissociation of water

$$\mathrm{H_2O} - \mathrm{H^+} \;\rightleftharpoons\; \mathrm{OH^-}, \tag{16}$$

ion-pairing reactions

$$\mathrm{Na^+ + Cl^-} \;\rightleftharpoons\; \mathrm{NaCl^\circ}, \tag{17}$$

complexing reactions

$$\mathrm{Ca^{2+} + SO_4^{2-}} \;\rightleftharpoons\; \mathrm{CaSO_4^\circ}, \tag{18}$$

and redox reactions

$$\mathrm{Fe^{2+}} + \mathrm{H^+} - \frac{1}{2}\,\mathrm{H_2O} + \frac{1}{4}\,\mathrm{O_2} \;\rightleftharpoons\; \mathrm{Fe^{3+}}. \tag{19}$$

In these reactions the species H_2O, H^+, Na^+, Cl^-, Ca^{2+}, SO_4^{2-}, Fe^{2+}, and O_2 are primary species. The species OH^-, $NaCl^\circ$, $CaSO_4^\circ$, and Fe^{3+} are secondary species.

Heterogeneous Reactions. Heterogeneous reactions occur in a variety of forms as mineral precipitation/dissolution reactions, ion-exchange and surface complexation. Mineral precipitation/dissolution reactions can be expressed in the general form

$$\sum_j \nu_{jm}\mathcal{A}_j \;\rightleftharpoons\; \mathcal{M}_m, \tag{20}$$

where $\mathcal{M}_m$ denotes the mth mineral. For example, the dissolution of K-feldspar can be written as

$$\mathrm{K^+} + \mathrm{Al^{3+}} + 3\,\mathrm{SiO_{2(aq)}} + \mathrm{H_2O} - 4\,\mathrm{H^+} \;\rightleftharpoons\; \mathrm{KAlSi_3O_8}, \tag{21}$$

in terms of primary species K^+, Al^{3+}, $SiO_{2(aq)}$, and H_2O.

Uniqueness

The choice of basis or primary species is not unique. Different sets of basis species are related by a linear transformation which may be represented by the matrix $\mathbf{\Gamma}$. The transformation from one basis $\boldsymbol{B} = (\mathcal{A}_1, \ldots, \mathcal{A}_{N_c})^T$ to another $\boldsymbol{B}' = (\mathcal{A}'_1, \ldots, \mathcal{A}'_{N_c})^T$, where the superscript $(\ldots)^T$ denotes the transpose resulting in a column vector, is then represented by a matrix equation written in the form

$$\mathbf{\Gamma}\boldsymbol{B} \;\rightleftharpoons\; \boldsymbol{B}'. \tag{22}$$

This equation represents the basis transformation as a set of chemical reactions written in canonical form. The only requirement for the species $\boldsymbol{B}'$ to form new basis species is that the transformation from one basis to another be nonsingular. The new basis set $\boldsymbol{B}'$ consists of some combination of the original primary and secondary species. Only those primary species which are different in the two bases are transformed—the indentity transformation is applied to those primary species which remain common to both bases. An explicit form of the transformation matrix $\mathbf{\Gamma}$ can be found by comparing Eqn.(22) with Eqn.(13). Writing out Eqn.(22) in component form yields

$$\sum_j \Gamma_{kj}\mathcal{A}_j \;\rightleftharpoons\; \mathcal{A}'_k. \tag{23}$$

If the new basis species $\mathcal{A}'_k$ is one of the original secondary species $\mathcal{A}_{i_k}$, then the kth row of $\mathbf{\Gamma}$ is equal to the kth column of the stoichiometric matrix ν_{ji_k}:

$$\Gamma_{kj} \;=\; \nu_{ji_k}, \quad (j = 1, \ldots, N_c). \tag{24}$$

On the other hand, if the new basis species $\mathcal{A}'_k$ is the same as one of the original basis species $\mathcal{A}_j$, then Γ_{kj} represents the identity transformation

$$\Gamma_{kj} \;=\; \delta_{jk}. \tag{25}$$

In writing this equation it is assumed that basis species which remain the same keep their place in the sequence of basis species. While this is not necessary it is convenient and simplifies the notation.

The inverse transformation

$$\boldsymbol{\Gamma}^{-1}\boldsymbol{B}' \rightleftharpoons \boldsymbol{B}, \tag{26}$$

expresses the original set of basis species $\boldsymbol{B}$ in terms of the new basis species $\boldsymbol{B}'$. Thus those original primary species which no longer belong to the set of new basis species become secondary species in the new basis. To express the remaining secondary species in terms of the new basis, the original set of homogeneous reactions are transformed to the new basis. According to Eqn.(13), these reactions read in matrix form

$$\boldsymbol{\nu}^T\boldsymbol{B} \rightleftharpoons \boldsymbol{S}, \tag{27}$$

where $\boldsymbol{S}$ denotes the column vector of secondary species which are common to both bases. The matrix $\boldsymbol{\nu}^T$, where the superscript T represents the transpose of the matrix $\boldsymbol{\nu}$, has the entries $(\boldsymbol{\nu}^T)_{ij}$=$\nu_{ji}$. Substituting for $\boldsymbol{B}$ from Eqn.(26) gives

$$\boldsymbol{\nu}'^T\boldsymbol{B}' \rightleftharpoons \boldsymbol{S}, \tag{28}$$

with

$$\boldsymbol{\nu}'^T = \boldsymbol{\nu}^T\boldsymbol{\Gamma}^{-1} = ((\boldsymbol{\Gamma}^{-1})^T\boldsymbol{\nu})^T. \tag{29}$$

To obtain the latter expression the property of the transpose of a matrix product $(\boldsymbol{AB})^T$= $\boldsymbol{B}^T\boldsymbol{A}^T$ has been used. From Eqn.(28) reactions for the remaining secondary species are obtained in terms of the new basis species $\boldsymbol{B}'$. Equations (26) and (28) may be combined into a single matrix equation as

$$\begin{bmatrix} \boldsymbol{\Gamma}^{-1} \\ \boldsymbol{\nu}^T\boldsymbol{\Gamma}^{-1} \end{bmatrix} \boldsymbol{B}' \rightleftharpoons \begin{bmatrix} \boldsymbol{B} \\ \boldsymbol{S} \end{bmatrix}. \tag{30a}$$

In terms of the original basis set the homogeneous reactions can be written as

$$\begin{bmatrix} \boldsymbol{\Gamma} \\ \boldsymbol{\nu}^T \end{bmatrix} \boldsymbol{B} \rightleftharpoons \begin{bmatrix} \boldsymbol{B}' \\ \boldsymbol{S} \end{bmatrix}, \tag{30b}$$

obtained by combining Eqns.(22) and (27). These equations will prove useful for transforming the mass transport equations to a new set of basis species [see Eqn.(125)].

The transformed equilibrium constants $\boldsymbol{K}'_S$ are related to the original constants by the equation

$$\log \boldsymbol{K}'_S = \log \boldsymbol{K}_S - \boldsymbol{\nu}^T\boldsymbol{\Gamma}^{-1}\log \boldsymbol{K}', \tag{31}$$

where $\boldsymbol{K}'$ refer to the equilibrium constants for the basis transformation reactions Eqn.(22). The activities of the new and old basis species $\boldsymbol{a}'$ and $\boldsymbol{a}$, respectively, are related by

$$\log \boldsymbol{a}' = \log \boldsymbol{K}' + \boldsymbol{\Gamma}\log \boldsymbol{a}, \tag{32}$$

corresponding to the mass action equations of basis transformation reactions.

For mineral precipitation/dissolution reactions as given in Eqn.(20) the transformation to the new basis set may be carried out in one step since minerals are not allowed to become

primary or basis species in the formulation presented here. Writing Eqn.(20) in matrix form yields

$$\boldsymbol{\nu}_M^T \boldsymbol{B} \rightleftharpoons \boldsymbol{M}, \tag{33}$$

with $(\boldsymbol{\nu}_M)_{jm} = \nu_{jm}$ and where $\boldsymbol{M}$ represents the column vector of minerals. The transformed reactions become

$$\boldsymbol{\nu}_M'^{\,T} \boldsymbol{B}' \rightleftharpoons \boldsymbol{M}, \tag{34}$$

where the transformed stoichiometric matrix is given by

$$\boldsymbol{\nu}_M'^{\,T} = \boldsymbol{\nu}_M^T \boldsymbol{\Gamma}^{-1} = ((\boldsymbol{\Gamma}^{-1})^T \boldsymbol{\nu}_M)^T. \tag{35}$$

Taking the transpose of both sides of this equation yields the alternative form

$$\boldsymbol{\nu}_M' = \left(\boldsymbol{\Gamma}^{-1}\right)^T \boldsymbol{\nu}_M. \tag{36}$$

The new values for the equilibrium constants may be obtained as follows. Noting that

$$\log \boldsymbol{K}_M' = -\boldsymbol{\nu}_M'^{\,T} \log \boldsymbol{a}', \tag{37}$$

for the transformed mineral reactions, where $\log \boldsymbol{a}'$ represents a column vector of the activities of transformed aqueous basis species, it follows that

$$\begin{aligned} \log \boldsymbol{K}_M' &= -\boldsymbol{\nu}_M'^{\,T} \left\{\log \boldsymbol{K}' + \boldsymbol{\Gamma} \log \boldsymbol{a}\right\}, \\ &= -\boldsymbol{\nu}_M^T \boldsymbol{\Gamma}^{-1} \left\{\log \boldsymbol{K}' + \boldsymbol{\Gamma} \log \boldsymbol{a}\right\}, \\ &= -\boldsymbol{\nu}_M^T \boldsymbol{\Gamma}^{-1} \log \boldsymbol{K}' - \log \boldsymbol{K}_M, \end{aligned} \tag{38}$$

making use of Eqn.(32). From the latter expression the new mineral equilibrium constants $\boldsymbol{K}_M'$ can be computed relative to the new set of basis species in terms of the original constants $\boldsymbol{K}_M$ and the equilibrium constants for the basis transformation reactions $\boldsymbol{K}'$.

To illustrate these relations with a concrete example consider a three-component system with basis species $\boldsymbol{B} = \{\mathrm{A}, \mathrm{B}, \mathrm{C}\}$, and four secondary species $\boldsymbol{S} = \{\mathrm{AB}, \mathrm{A_2B}, \mathrm{AC}, \mathrm{BC}\}$. In matrix form the chemical reactions become

$$\begin{bmatrix} 1 & 1 & 0 \\ 2 & 1 & 0 \\ 1 & 0 & 1 \\ 0 & 1 & 1 \end{bmatrix} \begin{bmatrix} \mathrm{A} \\ \mathrm{B} \\ \mathrm{C} \end{bmatrix} \rightleftharpoons \begin{bmatrix} \mathrm{AB} \\ \mathrm{A_2B} \\ \mathrm{AC} \\ \mathrm{BC} \end{bmatrix}. \tag{39}$$

Consider the new basis set $\boldsymbol{B}' = \{\mathrm{AB}, \mathrm{A_2B}, \mathrm{AC}\}$, and secondary species $\boldsymbol{S}' = \{\mathrm{A}, \mathrm{B}, \mathrm{C}, \mathrm{BC}\}$. For this example the transformation matrix $\boldsymbol{\Gamma}$ consists of the first three rows of the stoichiometric matrix. The basis transformation reads

$$\begin{bmatrix} 1 & 1 & 0 \\ 2 & 1 & 0 \\ 1 & 0 & 1 \end{bmatrix} \begin{bmatrix} \mathrm{A} \\ \mathrm{B} \\ \mathrm{C} \end{bmatrix} \rightleftharpoons \begin{bmatrix} \mathrm{AB} \\ \mathrm{A_2B} \\ \mathrm{AC} \end{bmatrix}. \tag{40}$$

Inverting this equation gives the reactions for the new secondary species with the exception of species BC as

$$\begin{bmatrix} -1 & 1 & 0 \\ 2 & -1 & 0 \\ 1 & -1 & 1 \end{bmatrix} \begin{bmatrix} \mathrm{AB} \\ \mathrm{A_2B} \\ \mathrm{AC} \end{bmatrix} \rightleftharpoons \begin{bmatrix} \mathrm{A} \\ \mathrm{B} \\ \mathrm{C} \end{bmatrix}. \tag{41}$$

The reaction involving secondary species BC may be found by transforming the original set of homogeneous reactions to give

$$\begin{bmatrix} 1 & 0 & 0 \\ 0 & 1 & 0 \\ 0 & 0 & 1 \\ 3 & -2 & 1 \end{bmatrix} \begin{bmatrix} \mathrm{AB} \\ \mathrm{A_2B} \\ \mathrm{AC} \end{bmatrix} \rightleftharpoons \begin{bmatrix} \mathrm{AB} \\ \mathrm{A_2B} \\ \mathrm{AC} \\ \mathrm{BC} \end{bmatrix}. \tag{42}$$

Notice that the first three rows form the identity matrix, since these former secondary species are now primary species in the new basis. The fourth row gives the desired reaction for the remaining secondary species. Combining the last equation with the basis transformation equations, gives the final relation for the new set of reactions in the new basis:

$$\begin{bmatrix} -1 & 1 & 0 \\ 2 & -1 & 0 \\ 1 & -1 & 1 \\ 3 & -2 & 1 \end{bmatrix} \begin{bmatrix} \mathrm{AB} \\ \mathrm{A_2B} \\ \mathrm{AC} \end{bmatrix} \rightleftharpoons \begin{bmatrix} \mathrm{A} \\ \mathrm{B} \\ \mathrm{C} \\ \mathrm{BC} \end{bmatrix}. \tag{43}$$

Besides predicting solution compositions and mineral abundances as functions of time and space, a reactive transport model can also be used to predict the form of the overall reactions which take place in the system. The insensitivity of solutions to the reactive transport equations to the choice of basis species, all other things being the same including kinetic rate laws, implies that the particular form of the reactions used in the calculations may have little resemblance to the actual overall reactions taking place in the system. These reactions can be very different from the reactions read from the thermodynamic database used as input to the calculation. This is considered in more detail below in the section discussing oxidation–reduction reactions.

KINETICS

For simplicity and because of lack of knowledge of detailed reaction mechanisms, mineral reactions are often represented by an overall reaction between the mineral and aqueous solution. The form of the reaction rate is based on transition state theory (Lasaga, 1981; Aagaard and Helgeson, 1982). An overall reaction consists, in principle, of a sequence of elementary steps. This implies that the overall reaction can be written as a linear combination of elementary steps. If the ith elementary step is written in the general form

$$\varnothing \rightleftharpoons \sum_j \nu_{ji} \mathcal{A}_j, \tag{44}$$

and the overall reaction has the form

$$\varnothing \rightleftharpoons \sum_j \nu_j \mathcal{A}_j, \tag{45}$$

then the stoichiometric coefficients of the overall reaction are related to the coefficients of the elementary reactions by the expression

$$\nu_j = \sum_i \nu_{ji} \sigma_i, \tag{46}$$

where the sum is over all elementary steps, and σ_i represents the stoichiometric number of the ith elementary reaction in the overall reaction. Determination of the elementary steps for any particular overall reaction is often a formidable task.

By definition of an elementary step the reaction rate is defined as the difference between the forward and backward rates with the explicit form

$$I_i \;=\; k_i^+ \prod_{j,\,\nu_{ji}<0} a_j^{-\nu_{ji}} - k_i^- \prod_{j,\,\nu_{ji}>0} a_j^{\nu_{ji}}, \tag{47}$$

where a_j denotes the activity of the jth reactant, and $k_i^{\pm}$ refer the effective forward and backward rate constants. By convention, a positive stoichiometric coefficient implies the corresponding species represents a product species, and a negative coefficient a reactant. The ratio of the forward and backward rate constants is equal to the equilibrium constant of the reaction

$$K_i \;=\; \frac{k_i^+}{k_i^-}. \tag{48}$$

The affinity A_i of the ith elementary reaction is defined by

$$A_i \;=\; -RT \ln \frac{Q_i}{K_i}, \tag{49}$$

with the ion activity product defined by

$$Q_i \;=\; \prod a_j^{\nu_{ji}}. \tag{50}$$

In terms of the affinity the reaction rate can be expressed as

$$I_i \;=\; k_i^+ \left[\prod_{j,\,\nu_{ji}<0} a_j^{-\nu_{ji}} \right] \left(1 - \mathrm{e}^{-A_i/RT}\right). \tag{51}$$

The affinity can be expressed in terms of the forward and backward reaction rates, defined respectively as r_i and r_{-i}, as

$$\mathrm{e}^{-A_i/RT} \;=\; \frac{r_{-i}}{r_i}, \tag{52}$$

with the forward rate defined as

$$r_i \;=\; k_i^+ \prod_{j,\,\nu_{ji}<0} a_j^{-\nu_{ji}}, \tag{53a}$$

and the backward rate as

$$r_{-i} \;=\; k_i^- \prod_{j,\,\nu_{ji}>0} a_j^{\nu_{ji}}. \tag{53b}$$

At equilibrium the affinity vanishes and the net rate is zero. The forward and backward rates are equal.

For steady-state conditions, a general relationship exists between the rates of the elementary steps and the rate of the overall reaction (Horiuti, 1957; Tempkin, 1973). The approach of Boudart and Djéga-Mariadasson (1984), who present a general discussion of the literature applied to heterogeneous catalytic reactions, is followed in the discussion below.

The following mathematical identity can be written between the rates of the elementary steps:

$$\begin{aligned}(r_1 - r_{-1})r_2 \cdots r_N + r_{-1}(r_2 - r_{-2})r_3 \cdots r_N + \cdots \\ + r_{-1}r_{-2} \cdots r_{-(N-1)}(r_N - r_{-N}) \\ = \; r_1 r_2 \cdots r_N - r_{-1}r_{-2} \cdots r_{-N}.\end{aligned} \tag{54}$$

This relation is referred to as Tempkin's identity (Tempkin, 1973).

Assuming a steady state has been reached, the difference in the rates of each elementary step is equal to the overall reaction rate times the stoichiometric number associated with the elementary step according to the expression

$$I_i \; = \; r_i - r_{-i} \; = \; \sigma_i I, \tag{55}$$

where I represents the overall reaction rate. Substituting this relation into Tempkin's identity, Eqn.(54), yields the following expression for the overall reaction rate

$$I \; = \; \frac{r_1 r_2 \cdots r_N - r_{-1}r_{-2} \cdots r_{-N}}{\sigma_1 r_2 \cdots r_N + r_{-1}\sigma_2 r_3 \cdots r_N + \cdots + r_{-1}r_{-2} \cdots r_{-(N-1)}\sigma_N}. \tag{56}$$

Forward and backward rates for the overall reaction may be defined according to the relations

$$I_+ \; = \; \frac{r_1 r_2 \cdots r_N}{\mathcal{D}}, \tag{57}$$

and

$$I_- \; = \; \frac{r_{-1}r_{-2} \cdots r_{-N}}{\mathcal{D}}, \tag{58}$$

where the quantity $\mathcal{D}$ represents the denominator in Eqn.(56) and is defined by

$$\mathcal{D} \; = \; \sigma_1 r_2 \cdots r_N + r_{-1}\sigma_2 r_3 \cdots r_N + \cdots + r_{-1}r_{-2} \cdots r_{-(N-1)}\sigma_N. \tag{59}$$

The ratio of the forward and backward rates is then equal to

$$\begin{aligned}\frac{I_+}{I_-} \; &= \; \frac{r_1 r_2 \cdots r_N}{r_{-1}r_{-2} \cdots r_{-N}}, \\ &= \; \prod_i \frac{r_i}{r_{-i}}.\end{aligned} \tag{60}$$

Making use of Eqn.(52) for an elementary step, it follows that

$$\frac{I_+}{I_-} \; = \; \exp\left\{\frac{1}{RT}\sum_i A_i\right\}. \tag{61}$$

The affinity of the overall reaction A is equal to the sum of the affinities of the elementary steps A_i weighted by the stoichiometric number of the step

$$A \; = \; \sum_i \sigma_i A_i. \tag{62}$$

Thus, defining the average stoichiometric coefficient $\overline{\sigma}$, referred to as Tempkin's number, by the relation

$$\overline{\sigma} \; = \; \frac{\sum_i \sigma_i A_i}{\sum_l A_l}, \tag{63}$$

it follows that the rate of the overall reaction may be expressed in a form analogous to that of an elementary reaction as

$$\begin{aligned} I &= I_+ - I_-, \\ &= I_+ \left[1 - \frac{I_-}{I_+}\right], \\ &= I_+ \left[1 - \mathrm{e}^{-A/(\overline{\sigma} RT)}\right], \end{aligned} \tag{64}$$

but where now the factor $\overline{\sigma}$ appears in the affinity term.

It should be noted that although formally Eqn.(64) and the rate for an elementary step Eqn.(51) appear similar, they are actually quite different in general. The forward overall reaction rate is a complicated function of the stoichiometric coefficients σ_i and the forward and backward elementary reaction rates $r_{\pm i}$ through Eqn.(57). Furthermore, $\overline{\sigma}$ depends on the stoichiometric coefficients as well. There is one particular case where these equations simplify greatly. This occurs when all elementary steps but one are sufficiently fast to be considered in equilibrium, while one step, the rate determining step, is kinetically controlled. Let the $i_\circ$ be the rate determining step, the remaining steps in thermodynamic equilibrium. In this case the rate of the overall reaction becomes simply

$$I = \frac{r_{i_\circ} - r_{-i_\circ}}{\sigma_{i_\circ}}. \tag{65}$$

Factoring out the forward rate gives

$$\begin{aligned} I &= \frac{r_{i_\circ}}{\sigma_{i_\circ}} \left[1 - \frac{r_{-i_\circ}}{r_{i_\circ}}\right], \\ &= I_+ \left[1 - \mathrm{e}^{-A/(\sigma_{i_\circ} RT)}\right], \end{aligned} \tag{66}$$

with

$$I_+ = \frac{r_{i_\circ}}{\sigma_{i_\circ}}. \tag{67}$$

Thus the stoichiometric coefficient of the rate determining step enters the expression for the overall reaction rate. This is a nontrivial result. One might ask whether it is possible to set $\sigma_{i_\circ} = 1$ by renormalizing the overall reaction. In the sum appearing in Eqn.(46), it is always possible to chose one $\sigma_i = 1$. However, when writing the overall reaction it is usually supposed that one species has already been singled out with unit stoichiometric coefficient. For example, if one where to attempt to apply this formalism to the overall reaction describing the dissolution of albite, albite would appear in the reaction with unit stoichiometric coefficient. The stoichiometric number $\sigma_{i_\circ}$ (if a rate determining step indeed exists!) is thus measured relative to albite, in this case, and further normalization is not possible.

Recently, Lasaga (1995) has questioned the validity of this equation suggesting that the form of Eqn.(64) is not fundamentally valid for $\overline{\sigma} \neq 1$. However, as the derivation given here demonstrates, this relation follows directly from Tempkin's mathematical identity Eqn.(54), assuming steady-state conditions and the definition of $\overline{\sigma}$ given in Eqn.(63). This approach has been used by Aagaard and Helgeson (1982), Helgeson et al. (1984), Oelkers et al. (1994) and others, to analyze kinetic reactions of silicate and other minerals.

Homogeneous Reactions

Homogeneous kinetic reactions are assumed to have the general form

$$\varnothing \rightleftharpoons \sum_{i=1}^{N} \nu_{ir}^{\mathrm{kin}} \mathcal{A}_i, \tag{68}$$

with all species $\mathcal{A}_i$ belonging to a single phase. The reaction rate is denoted by I_r^{kin}. For an elementary reaction the reaction rate can be expressed as the difference between the forward and backward rates as

$$I_r^{\mathrm{kin}} = k_r^f \prod_{\nu_{ir}^{\mathrm{kin}}<0} a_i^{-\nu_{ir}^{\mathrm{kin}}} - k_r^b \prod_{\nu_{ir}^{\mathrm{kin}}>0} a_i^{\nu_{ir}^{\mathrm{kin}}}, \tag{69}$$

where k_r^f and k_r^b denote the forward and backward rate constants, respectively. At equilibrium the net rate vanishes, the forward and backward rates being equal, resulting in a relation between the forward and backward rate constants and the equilibrium constant

$$K_r = \frac{k_r^f}{k_r^b}. \tag{70}$$

Factoring out the first term, the kinetic rate can be expressed in the form

$$I_r^{\mathrm{kin}} = k_r^f \left[\prod_{\nu_{ir}^{\mathrm{kin}}<0} a_i^{-\nu_{ir}^{\mathrm{kin}}} \right] \left(1 - \frac{Q_r}{K_r} \right), \tag{71}$$

with the ion activity product defined as

$$Q_r = \prod_i a_i^{\nu_{ir}^{\mathrm{kin}}}. \tag{72}$$

This form of the reaction rate, and variations of it, are used for both homogeneous and heterogeneous reactions. The term in round brackets is referred to as the affinity factor. At equilibrium the affinity factor vanishes and the net rate is zero.

Heterogeneous Reactions

The treatment of heterogeneous reactions is much more complicated than that of homogeneous reactions. Consider a heterogeneous reaction involving a solid phase reacting with an aqueous solution according to Eqn.(20). Because of the simplicity of describing rates of homogeneous reactions as a volume average, often an attempt is made to represent heterogeneous reactions in a similar manner. An additional descriptive parameter is required specifying the surface area per unit volume of bulk porous medium. Such a parameter is not required for truly homogeneous reactions. This parameter is also very problematical to pin down for any real system. The reaction rate is denoted by $\hat{I}_m$ for reasons which become apparent below [see Eqn.(78)], and is assumed to have the form

$$\widehat{I}_m = -k_m s_m \left[\prod_i a_i^{n_i} \right] \left(1 - \mathrm{e}^{-A_m/\sigma_m RT} \right), \tag{73a}$$

$$= -k_m s_m \left[\prod_i a_i^{n_i} \right] \left(1 - K_m Q_m \right), \tag{73b}$$

where k_m denotes the kinetic rate constant, s_m denotes the mineral surface area participating in the reaction, σ_m refers to Tempkin's constant, a_i represents the activity of the ith species, and n_i is a constant. The quantity K_m denotes the corresponding equilibrium constant for the mineral reaction as written in Eqn.(20) with the mineral on the right-hand side, and Q_m denotes the ion activity product defined by

$$Q_m \;=\; \prod_{j=1}^{N_c} (\gamma_j C_j)^{\widetilde{\nu}_{jm}} \,. \tag{74}$$

The affinity A_m of the reaction is defined by

$$A_m \;=\; -\sigma_m RT \ln K_m Q_m, \tag{75}$$

with R the gas constant, and T the temperature.

Note that because of writing reactions in the form of Eqn.(20), the product $K_m Q_m$ occurs in the formulation for the rate, rather than the often used form Q_m/K_m. The quantity in round brackets in Eqn.(73a,b) is referred to as the affinity factor and provides a measure of how far the reaction is from equilibrium. At equilibrium the affinity vanishes and the affinity factor is zero, ensuring that the overall reaction rate is zero. The quantity in square brackets accounts for the dependence of the rate on the concentration of dissolved species, such as the proton activity, in addition to the affinity factor. Precipitation ($\widehat{I}_m > 0$) occurs if $A_m < 0$, and dissolution ($\widehat{I}_m < 0$) if $A_m > 0$. The reaction rate has units of moles per unit time per unit volume of bulk porous medium. Thus it represents an average rate taken over a REV.

Far from equilibrium the expression for the reaction rate reduces to the forms

$$\widehat{I}_m \;=\; -k_m s_m \left[\prod_i a_i^{n_i}\right], \tag{76a}$$

for $A_m \gg 0$ corresponding to dissolution, and

$$\widehat{I}_m \;=\; k_m s_m \, \mathrm{e}^{|A_m|/\sigma_m RT} \left[\prod_i a_i^{n_i}\right], \tag{76b}$$

for $A_m \ll 0$ corresponding to precipitation. Close to equilibrium the rate becomes proportional to the chemical affinity according to the expression

$$\widehat{I}_m \;=\; k_m s_m \left[\prod_i a_i^{n_i}\right] \frac{A_m}{\sigma_m RT}, \tag{76c}$$

valid for $|A_m/\sigma_m RT| \ll 1$. There is an inherent asymmetry in the rate law regarding precipitation and dissolution that should be noted. According to Eqn.(76b), the precipitation rate grows indefinitely as $A_m \to -\infty$, whereas according to Eqn.(76a) the dissolution rate tends to a finite constant times the factor in square brackets as $A_m \to \infty$. Of course physically the reaction rate cannot grow indefinitely, but must be limited by the rate of transport of reactants and products to the site where the reaction takes place. Note that under such far-from-equilibrium conditions, although the rate is transport limited, the reaction is not in local chemical equilibrium.

The temperature dependence of the kinetic rate constant may be calculated from the Arrhenius equation (Lasaga, 1981)

$$k_m(T) \;=\; k_m^0 \,\frac{A(T)}{A(T_0)}\,\exp\left[-\frac{1}{R}\,\left(\frac{1}{T}-\frac{1}{T_0}\right)\Delta E_m\right], \tag{77}$$

where k_m^0 denotes the rate constant at T_0, $A(T)$ represents a pre-exponential factor, and ΔE_m denotes the activation energy.

Moving Boundary Problem

The expression for the reaction rate that enters the mass transport equations must take into account the distribution in space of the various minerals in the system. This distribution changes continually with time as mineral alteration zones form and advance with time, dissolving and re-precipitating. Dissolution can occur at some point in space only if the particular mineral in question is actually present. For precipitation, on the other hand, it is only necessary that the mineral be supersaturated with respect to the aqueous solution. In this sense the reactive transport equations define a moving boundary problem and part of the problem is to determine the regions in space each mineral occupies. This can be accomplished with the following form of the rate

$$I_m(\boldsymbol{r},\,t) \;=\; \begin{cases} \widehat{I}_m(\boldsymbol{r},\,t), & \text{if } \phi_m(\boldsymbol{r},\,t)>0, \text{ or if } \phi_m(\boldsymbol{r},\,t)=0 \text{ and } A_m(\boldsymbol{r},\,t)<0, \\ \\ 0, & \text{otherwise,} \end{cases} \tag{78}$$

with $\widehat{I}_m$ the kinetic rate law for the mineral as determined by the assumed reaction mechanism and where ϕ_m denotes the mineral volume fraction. According to this relation the rate $I_m(\boldsymbol{r},\,t)$ is zero unless the mineral is present at point $\boldsymbol{r}$ and time t, or the mineral is not present but the fluid is supersaturated with respect to the mineral. In these latter cases the rate is determined by the specified rate law $\widehat{I}_m(\boldsymbol{r},\,t)$.

The rate law given by Eqn.(73a) should really be referred to as a pseudo-kinetic rate law. This is because it refers to the overall mineral precipitation/dissolution reaction, and generally does not describe the actual kinetic mechanism by which the mineral reacts. Nevertheless, it provides a useful form to describe departures from equilibrium and is certainly no worse than the assumption of local equilibrium. Other forms have also been proposed for the for of the rate law (Steefel and Van Cappellen, 1990; Lasaga, 1995).

Flow Past a Boundary Layer

To illustrate the difficulties inherent in determining the rate law for heterogeneous reactions, the rate law for flow past a boundary layer at the mineral surface is considered briefly (Murphy et al., 1989). In this case, a stagnant region of fluid borders the mineral surface, and solute species must diffuse from the bulk fluid across the boundary layer to the mineral surface. The reaction rate at the mineral surface must be balanced by the diffusive flux of species across the boundary layer to the surface. In symbols

$$I_{\rm surf} \;=\; k's(C_{\rm surf}-C_{\rm eq}) \;=\; s'D\left(\frac{\partial C}{\partial x}\right)_{\rm surf} \;=\; s'D\frac{C_{\rm bulk}-C_{\rm surf}}{\Delta l}, \tag{79}$$

where Δl denotes the boundary layer thickness, $C_{\rm bulk}$ denotes the bulk fluid composition, $C_{\rm surf}$ the concentration at the mineral surface, s denotes the effective reactive surface area of the mineral, and s' refers to the geometric area. Solving this relation for the surface concentration yields

$$C_{\rm surf} \;=\; (1-\beta)\, C_{\rm eq} + \beta\, C_{\rm bulk}, \tag{80}$$

where

$$\beta \;=\; \frac{1}{1+{\rm Da}}. \tag{81}$$

and

$$ {\rm Da} \;=\; \frac{k' s \Delta l}{s' D}, \tag{82}$$

represents the Damköhler number (Damköhler, 1936). Substituting this result into the equation for the reaction rate, yields the following expression for the effective rate constant

$$k_{\rm eff} \;=\; \frac{k' s}{1+{\rm Da}}. \tag{83}$$

The following limiting values are obtained for the effective rate constant

$$k_{\rm eff} \;=\; \left\{ \begin{array}{ll} k' s, & (\Delta l \rightarrow 0) \\ \dfrac{s' D}{\Delta l}, & (\Delta l \gg s' D / k' s) \end{array} \right. . \tag{84}$$

This result indicates the complex relation the effective rate constant can have to measurable quantities. It may not be enough to know the rate constant and surface area alone. For intrinsically fast reactions, ${\rm Da} \gg 1$, geometry can also be an important factor.

REACTIVE MASS TRANSPORT EQUATIONS

Homogeneous Reactions

First the simplest case of transport of solute species in the aqueous phase is considered involving homogeneous reactions, but in the absence of heterogeneous reactions. Partial differential equations describing transport of N solute species with concentrations C_i in a porous medium with porosity ϕ and reacting according to the general set of reactions given in Eqn.(10) with corresponding reaction rates I_r have the form

$$\frac{\partial}{\partial t}\left(\phi C_i\right) + \boldsymbol{\nabla} \cdot \boldsymbol{J}_i \;=\; \sum_{r=1}^{N_R} \nu_{ir} I_r. \tag{85}$$

The solute flux $\boldsymbol{J}_i$ consists of contributions from advection and diffusion according to the definition

$$\boldsymbol{J}_i \;=\; -\phi D \boldsymbol{\nabla} C_i + \boldsymbol{v} C_i, \tag{86}$$

with an effective diffusion coefficient D, assumed for simplicity to be the same for all species, and Darcy flow velocity $\boldsymbol{v}$. Making use of the equivalent canonical form of the chemical reactions given by Eqn.(13), the transport equations become

$$\frac{\partial}{\partial t}\left(\phi C_j\right) + \boldsymbol{\nabla} \cdot \boldsymbol{J}_j \;=\; -\sum_{i=1}^{N_R} \nu_{ji} I_i, \tag{87}$$

for primary species, and

$$\frac{\partial}{\partial t}\left(\phi C_i\right) + \boldsymbol{\nabla}\cdot\boldsymbol{J}_i \;=\; I_i, \tag{88}$$

for secondary species. The reaction rates I_i for reactions written in canonical form are related to the rates I_r of the original reactions through the linear combination

$$I_i \;=\; \sum_{r=1}^{N_R} \nu_{ir} I_r. \tag{89}$$

Thus if the original reaction rates I_r are described by elementary kinetic rate laws, the rates in canonical form are no longer elementary.

Note the simplicity of the rate term in the transport equations for the secondary species compared to the original set of transport equations, Eqn.(85). It is this feature that distinguishes the canonical representation from the original set of reactions given by Eqn.(10). With reactions written in canonical form it is an easy matter to eliminate the reaction rates I_i appearing in the primary species transport equations by substituting Eqn.(88) into Eqn.(87) to give

$$\frac{\partial}{\partial t}\left(\phi\Psi_j\right) + \boldsymbol{\nabla}\cdot\boldsymbol{\Omega}_j \;=\; 0, \tag{90}$$

where Ψ_j and $\boldsymbol{\Omega}_j$ are defined by

$$\Psi_j \;=\; C_j + \sum_i \nu_{ji} C_i, \tag{91}$$

and

$$\boldsymbol{\Omega}_j \;=\; \boldsymbol{J}_j + \sum_i \nu_{ji} \boldsymbol{J}_i. \tag{92}$$

With species-independent diffusion coefficients the expression for $\boldsymbol{\Omega}_j$ reduces to

$$\boldsymbol{\Omega}_j \;=\; \left(-\phi D\boldsymbol{\nabla} + \boldsymbol{v}\right)\Psi_j. \tag{93}$$

For the case when the stoichiometric coefficients are positive, the quantities Ψ_j and $\boldsymbol{\Omega}_j$ have a simple interpretation as the total concentration and flux of the jth primary species.

Intrinsically Fast Reactions. The mass conservation equations simplify for reactions which are intrinsically fast, enabling the concept of local chemical equilibrium to be utilized. The actual rate of a reaction in thermodynamic equilibrium in a open system is determined by the rate of transport of solute species to the site of reaction. This is quite different from a closed system in which the net rate of a reaction in equilibrium is zero, the forward and backward rates being equal. In an open system, the rates of "fast" reactions must be such that they balance advective and diffusive transport of solute species to maintain equilibrium at each "point" (i.e. control volume) of the system. Neighboring points, however, are generally not equilibrium with each other. The actual rate of an intrinsically fast reaction may, in fact, not be very fast at all if the transport rate of solute species is slow.

The mass action equation corresponding to the canonical form of a homogeneous reaction, provides an algebraic relation between the concentration of the corresponding secondary species and the concentrations of the primary species. For the homogeneous reaction as written in Eqn.(15), the mass action equation can be expressed in the form

$$C_i \;=\; \gamma_i^{-1} K_i \prod_{j=1}^{N_c} \left(\gamma_j C_j\right)^{\nu_{ji}}, \tag{94}$$

where K_i denotes the equilibrium constant of the reaction, and γ_j and γ_i refer to activity coefficients of primary and secondary species. Accordingly, the transport equation for the ith secondary species, Eqn.(88), is no longer needed. It may be used to eliminate the unknown reaction rate I_i from the transport equations for the primary species.

For the common situation when the aqueous reactions may be considered in local chemical equilibrium, the number of partial differential equations necessary to solve reduces to the number of primary species. In this case the partial differential equations for the secondary species, Eqn.(88), are replaced by the mass action equations, Eqn.(94), and the problem becomes a differential-algebraic system of nonlinear equations. For the case of species-independent diffusion coefficients, the primary species transport equations, Eqn.(90), become independent of each other and may be solved directly for Ψ_j as in the case of nonreactive transport equations. The case of species-dependent diffusion coefficients is more complicated and is not considered further here (see Lichtner, 1995; Lichtner et al., 1996).

As is apparent from the above discussion, use of the canonical form of chemical reactions greatly reduces the number of partial differential equations necessary to solve to N_c rather than N corresponding to the total number of species in the system. For a multicomponent system this can be a considerable reduction in the number of partial differential equations.

Partial Equilibrium System

For a system in which some of the aqueous reactions are described by kinetic rate laws, additional partial differential equations are required, one for each kinetic reaction (Lichtner, 1995). Assuming that the first $N_R^{\rm eq}$ reactions in Eqn.(10) may be considered in local equilibrium and remaining reactions described by kinetic rates laws of the form of Eqn.(68), the transport equations become

$$\widehat{\mathcal{L}}C_i \;=\; \sum_{r=1}^{N_R^{\rm eq}} \nu_{ir}^{\rm eq} I_r^{\rm eq} + \sum_{r=N_R^{\rm eq}+1}^{N_R} \nu_{ir}^{\rm kin} I_r^{\rm kin}, \quad (i=1,\ldots,N), \tag{95}$$

where the differential operator $\widehat{\mathcal{L}}$ defined by

$$\widehat{\mathcal{L}}C_i \;=\; \frac{\partial}{\partial t}\left(\phi C_i\right) + \boldsymbol{\nabla}\cdot\boldsymbol{J}_i, \tag{96}$$

has been introduced. Superscripts 'eq' and 'kin' have been added to distinguish between local equilibrium and kinetic reactions. The reaction rates $I_r^{\rm eq}$ for the local equilibrium reactions are unknowns and can be eliminated in favor of mass action equations. To do this, $N_R^{\rm eq}$ solute species are selected such that the stoichiometric matrix $\nu_{ir}^{\rm eq}$ is a square, nonsingular matrix and hence can be inverted. This is always possible provided the set of chemical reactions are linearly independent. This prescription leads to a partitioning of the N solute species into $N_c = N - N_R^{\rm eq}$ primary species and $N_R^{\rm eq}$ secondary species. In this case because $N_R^{\rm eq} < N_R$, there are fewer secondary species and a greater number of primary species compared to the case when all reactions are described by local equilibrium conditions. Writing separate statements of Eqn.(95) for primary and secondary species gives

$$\widehat{\mathcal{L}}C_l \;=\; \sum_{r=1}^{N_R^{\rm eq}} \nu_{lr}^{\rm eq} I_r^{\rm eq} + \sum_{r=N_R^{\rm eq}+1}^{N_R} \nu_{lr}^{\rm kin} I_r^{\rm kin}, \quad (l=1,\ldots,N_c), \tag{97a}$$

and

$$\widehat{\mathcal{L}}C_i \;=\; \sum_{r=1}^{N_R^{\rm eq}} \nu_{ir}^{\rm eq} I_r^{\rm eq} + \sum_{r=N_R^{\rm eq}+1}^{N_R} \nu_{ir}^{\rm kin} I_r^{\rm kin}, \quad (i = N_c+1,\ldots,N). \tag{97b}$$

Solving the second set of transport equations for the local equilibrium reaction rates $I_r^{\rm eq}$ yields

$$I_r^{\rm eq} \;=\; \sum_i (\nu^{\rm eq})^{-1}_{ri} \left[\widehat{\mathcal{L}}C_i - \sum_{r'} \nu_{ir'}^{\rm kin} I_{r'}^{\rm kin} \right]. \tag{98}$$

Substituting this result into Eqn.(97a) then yields the desired result

$$\widehat{\mathcal{L}}\Psi_l \;=\; \sum_{r=N_R^{\rm eq}+1}^{N_R} \nu_{lr}^{\rm kin\prime} I_r^{\rm kin}, \tag{99}$$

where Ψ_l is defined by

$$\Psi_l \;=\; C_l + \sum_i \nu_{li}^{\rm eq} C_i, \tag{100}$$

the stoichiometric matrix $\nu_{lr}^{\rm kin\prime}$ is defined by

$$\nu_{lr}^{\rm kin\prime} \;=\; \nu_{lr}^{\rm kin} + \sum_i \nu_{li}^{\rm eq} \nu_{ir}^{\rm kin}, \tag{101}$$

and where the canonical stoichiometric matrix $\nu_{li}^{\rm eq}$ is defined by an equation similar to Eqn.(14)

$$\nu_{li}^{\rm eq} \;=\; -\sum_r \nu_{lr}^{\rm eq} (\nu^{\rm eq})^{-1}_{ri}. \tag{102}$$

In terms of chemical reactions the primary species transport equations correspond to transforming the local equilibrium reactions to the canonical form Eqn.(13), and representing the kinetic reactions as

$$\varnothing \;\rightleftharpoons\; \sum_{r=1}^{N_c} \nu_{lr}^{\rm kin\prime} \mathcal{A}_l, \tag{103}$$

in which only primary species appear. This form of the kinetic reactions is obtained by eliminating the secondary species $\mathcal{A}_i$ from Eqn.(68) using Eqn.(13).

Simplification of the transport equations may be carried one step further by transforming the kinetic reactions in the form of Eqn.(103) to canonical form. In a similar fashion as the local equilibrium reactions, the kinetic reactions may be rewritten in the canonical form

$$\sum_j \nu_{jk}^{\rm kin} \mathcal{A}_j \;\rightleftharpoons\; \mathcal{A}_k, \tag{104}$$

based on the partitioning of primary species into the sets $\{\mathcal{A}_j\}$ and $\{\mathcal{A}_k\}$, where

$$\nu_{jk}^{\rm kin} \;=\; -\sum_r \nu_{jr}^{\rm kin} (\nu^{\rm kin})^{-1}_{rk}. \tag{105}$$

The local equilibrium reactions have the form

$$\sum_j \nu_{ji}^{\rm eq} \mathcal{A}_j + \sum_k \nu_{ki}^{\rm eq} \mathcal{A}_k \;\rightleftharpoons\; \mathcal{A}_i, \tag{106}$$

involving both sets of primary species $\{\mathcal{A}_j\}$ and $\{\mathcal{A}_k\}$. Note that it is not possible to eliminate the species $\mathcal{A}_k$ from the local equilibrium reactions because reactions (104) are kinetically controlled and mass action equations do not apply. With reactions given by Eqns.(104) and (106) the transport equations become

$$\widehat{\mathcal{L}}C_j \;=\; -\sum_i \nu_{ji}^{\rm eq} I_i^{\rm eq} - \sum_k \nu_{jk}^{\rm kin} I_k^{\rm kin}, \tag{107a}$$

$$\widehat{\mathcal{L}}C_k \;=\; I_k^{\rm kin} - \sum_i \nu_{ki}^{\rm eq} I_i^{\rm eq}, \tag{107b}$$

and

$$\widehat{\mathcal{L}}C_i \;=\; I_i^{\rm eq}. \tag{107c}$$

Eliminating the local equilibrium reaction rates using Eqn.(107c) yields the following form for the transport equations for the primary species

$$\widehat{\mathcal{L}}\Psi_j \;=\; -\sum_k \nu_{jk}^{\rm kin} I_k^{\rm kin}, \tag{108a}$$

and

$$\begin{aligned} \widehat{\mathcal{L}}\Psi_k \;&=\; I_k^{\rm kin}, \\ &=\; \sum_r \nu_{kr}^{\rm kin\prime} I_r^{\rm kin}, \end{aligned} \tag{108b}$$

where Ψ_j and Ψ_l are defined by Eqn.(100) with the appropriate species subscript. Finally eliminating the kinetic reaction rates from the first set of primary species transport equations, Eqn.(108a), yields

$$\widehat{\mathcal{L}}\left(\Psi_j + \sum_k \nu_{jk}^{\rm kin}\Psi_k\right) \;=\; 0. \tag{109}$$

The quantity in brackets on the left-hand side of Eqn.(109) can be expressed in terms of the individual species concentrations as follows

$$\begin{aligned} \Psi_j + \sum_k \nu_{jk}^{\rm kin}\Psi_k \;&=\; C_j + \sum_i \nu_{ji}^{\rm eq} C_i + \sum_k \nu_{jk}^{\rm kin} C_k + \sum_{ki} \nu_{jk}^{\rm kin}\nu_{ki}^{\rm eq} C_i, \\ &=\; C_j + \sum_i \widetilde{\nu}_{ji} C_i + \sum_k \nu_{ki}^{\rm eq} C_k, \end{aligned} \tag{110}$$

where

$$\widetilde{\nu}_{ji} \;=\; \nu_{ji}^{\rm eq} + \sum_k \nu_{jk}^{\rm kin}\nu_{ki}^{\rm eq}. \tag{111}$$

Note that the reaction rates $I_k^{\rm kin}$ involve a sum of elementary rates $I_r^{\rm kin}$ as in Eqn.(108b) and thus are no longer elementary themselves. Equations (109) and (108b) represent a coupled set of nonlinear reactive transport equations which when combined with the mass action equations for homogeneous local equilibrium reactions can be solved for the primary species concentrations.

Homogeneous and Heterogeneous Reactions

Adding mineral precipitation/dissolution to the set of homogeneous reactions (104) and (106) leads to additional reactions which are assumed to have the canonical form

$$\sum_j \nu_{jm}\mathcal{A}_j + \sum_k \nu_{km}\mathcal{A}_k \;\rightleftharpoons\; \mathcal{M}_m, \tag{112}$$

for the mth mineral $\mathcal{M}_m$ with reaction rate I_m. The mass conservation equations for the primary species for a system in partial equilibrium can now be written in the form

$$\widehat{\mathcal{L}}\left(\Psi_j + \sum_k \nu_{jk}^{\rm kin}\Psi_k\right) \;=\; -\sum_m \widetilde{\nu}_{jm} I_m, \tag{113}$$

where

$$\widetilde{\nu}_{jm} \;=\; \nu_{jm} + \sum_k \nu_{jk}^{\rm kin}\nu_{km}, \tag{114}$$

and

$$\widehat{\mathcal{L}}\Psi_k \;=\; I_k^{\rm kin} - \sum_m \nu_{km} I_m. \tag{115}$$

The mineral reaction rate could be determined either through a kinetic rate law or under conditions of local equilibrium. Mineral mass transfer equations have the form

$$\frac{\partial \phi_m}{\partial t} \;=\; \overline{V}_m I_m, \tag{116}$$

where ϕ_m denotes the mth mineral volume fraction with molar volume $\overline{V}_m$. The mineral volume fractions may be related to the porosity by the equation

$$\phi \;=\; 1 - \sum_m \phi_m. \tag{117}$$

As self-evident as this equation may seem, it is based on some far-reaching assumptions. For one to use the porosity calculated by this relation it is necessary to assume that the total porosity is identical to the connected or flow porosity. Furthermore, the relation assumes that the intrinsic porosity associated with a mineral phase is zero.

There are two fundamental distinctions to be made between the mass action equations for homogeneous reactions and those for heterogeneous reactions. Considering reactions between pure phases (solid solutions are not considered in what follows), the thermodynamic activity of the phase may always be chosen as unity by appropriate choice of standard state (Denbigh, 1981). Equilibrium between the different phases requires that their chemical potentials be equal. Equilibrium between a pure solid and an aqueous solution limits the degrees of freedom in the aqueous solution, but does not place any limitation on the amount of solid that must be present. For homogeneous reactions the mass action equations lead directly to a relationship between the concentrations (or more precisely activities) of the reacting species as in Eqn.(94). By contrast, for heterogeneous reactions, because of the moving boundary aspect of the problem, local equilibrium of the mth mineral yields an inequality for the mass action equation

$$K_m \prod_{j=1}^{N_c} (\gamma_j C_j)^{\nu_{jm}} \prod_{k=1}^{N_c'} (\gamma_k C_k)^{\nu_{km}} \leq 1. \tag{118}$$

Equality holds in regions of the host rock where the mineral in question is present. Where the mineral is not present, the inequality applies. In regions where the mineral is present, the mass action equation provides a single relation among the concentrations of the primary species, which are thus no longer independent. Assuming local equilibrium of both homogeneous and heterogeneous reactions, the primary species transport equations can be expressed in terms of the mineral volume fractions as

$$\frac{\partial}{\partial t}\left(\phi\Psi_j + \sum_m \nu_{jm}\overline{V}_m^{-1}\phi_m\right) + \boldsymbol{\nabla}\cdot\boldsymbol{\Omega}_j \;=\; 0, \tag{119}$$

in which all reaction rates have been eliminated. The unknowns are the concentrations of the primary species C_j and the mineral volume fractions ϕ_m. An equal number of equations are provided by the mineral and aqueous species mass action equations and the primary species transport equations.

Because of the inequality nature of the mineral mass action equations, in practice it is often easier to simply employ sufficiently fast kinetic rate constants to approximate conditions of local equilibrium. In this respect it is important to distinguish between local equilibrium on a macroscale and on a microscale. Macroscale refers to the continuum scale of the representative elemental volume on which the macroscopic transport equations are based. Microscale refes to the pore scale of the porous medium. For very fast reactions, such as calcite or brucite for example, reaction rates may be so fast as to result in concentration gradients within an individual pore volume (Murphy et al., 1989). In such a situation the concentration at the surface of the reacting mineral is no longer the same as the bulk fluid composition. The formulation of such reactions lies outside the scope of the single continuum model.

The mass conservation equations for aqueous species and minerals consistent with reactions (104), (106) and (112) have the form of Eqns.(109), (108b) and (116). These equations combined with initial and boundary conditions and various constitutive relations fully determine the time evolution of the system. The constitutive relations provide kinetic rate laws for the redox reactions (104) and mineral reactions (112), and mass action equations for local equilibrium reactions (106).

With homogeneous kinetic reactions written in the form of Eqn.(104), it is easy to switch from local equilibrium to kinetic controlled reaction rates. Thus if the reaction involving the kth species is to be described by local equilibrium, the transport equation, Eqn.(109), is eliminated and replaced by the corresponding mass action equation in the form of Eqn.(94). The reaction rate can be determined from Eqn.(98) once the transport equations have been solved. The transport equations given by Eqns.(109), (108b), and (116) have the desired form for incorporating either kinetic or local equilibrium descriptions of reactions.

Basis Transformation

As stated above the choice of basis species is arbitrary provided only that basis species are restricted to the set of aqueous species so that it is possible to use the same basis over the entire computational domain, and that they indeed form a basis for the chemical system being considered. Under a basis transformation the transport equations must be expressed in terms of the new set of primary species. The transport equations may be formulated either directly from the transformed set of chemical reactions expressed in terms

of the new basis, or the transport equations themselves may be transformed to the new basis set from the old one. Either way the same end result must be obtained. The latter approach may have some advantages over the former especially if it is desired to relate various physical and chemical properties in the different bases. For a system involving homogeneous aqueous reactions in local equilibrium and heterogeneous mineral reactions, the mass transport equations can be written in matrix form as

$$\widehat{\mathcal{L}}\boldsymbol{\Psi} \;=\; -\boldsymbol{\nu}_M \boldsymbol{I}_M. \tag{120}$$

The column vector $\boldsymbol{\Psi}$ can be expressed in matrix form as

$$\begin{aligned}\boldsymbol{\Psi} \;&=\; \boldsymbol{C_B} + [\boldsymbol{\Gamma}^T, \boldsymbol{\nu}] \begin{bmatrix} \boldsymbol{C_{B'}} \\ \boldsymbol{C_S} \end{bmatrix}, \\ &=\; \boldsymbol{C_B} + \boldsymbol{\Gamma}^T \boldsymbol{C_{B'}} + \boldsymbol{\nu} \boldsymbol{C_S},\end{aligned} \tag{121}$$

where $\boldsymbol{C_B}$, $\boldsymbol{C_{B'}}$ and $\boldsymbol{C_S}$ refer to column vectors composed of the concentrations of the old and new basis species and secondary species common to the two basis sets, respectively. Multiplying through by the matrix $(\boldsymbol{\Gamma}^T)^{-1}$ gives

$$\begin{aligned}(\boldsymbol{\Gamma}^T)^{-1}\boldsymbol{\Psi} \;&=\; (\boldsymbol{\Gamma}^T)^{-1}\boldsymbol{C_B} + \boldsymbol{C_{B'}} + (\boldsymbol{\Gamma}^T)^{-1}\boldsymbol{\nu}\boldsymbol{C_S}, \\ &=\; \boldsymbol{C_{B'}} + [(\boldsymbol{\Gamma}^{-1})^T, (\boldsymbol{\Gamma}^{-1})^T\boldsymbol{\nu}] \begin{bmatrix} \boldsymbol{C_B} \\ \boldsymbol{C_S} \end{bmatrix}.\end{aligned} \tag{122}$$

The latter expression will be recognized as the definition of $\boldsymbol{\Psi}'$, the definition of $\boldsymbol{\Psi}_j$ expressed in terms of the new basis set. Thus

$$\boldsymbol{\Psi}' \;=\; (\boldsymbol{\Gamma}^{-1})^T\boldsymbol{\Psi}, \tag{123}$$

recalling that $(\boldsymbol{\Gamma}^T)^{-1}$=$(\boldsymbol{\Gamma}^{-1})^T$, i.e. the transpose and inverse operations commute. With this result it is a simple manner to transform the mass transport equations. It follows that

$$\widehat{\mathcal{L}}(\boldsymbol{\Gamma}^{-1})^T\boldsymbol{\Psi} \;=\; -(\boldsymbol{\Gamma}^{-1})^T\boldsymbol{\nu}_M\boldsymbol{I}_M, \tag{124}$$

obtained by multiplying Eqn.(120) through by $(\boldsymbol{\Gamma}^{-1})^T$. Thus the following desired result for the transformed transport equations is obtained

$$\widehat{\mathcal{L}}\boldsymbol{\Psi}' \;=\; -\boldsymbol{\nu}'_M\boldsymbol{I}_M, \tag{125}$$

with $\boldsymbol{\nu}'_M$ defined in Eqn.(36). Note that the mineral reaction rates $\boldsymbol{I}_M$ are independent of the choice of basis species. This is not true, however, for the rates of some of the homogeneous reactions. Denoting the rates of reactions (22) and (26) by $\boldsymbol{I_{B'}}$ and $\boldsymbol{I_B}$, respectively, it follows that

$$\boldsymbol{I_{B'}} \;=\; (\boldsymbol{\Gamma}^{-1})^T\boldsymbol{I_B}. \tag{126}$$

The rates of the remaining reactions for the secondary species $\boldsymbol{S}$ common to both bases are also independent of the choice of basis species.

It follows that the overall reaction, determined by summing the homogeneous and heterogeneous reactions multiplied by their respective reaction rates, is independent of the choice of basis species. The overall reaction may be expressed in matrix form as

$$\boldsymbol{B}^T\left(\boldsymbol{\nu}_M\boldsymbol{I}_M + \boldsymbol{\nu}\boldsymbol{I_S} + \boldsymbol{\Gamma}^T\boldsymbol{I_{B'}}\right) - \boldsymbol{S}^T\boldsymbol{I_S} - \boldsymbol{B'}^T\boldsymbol{I_{B'}} \;\rightleftharpoons\; \boldsymbol{M}^T\boldsymbol{I}_M. \tag{127}$$

Exchanging the roles of $\boldsymbol{B}$ and $\boldsymbol{B}'$ using the relation

$$\boldsymbol{B}^T \rightleftharpoons \boldsymbol{B}'^T(\boldsymbol{\Gamma}^{-1})^T, \tag{128}$$

which follows from Eqn.(26), and taking into account the transformation of the homogeneous reaction rates according to Eqn.(126), yields the equivalent overall reaction expressed in terms of the new basis set

$$\boldsymbol{B}'^T\left(\boldsymbol{\nu}'_M\boldsymbol{I}_M+\boldsymbol{\nu}'\boldsymbol{I}_{\boldsymbol{S}}+\boldsymbol{\Gamma}^T\boldsymbol{I}_{\boldsymbol{B}}\right)-\boldsymbol{S}^T\boldsymbol{I}_{\boldsymbol{S}}-\boldsymbol{B}^T\boldsymbol{I}_{\boldsymbol{B}} \rightleftharpoons \boldsymbol{M}^T\boldsymbol{I}_M. \tag{129}$$

Changes in pH and oxygen fugacity, as examples, can lead to very different sets of dominant species in different regions of space and at different times. For example, part of the system may be under oxidizing conditions, and another part reducing. Nevertheless, the transport equations may be solved using a single set of basis species regardless of how small the concentrations of the primary species become. This is achieved numerically by solving for the logarithms of the concentrations (Lichtner, 1992), rather than directly for the concentrations themselves. In this way, for example, a complete redox ladder made up of a sequence of distinct redox states can be described using a single set of basis species to represent all possible reactions in the system.

SINGLE COMPONENT SYSTEM

In this section the reactive transport equations are applied to the simplest system possible, that of a single component reacting with a solid phase with linear kinetics. First flow in a one-dimensional porous medium is considered, and the question of validity of the local equilibrium approximation is addressed. This is followed by a two-dimensional problem involving fracture-matrix chemical interaction.

One-Dimensional Porous Medium

A single aqueous species is allowed to react with a solid phase according to the reaction

$$\mathcal{A} \rightleftharpoons \mathcal{A}_{(s)}. \tag{130}$$

An example of such a system is the system SiO_2 + H_2O reacting with quartz. Rimstidt and Barnes (1980) have shown that the rate law for the dissolution of quartz may be assumed to be linear of the form

$$I = -ks\left[1-KC\right], \tag{131}$$

with rate constant k, specific surface area s, and equilibrium constant K corresponding to the reaction as written in Eqn.(130). The equilibrium concentration $C_{\rm eq}$ of the solute is thus

$$C_{\rm eq} = K^{-1}. \tag{132}$$

It is convenient to rewrite the reaction rate in the form

$$I = k's\left(C-C_{\rm eq}\right). \tag{133}$$

The relation between k and k' is

$$k = k'C_{\rm eq}. \tag{134}$$

With this rate law the volume averaged solute mass transport equation describing advective and diffusive transport and reaction with the solid porous medium is given by

$$\phi\frac{\partial C}{\partial t} - \phi D\frac{\partial C}{\partial x^2} + v\frac{\partial C}{\partial x} \;=\; ks\left[1 - KC\right]. \tag{135}$$

To solve this equation it is necessary to impose the appropriate initial and boundary conditions. The initial conditions set the concentration at time t=0 over all space, for example, equal to the equilibrium concentration of the solid

$$C(x,\, t = 0) \;=\; C_{\rm eq}. \tag{136}$$

The boundary conditions specify the concentration or flux at either end of the flow domain. For example, at the inlet defined by x=0 the concentration is set to some value C_0:

$$C(x = 0,\, t) \;=\; C_0. \tag{137}$$

At the outlet one might impose a zero gradient boundary condition:

$$\lim_{x\to\infty}\frac{\partial C}{\partial x}(x,\, t) \;=\; 0. \tag{138}$$

This boundary condition allows flow of solute to take place across the boundary, but not diffusion.

To simplify the analysis it is assumed that the porosity changes only slightly during reaction and thus may be assumed constant. The case where both the porosity and permeability are allowed to change with reaction can give rise to instabilities in the reaction front (Lichtner, 1996) which is not considered here. With these assumptions a planar front is obtained. It should be kept in mind that this need not, and in fact does not, often correspond to reality. However, it is useful to first understand the simple, albeit unrealistic, case of constant porosity and fluid flow velocity.

To investigate the question of validity of local chemical equilibrium for describing this system, it is necessary to determine the path length over which the aqueous solution comes to equilibrium with respect to the solid. Local equilibrium is defined by requiring that this length be some small distance, for example characterized by the pore size. To determine this length dimensionless variables x' and t' are introduced defined by

$$x' \;=\; \frac{x}{l}, \tag{139}$$

and

$$t' \;=\; \frac{Dt}{l^2}, \tag{140}$$

where l represent the length scale in question. The dimensionless concentration C' is also introduced defined by

$$C' \;=\; \frac{C - C_{\rm eq}}{C_0 - C_{\rm eq}}, \tag{141}$$

where C_0 denotes the injected concentration at one end of the porous column. Transforming the partial differential equation Eqn.(135) to the new variables, after some manipulation, yields

$$\frac{\partial C'}{\partial t'} - \frac{\partial C'}{\partial x'^2} + \mathrm{Pe}\,\frac{\partial C'}{\partial x'} \;=\; \mathrm{Da}\,C'. \tag{142}$$

In this equation Pe denotes the Peclet number defined by

$$\mathrm{Pe} \;=\; \frac{vl}{\phi D}, \tag{143}$$

and Da denotes the Damköhler number defined by (Damköhler, 1936)

$$\mathrm{Da} \;=\; \frac{ksl^2}{\phi D C_{\mathrm{eq}}} \;=\; \frac{k's l^2}{\phi D}. \tag{144}$$

As can be seen from Eqn.(142), the partial differential equation involves only two dimensionless parameters: the Peclet number Pe and the Damköhler number Da. By investigating how the solution behaves as a function of these two parameters it should be possible to map out regions in $\mathrm{Pe}-\mathrm{Da}$ space where local equilibrium applies.

To simplify the problem even further, focus on the stationary state solution to Eqn.(142) (Lichtner, 1988). Neglecting the partial time derivative the partial differential becomes the ordinary differential equation

$$\frac{d^2C'}{dx'^2} - \mathrm{Pe}\frac{dC'}{dx'} + \mathrm{Da}C' \;=\; 0, \tag{145}$$

with boundary conditions

$$C'(0) \;=\; 1, \quad C'(\infty) \;=\; 0. \tag{146}$$

Note that to determine the stationary state solution initial conditions are not required. Substituting a solution of the form of a simple exponential function

$$C' \;=\; \mathrm{e}^{-q'x'}, \tag{147}$$

which satisfies Eqn.(146), yields a quadratic equation for q':

$$q'^2 + \mathrm{Pe}\, q' - \mathrm{Da} \;=\; 0. \tag{148}$$

This has the single physically possible solution

$$q'(\mathrm{Pe},\, \mathrm{Da}) \;=\; \frac{1}{2}\left[\sqrt{\mathrm{Pe}^2 + 4\,\mathrm{Da}} - \mathrm{Pe}\right]. \tag{149}$$

Notice that if there is no reaction (Da=0), then q' vanishes and the concentration is constant equal to the inlet concentration C_0. This result is the only stationary state solution for the nonreactive transport problem in an infinitely long system. There are two limiting cases to consider: $\mathrm{Pe} \gg \mathrm{Da}$, and $\mathrm{Pe} \ll \mathrm{Da}$. It follows that

$$q'(\mathrm{Pe},\, \mathrm{Da}) \;=\; \begin{cases} \sqrt{\mathrm{Da}}, & (\mathrm{Da} \gg \mathrm{Pe}), \\ \\ \mathrm{Da}/\mathrm{Pe}, & (\mathrm{Pe} \gg \mathrm{Da}). \end{cases} \tag{150}$$

From the definitions of Pe and Da, the expression for q' is equal to the ratio

$$\frac{\mathrm{Da}}{\mathrm{Pe}} \;=\; \frac{ksl}{vC_{\mathrm{eq}}}, \tag{151}$$

which is independent of the porosity and diffusion coefficient.

With these results it is now possible to answer the question when is the system described by conditions of local equilibrium. The complete stationary state solution is given by

$$C(x;\,\mathrm{Pe},\,\mathrm{Da}) \;=\; (C_0 - C_{\mathrm{eq}})\;\mathrm{e}^{-q(\mathrm{Pe},\,\mathrm{Da})\,x} + C_{\mathrm{eq}}, \tag{152}$$

where the quantity q related to q' by

$$q \;=\; \frac{q'}{l}, \tag{153}$$

is introduced to express the solution in terms of actual distance. The inverse of q is referred to as the equilibration length λ. In symbols

$$\lambda \;=\; q^{-1}. \tag{154}$$

The equilibration length provides a measure of the distance required for the aqueous solution to come to equilibrium with the solid. It is apparent that the solute concentration is close to equilibrium over the characteristic length $\lambda{\sim}l$ ($x'{=}1$), provided the first term on the right hand side of Eqn.(152) is close to zero. This will occur provided $q'(\mathrm{Pe},\,\mathrm{Da}){\sim}1$. Thus it is possible by plotting q' as a function of the variables Pe and Da to map out the regions where $q'{>}1$ and $q'{<}1$. The former region corresponds to local equilibrium and the latter to surface controlled reaction. The results are exhibited in Figure 1. It is interesting to note that the Damköhler number alone does not determine whether the reaction rate is surface or transport controlled, unless there is no advection. For sufficiently large Peclet numbers it is possible for $q'{<}1$ even for Damköhler numbers much larger than one. For pure diffusive transport, a Damköhler number of one corresponds to $q'{=}1$.

It is important to distinguish between micro- and macroscales when referring to the concept of local equilibrium. Here microscale refers to the pore scale and macroscale to the continuum scale which is an average over many pore volumes. The limit as the rate constant approaches infinity in the continuum formulation refers to macroscale local equilibrium. At this scale each REV attains thermodynamic equilibrium; however, any particular REV is generally in disequilibrium with its neighbors. This is quite different from local equilibrium on a microscale for which the detailed pore geometry plays a role. It must be kept in mind that it is meaningless within the continuum framework to use a kinetic rate constant which gives an equilibration length that is smaller than the characteristic length associated with a REV. For microscale local equilibrium the pore geometry must be taken into account in the calculations. This becomes a very difficult task especially if the computation domain is at the macroscale.

Fracture-Matrix Interaction

Many circumstances involving fluid flow and transport in natural systems involve flow through fractures accompanied by diffusion into the surrounding rock matrix. Of interest is the extent to which the rock matrix and fracture fluids are altered by their mutual interaction. As a result of this interaction, mineral products are formed in the matrix and as fracture fillings, possibly causing sealing or opening of the matrix and fractures to further transport of solute species. Recently this situation has been investigated by Steefel and Lichtner (1997) for the situation of infiltration of a hyperalkaline fluid emanating from a cementitious barrier into a fracture.

For the geometry shown in Figure 2, flow through a single fracture with simultaneous diffusion into the adjacent rock matrix can be represented by the coupled partial differential

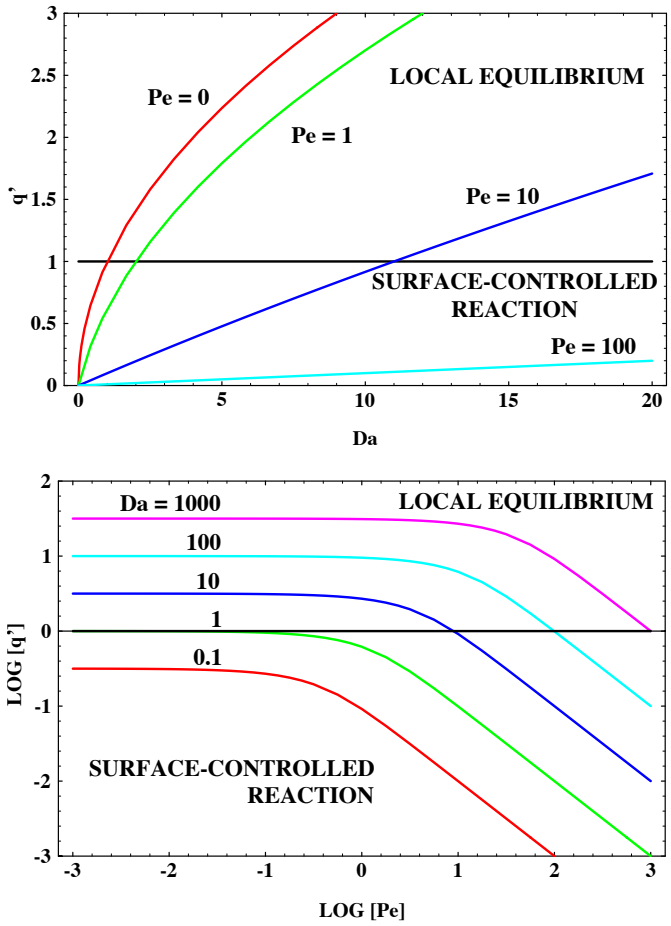

Figure 1. Regions of surface-controlled reaction and local equilibrium for different Damköhler and Peclet numbers separated by the horizontal line $q' = 1$.

equations

$$\frac{\partial C_f}{\partial t} + v_f \frac{\partial C_f}{\partial z} - s_f \phi D \frac{\partial C_m}{\partial x}\bigg|_{x=\delta} = -k s_f \left(C_f - C_{\text{eq}}\right), \tag{155a}$$

for the fracture, and

$$\frac{\partial}{\partial t}\left(\phi C_m\right) - \phi D \frac{\partial^2 C_m}{\partial x^2} = -k s_m \left(C_m - C_{\text{eq}}\right), \tag{155b}$$

for the matrix, where

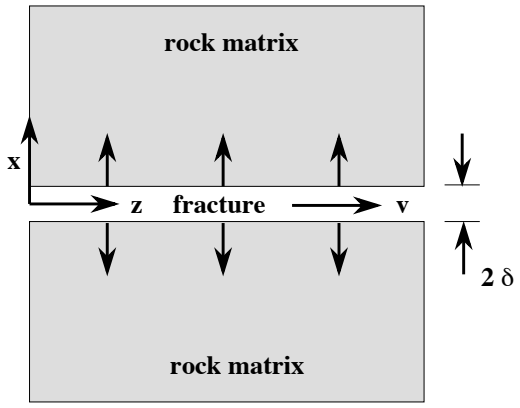

Figure 2. Geometry and definition of coordinate system used in the fracture-matrix interaction problem.

z = coordinate along the length of the fracture [L],
x = coordinate perpendicular to fracture [L],
t = time [T],
v_f = groundwater velocity in the fracture [L/T],
C_f = solute concentration in fracture [mole/L^3],
C_m = solute concentration in rock matrix [mole/L^3],
ϕ = rock matrix porosity [dimensionless],
k = mineral kinetic rate constant [L/T],
D = effective matrix diffusion coefficient [L^2/T],
s_f = fracture surface area per unit fracture volume [1/L],
s_m = matrix surface area per unit bulk matrix volume [1/L],

A linear kinetic rate expression is used for the fracture and matrix. The fracture surface area per unit fracture volume is equal to the reciprocal of half the fracture aperture 2δ

$$s_f \;=\; \frac{1}{\delta}. \tag{156}$$

The third term on the left-hand side of Eqn.(155a) represents the flux from the matrix into the fracture coupling the fracture and matrix equations. The matrix transport equation is coupled to the fracture equation by the boundary condition

$$C_m(0,\, t;\, z) \;=\; C_f(z,\, t), \tag{157}$$

equating the matrix concentration at the wall rock to the concentration in the fracture along the entire fracture length. For simplicity, pure advective transport is assumed for the fracture equation, and diffusion in the matrix is required to take place in the direction perpendicular to the fracture. Steefel and Lichtner (1997) consider the general case by solving the transport equations numerically for a multicomponent system.

To solve the fracture and matrix transport equations the initial fluid concentrations in the fracture and matrix, and the initial mineral concentration in the matrix must be specified. In addition boundary conditions must be specified at the inlet and outlet to the fracture

and at the boundary of the matrix, normally taken as zero concentration gradient at the symmetry plane between two fractures. These conditions can be represented by the equations

$$C_f(z,\,0) = C_f^{\infty}, \tag{158a}$$

$$C_m(x,\,0;\,z) = C_m^{\infty}, \tag{158b}$$

$$C_f(0,\,t) = C_f^{0}, \tag{158c}$$

$$\frac{\partial C_f}{\partial z}(\infty,\,t) = 0, \tag{158d}$$

$$\frac{\partial C_m}{\partial x}(d/2,\,t) = 0, \tag{158e}$$

where d denotes the fracture spacing. With these initial and boundary conditions an analytical solution exists to the transient transport equations (Tang et al., 1981; Steefel and Lichtner, 1997).

Stationary State Solution. To study the qualitative nature of the solution to these equations it is instructive to consider the stationary state solution. To this end the transport equations are first written in terms of dimensionless independent variables corresponding to distances x' and z' and time t' defined in terms of the fracture aperture as the characteristic length scale as

$$x' \;=\; \frac{x}{\delta}, \quad z' \;=\; \frac{z}{\delta}, \quad \text{and } t' \;=\; \frac{Dt}{\delta^2}. \tag{159}$$

New concentration variables are defined as

$$C_f' \;=\; C_f - C_{\rm eq}, \tag{160a}$$

and

$$C_m' \;=\; C_m - C_{\rm eq}. \tag{160b}$$

With these new variables the transport equations become

$$\frac{\partial C_f'}{\partial t'} + \mathrm{Pe}\frac{\partial C_f'}{\partial z'} - \left.\frac{\partial C_m'}{\partial x'}\right|_{x'=1} \;=\; -\mathrm{Da}_f C_f', \tag{161a}$$

for the fracture, and

$$\frac{\partial C_m'}{\partial t'} - \frac{\partial^2 C_m'}{\partial x'^2} \;=\; -\mathrm{Da}_m C_m', \tag{161b}$$

for the matrix. The dimensionless constants, the Peclet number Pe, and Damköhler numbers Da_f and Da_m, are defined by

$$\mathrm{Pe} \;=\; \frac{v_f \delta}{\phi D}, \tag{162}$$

and

$$\mathrm{Da}_f \;=\; \frac{k\delta}{\phi D}, \tag{163a}$$

$$\mathrm{Da}_m \;=\; \frac{k s_m \delta^2}{\phi D}. \tag{163b}$$

These dimensionless constants are not independent. The two Damköhler numbers are related by the ratio of the matrix and fracture surface areas

$$\mathrm{Da}_m \;=\; \frac{s_m}{s_f}\mathrm{Da}_f. \tag{164}$$

The Peclet number and fracture Damköhler number are related by the expression

$$\mathrm{Pe} \;=\; \frac{v_f}{k}\mathrm{Da}_f. \tag{165}$$

The stationary state solution, obtained by ignoring the time derivative terms in the transport equations, is separable into a product of two functions, one which depends only on z and the other only on x. This is not the case generally for the transient solution, however. The resulting solution is given by

$$C'_f(z') \;=\; (C_0 - C_{\mathrm{eq}})\,\mathrm{e}^{-z'/\lambda'_f}, \tag{166a}$$

and

$$\begin{aligned} C'_m(x',\,z') &= C'_f(z')\exp\left[-\frac{x'-1}{\lambda'_m}\right], \\ &= (C_0 - C_{\mathrm{eq}})\exp\left[-\left(\frac{-z'}{\lambda'_f} + \frac{x'-1}{\lambda'_m}\right)\right]. \end{aligned} \tag{166b}$$

The boundary conditions are satisfied for both of these expressions provided the fracture spacing is infinite $d{\rightarrow}\infty$, i.e. only a single fracture is considered. The case of finite fracture spacing is considered in more detail below. The quantities λ'_f and λ'_m refer to dimensionless equilibration lengths in the fracture and rock matrix, respectively. The matrix equilibration length is defined similarly to Eqn.(150) for pure diffusion as

$$\lambda'_m \;=\; \frac{1}{\sqrt{\mathrm{Da}_m}}. \tag{167}$$

The fracture equilibration length also involves λ'_m according to the expression

$$\lambda'_f \;=\; \frac{1}{\dfrac{1}{\lambda_f^{0\prime}} + \dfrac{1}{\mathrm{Pe}\lambda'_m}}, \tag{168}$$

where $\lambda_f^{0\prime}$ refers to the fracture equilibration length in the absence of interaction with the matrix

$$\lambda_f^{0\prime} \;=\; \frac{v_f}{k}. \tag{169}$$

As might have been anticipated, a wedge-shaped concentration profile in the matrix is obtained. Remarkable is that the slope of equal concentration contours are given by the simple form as the ratio of the equilibration lengths in the matrix and fracture (Steefel and Lichtner, 1997)

$$\mathrm{slope} \;=\; \frac{dx}{dz} \;=\; \frac{\lambda_m}{\lambda_f}. \tag{170}$$

The slope can be expressed in terms of the dimensionless Peclet and matrix Damköhler numbers as

$$\frac{dx}{dz} \;=\; \frac{1}{\mathrm{Pe}}\left(1 + \frac{1}{s_m\delta}\sqrt{\mathrm{Da}_m}\right). \tag{171}$$

As discussed by Steefel and Lichtner (1997) for a sufficiently large value of the Peclet number the slope becomes zero and the equiconcentration contour lines are parallel to the fracture. This situation is indicative of weak interaction between fracture and matrix. In the

opposite extreme for $\mathrm{Da}_m \gg 1$, the slope approaches a very large number and the equiconcentration contour lines become perpendicular to the fracture. In this case strong coupling exists between the fracture and matrix. In this latter case the dual porosity system consisting of fracture and matrix may be replaced by a single porosity system greatly simplifying the problem.

Finite Fracture Spacing. For equally spaced fractures with separation distance d it is necessary to take into account the no flow boundary condition at the symmetry plane between fractures given by Eqn.(158e). This leads to the following stationary state solution for the matrix concentration

$$C'_m(x',\, z') \;=\; C'_f(z') \frac{\cosh\left[\dfrac{x' - d/2\delta}{\lambda'_m}\right]}{\cosh\left[\dfrac{1 - d/2\delta}{\lambda'_m}\right]}, \tag{172}$$

where cosh denotes the hyperbolic cosine function defined as $\cosh(x) = (\mathrm{e}^x + \mathrm{e}^{-x})/2$. The fracture coupling term evaluates to

$$\left.\frac{dC'_m}{dx'}\right|_{x'=1} \;=\; \frac{1}{\lambda'_m} \tanh\left[\frac{1 - d/2\delta}{\lambda'_m}\right] C'_f(z'), \tag{173}$$

defined in terms of the hyperbolic tangent $\tanh(x) = (\mathrm{e}^x - \mathrm{e}^{-x})/(\mathrm{e}^x + \mathrm{e}^{-x})$. With this result the stationary state fracture transport equation can be expressed as

$$\mathrm{Pe} \frac{dC'_f}{dz'} \;=\; -\left\{ \mathrm{Da}_f + \frac{1}{\lambda'_m} \tanh\left[\frac{1 - d/2\delta}{\lambda'_m}\right] \right\} C'_f. \tag{174}$$

An effective rate term appears on the right-hand side which accounts for interaction with the rock matrix.

For the situation when the matrix equilibration length is much larger than the fracture spacing ($\lambda_m \gg d \gg \delta$), the coupling term reduces to

$$\begin{aligned} \left.\frac{dC'_m}{dx'}\right|_{x'=1} &= \frac{1}{{\lambda'_m}^2} \left(1 - \frac{d}{2\delta}\right) C'_f(z'), \\ &= -\left(\frac{1 - \phi_f}{\phi_f}\right) \mathrm{Da}_m\, C'_f(z'), \end{aligned} \tag{175}$$

where the fracture porosity ϕ_f is defined by

$$\phi_f \;=\; \frac{V_f}{V_{\mathrm{REV}}} \;=\; \frac{2\delta}{d}. \tag{176}$$

Substituting this result into the stationary state fracture transport equation, multiplying through by ϕ_f and converting the equation back to dimensional form, gives

$$\phi_f v_f \frac{dC_f}{dz} \;=\; -k \left[\phi_f s_f + (1 - \phi_f)\, s_m\right] (C_f - C_{\mathrm{eq}}), \tag{177}$$

The term in square brackets on the right-hand side will be recognized as the surface area per unit bulk volume of an equivalent porous medium made up of the fracture network and rock matrix. To see this consider a REV of the fracture-matrix equivalent continuum. The

total equivalent continuum model surface area $s_{\rm ecm}$ consisting of an average of fracture and matrix surface areas can be expressed as

$$\begin{aligned} s_{\rm ecm} &= \frac{A_f + A_m}{V_{\rm REV}}, \\ &= \frac{A_f}{V_f}\frac{V_f}{V_{\rm REV}} + \frac{A_m}{V_m}\frac{V_m}{V_{\rm REV}}, \\ &= \phi_f s_f + (1-\phi_f) s_m, \end{aligned} \tag{178}$$

noting that

$$\begin{aligned} \frac{V_m}{V_{\rm REV}} &= \frac{V_{\rm REV} - V_f}{V_{\rm REV}}, \\ &= 1 - \phi_f. \end{aligned} \tag{179}$$

The flow velocity appearing on the left-hand side of Eqn.(177) will be recognized as the Darcy velocity in the equivalent continuum medium. Thus in the limit when the matrix equilibration length is much larger than the fracture spacing, a description based on the dual fracture-matrix continuum can be replaced by a single continuum in which the mineral surface area is averaged over the fracture and matrix continua. This simplification can also be shown to apply to the transient transport equations in which the porosity in the single continuum transport equation $\phi_{\rm ecm}$ is taken as the average of the fracture network and matrix porosity defined as

$$\phi_{\rm ecm} \;=\; \phi_f + (1-\phi_f)\phi_m, \tag{180}$$

with ϕ_m representing the matrix porosity.

MULTICOMPONENT SYSTEMS

Parallel Linearly-Dependent Reactions

It is common for the reaction mechanism of a particular reaction to change as the environment in which the reaction takes place changes. For example, the dissolution rates of silicate minerals are often pH-dependent with hydrolysis reaction rate constants which have different pH dependencies in different pH regimes. To account for this behavior simultaneous parallel reactions which are linearly dependent are introduced (Lichtner, 1996; Steefel and MacQuarrie, 1996).

Consider the set of linearly-independent reactions represented in Eqns.(104), (106), and (112) involving species $\mathcal{A}_j$, $\mathcal{A}_k$, $\mathcal{A}_i$, and $\mathcal{M}_m$, which consist of homogeneous reactions whose rates are controlled by kinetic and local equilibrium controlled homogeneous reactions, and heterogeneous reactions. Then a set of linearly-dependent heterogeneous reactions to these reactions may be written as

$$\sum_j \nu_{jm}^{\tau} \mathcal{A}_j + \sum_k \nu_{km}^{\tau} \mathcal{A}_k \;\rightleftharpoons\; \mathcal{M}_m, \tag{181}$$

where the superscript τ labels the parallel reactions. Without loss in generality, the stoichiometric coefficient for mineral $\mathcal{M}_m$ is taken as unity. Any appearance of secondary species

$\mathcal{A}_i$ can be eliminated using the associated local equilibrium reaction. There must exist coefficients c_{km}^{τ} not all zero such that the linearly-dependent reactions can be expressed as linear combinations of the original reactions

$$\sum_j \nu_{jm}\mathcal{A}_j + \sum_k \nu_{km}\mathcal{A}_k + \sum_k c_{km}^{\tau}\left(\mathcal{A}_k - \sum_j \nu_{jk}\mathcal{A}_j\right) \rightleftharpoons \mathcal{M}_m. \tag{182}$$

The reaction coefficients can be regrouped as

$$\sum_j \left(\nu_{jm} - \sum_k \nu_{jk}c_{km}^{\tau}\right)\mathcal{A}_j + \sum_k \left(\nu_{km} + c_{km}^{\tau}\right)\mathcal{A}_k \rightleftharpoons \mathcal{M}_m. \tag{183}$$

Comparing coefficients of this reaction with Eqn.(181) implies the identities

$$\nu_{jm}^{\tau} = \nu_{jm} - \sum_k \nu_{jk}c_{km}^{\tau}, \tag{184}$$

and

$$\nu_{km}^{\tau} = \nu_{km} + c_{km}^{\tau}. \tag{185}$$

These equations relate the linearly-dependent reaction stoichiometries to the stoichiometries of the original set of linearly-independent reactions.

The mass transport equations, including the contribution from linearly-dependent reactions, now become

$$\widehat{\mathcal{L}}C_j = -\sum_i \nu_{ji}I_i - \sum_k \nu_{jk}I_k - \sum_m \nu_{jm}I_m - \sum_{\tau m} \nu_{jm}^{\tau}I_m^{\tau}, \tag{186a}$$

and

$$\widehat{\mathcal{L}}C_k = I_k - \sum_i \nu_{ki}I_i - \sum_m \nu_{km}I_m - \sum_{\tau m} \nu_{km}^{\tau}I_m^{\tau}, \tag{186b}$$

for primary species, and

$$\widehat{\mathcal{L}}C_i = I_i, \tag{186c}$$

for aqueous secondary species, and

$$\frac{\partial \phi_m}{\partial t} = \overline{V}_m\left(I_m + \sum_{\tau} I_m^{\tau}\right), \tag{186d}$$

for minerals. Eliminating the reaction rates I_i and I_k from the primary species transport equations Eqn.(186a) leads to

$$\widehat{\mathcal{L}}\left(\Psi_j + \sum_k \nu_{jk}\Psi_k\right) = -\sum_m \nu_{jm}\left(I_m + \sum_{\tau} I_m^{\tau}\right). \tag{187}$$

This relation is obtained by making use of Eqns.(184) and (185). The source/sink term in this equation involves the sum of the linearly-independent and -dependent reaction rates multiplied by the same stoichiometric coefficients ν_{jm} corresponding to the original form

of the mth mineral reaction, and does not involve the coefficients c_{km}^τ or ν_{jm}^τ. The transport equations for the remaining primary species become

$$\begin{aligned}\widehat{\mathcal{L}}\Psi_k &= I_k - \sum_m \left(\nu_{km} I_m + \sum_\tau \nu_{km}^\tau I_m^\tau \right), \\ &= I_k - \sum_m \nu_{km} \left(I_m + \sum_\tau I_m^\tau \right) - \sum_{\tau m} c_{km}^\tau I_m^\tau. \end{aligned} \tag{188}$$

In these transport equations the specific stoichiometric coefficients for the linearly-dependent reactions also enter through the coefficients c_{km}^τ.

The reaction rates for the linearly-dependent reactions are assumed to have a form similar to that of the linearly-independent mineral reactions given by

$$I_m^\tau = -k_m^\tau s_m \left[1 - K_m^\tau Q_m^\tau \right], \tag{189}$$

where the ion activity product Q_m^τ is defined by

$$Q_m^\tau = \prod_j \left(\gamma_j C_j \right)^{\nu_{jm}^\tau} \prod_k \left(\gamma_k C_k \right)^{\nu_{km}^\tau}. \tag{190}$$

The equilibrium constants for the linearly-dependent reactions K_m^τ are related to the linearly-independent equilibrium constants K_m by the equation

$$K_m^\tau = K_m \prod_k K_k^{-c_{km}^\tau}, \tag{191a}$$

or in logarithmic form

$$\log K_m^\tau = \log K_m - \sum_k c_{km}^\tau \log K_k. \tag{191b}$$

It follows after some manipulation that the products $K_m Q_m$ and $K_m^\tau Q_M^\tau$ are related by the expression

$$K_m^\tau Q_m^\tau = K_m Q_m \prod_k \left[\frac{C_k}{C_k^{\mathrm{eq}}} \right]^{c_{km}^\tau}. \tag{192}$$

The concentration C_k^{eq} is defined as the concentration of the kth primary species computed as if it were in equilibrium as derived from the mass action equation

$$C_k^{\mathrm{eq}} = \gamma_k^{-1} K_k \prod_j \left(\gamma_j C_j \right)^{\nu_{jk}}. \tag{193}$$

Making use of this relation, the total source/sink term corresponding to the jth primary species resulting from parallel linearly-dependent heterogeneous kinetic reactions can be written as

$$\begin{aligned} R_j &= -\sum_m \nu_{jm} \left(I_m + \sum_\tau I_m^\tau \right), \\ &= -\sum_m \nu_{jm} \left(k_m \left[1 - K_m Q_m \right] + \sum_\tau k_m^\tau \left[1 - K_m^\tau Q_m^\tau \right] \right) s_m. \end{aligned} \tag{194}$$

The quantities k_m, k_m^τ, are effective rate "constants" which may depend on pH, f_{O_2}, and other solution variables.

For conditions of local equilibrium among the homogeneous reactions it follows that

$$K_m^\tau Q_m^\tau \;=\; K_m Q_m, \tag{195}$$

and the source/sink term reduces to

$$R_j \;=\; -\sum_m \nu_{jm} \left(k_m + \sum_\tau k_m^\tau \right) s_m \left[1 - K_m Q_m \right]. \tag{196}$$

According to this relation the effect of adding linearly-dependent reactions is to modify the kinetic rate constants by adding an additional term for each linearly-dependent reaction. However, the stoichiometric coefficients are not affected. For the local equilibrium case the only transport equations necessary to solve are those for the primary species $\{\mathcal{A}_j\}$ and minerals. Neither of these equations contains reference to the stoichiometry of the parallel linearly-dependent reactions. Thus, in the local equilibrium case, the only effect of adding parallel, linearly-dependent reactions is to modify the reaction rates, but not the stoichiometry of the reaction coefficients appearing in the transport equations. For a kinetic representation of homogeneous aqueous reactions, however, the stoichiometric coefficients of the linearly-dependent parallel reactions enter as well in the transport equations for the kinetically reacting species, as in Eqn.(188) through the coefficients c_{km}^τ.

One application of incorporating linearly-dependent parallel reactions in the formulation of reactive mass transport equations is accounting for pH-dependent rates for mineral hydrolysis reactions (Steefel and MacQuarrie, 1996). Shown in Figure 3 is the pH dependence of the effective albite rate constant. The experimental data are fitted by the pH-dependent rate constant

$$k \;=\; k_0 + k_a a_{H^+}^{\beta_a} + k_b a_{H^+}^{\beta_b}, \tag{197}$$

with values for the various constants of $\log k_0 = -16$, $\log k_a = -13.875$, $\log k_b = -18.475$, $\beta_a = 0.5$, and $\beta_b = -0.3$ (Blum and Stillings, 1995). The subscripts a and b refer to the acidic and basic ranges of the pH dependence. This form for the fit expression can be justified by considering each term in the rate expression as resulting from a parallel linearly-dependent reaction. Note that the effective rate constant at neutral pH results form the superposition of all three parallel reactions and is not simply equal to k_0.

Oxidation–Reduction Reactions. It is not uncommon in natural systems for oxidation–reduction reactions to be kinetically controlled rather than governed by conditions of chemical equilibrium (Lindberg and Runnells, 1984). Thus to treat redox reactions properly in a reactive transport description, a kinetic formulation must often be used. An additional complication of redox reactions often involve multiple pathways, each pathway related to the oxidation state of the aqueous solution. Microbial-mediated oxidation of organic matter also involves multiple pathways (Rittmann and VanBriesen, 1996; Van Cappellen and Gaillard, 1996; Steefel and MacQuarrie, 1996). For example, a series of heterotrophic reactions occur as organic carbon is oxidized by aerobic respiration ($O_{2(aq)}$), denitrification (NO_3^-), manganese reduction ($MnO_{2(s)}$), iron III reduction ($Fe(OH)_{3(s)}$), and sulfate reduction (SO_4^{2-}). These reactions generally involve parallel linearly-dependent and -independent reactions. Furthermore, the aqueous solution is commonly not in simultaneous redox equilibrium. Other examples of multiple redox pathways include oxidation of chalcopyrite, uraninite and other redox-sensitive ore bodies.

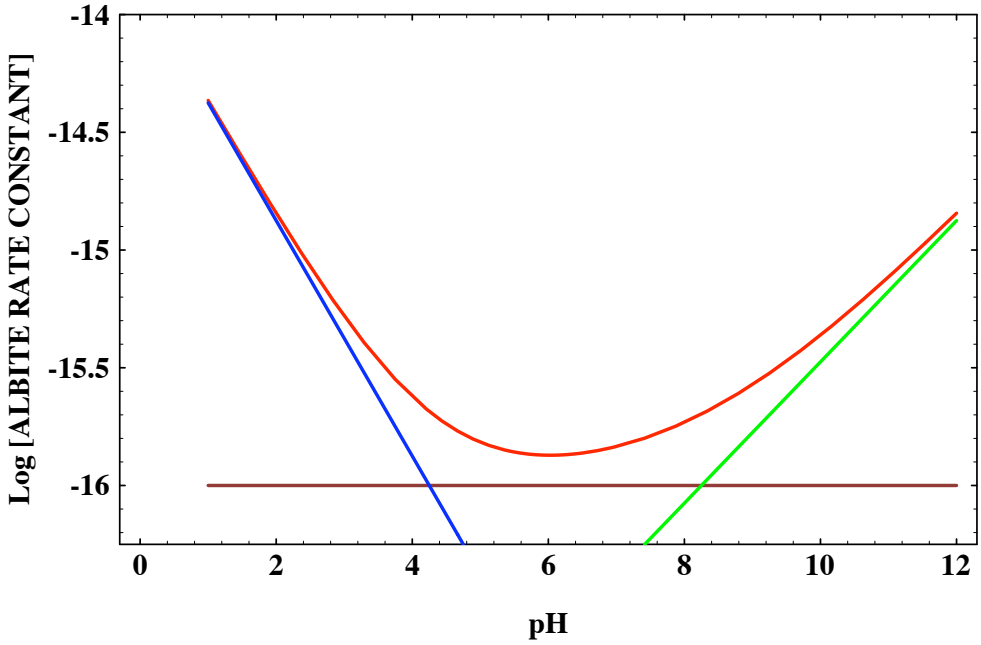

Figure 3. The pH-dependence of the albite rate constant. The blue and green lines refer to the acidic and basic rate constants, and the brown line to the neutral rate constant. The red curve is the sum of the different rate constants.

The oxidation of pyrite provides another example of parallel reactions. Pyrite may be oxidized directly by dissolved oxygen according to the reaction

$$\mathrm{Fe^{2+}} + 2\,\mathrm{SO_4^{2-}} + 2\,\mathrm{H^+} - \mathrm{H_2O} - \frac{7}{2}\,\mathrm{O_{2(aq)}} \rightleftharpoons \mathrm{FeS_2}, \tag{198a}$$

or, in the presence of $\mathrm{Fe^{3+}}$ by the reaction

$$15\,\mathrm{Fe^{2+}} - 14\,\mathrm{Fe^{3+}} + 2\,\mathrm{SO_4^{2-}} + 16\,\mathrm{H^+} - 8\,\mathrm{H_2O} \rightleftharpoons \mathrm{FeS_2}, \tag{198b}$$

in which $\mathrm{Fe^{3+}}$ acts as the oxidant. In the first reaction, primary species consist of the species $\mathrm{Fe^{2+}}$, $\mathrm{SO_4^{2-}}$, $\mathrm{O_{2(aq)}}$, $\mathrm{H^+}$, and $\mathrm{H_2O}$, whereas in the second reaction they consist of the species $\mathrm{Fe^{2+}}$, $\mathrm{Fe^{3+}}$, $\mathrm{SO_4^{2-}}$, $\mathrm{H^+}$, and $\mathrm{H_2O}$. A linear transformation can be written relating the two basis sets and therefore they provide equivalent representations of pyrite oxidation. Note that these two reactions for pyrite oxidation are linearly-dependent with the homogeneous redox reaction coupling $\mathrm{Fe^{2+}}$ and $\mathrm{Fe^{3+}}$.

Williamson and Rimstidt (1994) proposed several different forms for the oxidation rate of pyrite depending on the presence or absence of dissolved oxygen and pH. In the pH range 2–10 in the presence of dissolved oxygen the rate constant is described by

$$k \;=\; k_1\, m_{\mathrm{O_{2(aq)}}}^{0.5}\, m_{\mathrm{H^+}}^{-0.11}. \tag{199a}$$

with $\log_{10} k_1 = -12.19$. For the pH range 0.5–3, in a N_2-purged solution the rate constant has the form

$$k \;=\; k_2\, m_{\mathrm{Fe^{3+}}}^{0.3}\, m_{\mathrm{Fe^{2+}}}^{-0.47}\, m_{\mathrm{H^+}}^{-0.32}, \tag{199b}$$

with $\log_{10} k_2 = -12.58$, and when dissolved oxygen is present the form

$$k \;=\; k_3\, m_{\mathrm{Fe^{3+}}}^{0.93}\, m_{\mathrm{Fe^{2+}}}^{-0.4}, \tag{199c}$$

Table 1. Oxidation of pyrite by different iron III complexes.

$FeS_2 + 14\,Fe^{3+} + 8\,H_2O$	$\rightleftharpoons$	$15Fe^{2+} + 2\,SO_4^{2-} + 16\,H^+$
$FeS_2 + 14\,Fe(OH)^{2+}$	$\rightleftharpoons$	$15Fe^{2+} + 2\,SO_4^{2-} + 6\,H^+ + 6\,H_2O$
$FeS_2 + 14\,Fe(OH)_2^+ + 8\,H^+$	$\rightleftharpoons$	$15Fe^{2+} + 2\,SO_4^{2-} + 20\,H_2O$
$FeS_2 + 14\,Fe(OH)_3^\circ + 22\,H^+$	$\rightleftharpoons$	$15Fe^{2+} + 2\,SO_4^{2-} + 34\,H_2O$
$FeS_2 + 14\,Fe(OH)_4^- + 40\,H^+$	$\rightleftharpoons$	$15Fe^{2+} + 2\,SO_4^{2-} + 48\,H_2O$

with $\log_{10} k_3 = -10.07$. Reaction rate laws such as these could be used in parallel to provide a mechanism for pyrite oxidation over a wide range of conditions that can be expected to occur along a flow path.

The form of the overall reaction which actually occurs in a geochemical system is a complicated function of solution speciation, reaction rates and transport rates. In the case of pyrite oxidation, reaction (198b) is often quoted as resulting in more acid conditions compared to the first because of the greater number of protons produced per mole of pyrite oxidized (e.g. Langmuir, 1997). Yet when used in a reactive transport model, identical results must be obtained regardless of which reaction is used in the calculation, provided, of course, the same rate laws are used in each case. The mechanism for pyrite oxidation resulting from solving the mass conservation equations will depend, for example, on the pH which in turn determines the dominant iron species in solution, and the oxidant. Consider replacing Fe^{3+} in the reaction (198b) by various hydrolysis complexes $FeOH^{2+}$, $Fe(OH)_2^+$, $Fe(OH)_3^\circ$, and $Fe(OH)_4^-$ which become the most stable form of Fe(III) at pH values of approximately 3, 5, 8, and 9, respectively (Langmuir, 1997). One then has the reactions listed in Table 1. For the latter three reactions shown in Table 1 the pH change is reversed. Other reactions such as complexing Fe^{2+} with sulfate to form $FeSO_4^\circ$ can also affect the pH. In a reactive transport calculation neither one of these reactions would be expected to apply over the entire computational domain where pyrite was being oxidized. Rather the pH and hence complexing are expected to vary spatially and temporally, and as a consequence so would the pyrite oxidation mechanism. What is interesting about the form of the reactions listed in Table 1 is that at low pH, hydrogen ions are produced tending to lower the pH even further. Whereas at high pH hydrogen ions are consumed tending to raise the pH further. Clearly, attempting to predict the direction of change in solution composition from a single reaction can be difficult if not misleading.

For the situation of complete redox equilibrium between all redox pairs, there is no need in fact to distinguish redox reactions from any other reactions such as acid-base reactions in formulating and solving the mass conservation equations. However, to incorporate kinetic reactions between redox couples requires some care in setting up the various chemical reactions in the system—some of which involve transfer of electrons and others which do not. Once the reaction scheme is formulated, formulating the mass conservation equations corresponding to these reactions becomes a straightforward task. The situation is complicated by the requirement that reactions between redox couples are generally to be described kinetically, whereas reactions involving species in the same oxidation state are considered to be in local equilibrium.

To handle the distinction between kinetic and local equilibrium controlled reaction rates, the first step is to write reactions in which electron transfer processes are absent. The rates of these reactions are presumed to be controlled by local equilibrium. These reactions can be written in canonical form as defined previously by Eqn.(13). By construction these reactions preserve the oxidation state of each species. The set of primary species $\{\mathcal{A}_l\}$

contains all redox pairs relevant to the problem. For example, for pyrite oxidation the set of primary species includes the species $\{Fe^{2+}, Fe^{3+}, SO_4^{2-}, HS^-, S^{2-}, O_{2(aq)}\}$. Secondary species $\mathcal{A}_i$ are required to have the same oxidation state as the reactants $\mathcal{A}_l$ appearing on the left-hand side of the reaction. These reactions include reactions of the form listed in Table 2 for homogeneous local equilibrium reactions. Reactions with minerals cannot always be written in terms of aqueous species with the same oxidation state, because the oxidation state of a species in the solid may be different from that in an aqueous solution. For example, the oxidation state of sulfur in pyrite may be formally assigned the value -1, which is not present in an aqueous solution.

The second step is to combine electron transfer reactions in the aqueous phase with reactions involving species with the same oxidation state. The most general form of a reaction involving transfer of electrons can be represented as reactions between the original set of primary species $\{\mathcal{A}_l\}$ which are used to formulate nonredox reactions. Thus to reactions (13), each presumed to involve species in the identical oxidation state, are added the redox reactions of the form

$$\varnothing \rightleftharpoons \sum_l \nu_{lr}\mathcal{A}_l, \quad (r = 1, \ldots, N_{\rm rdx}). \tag{200}$$

It is assumed that there are $N_{\rm rdx}$ linearly-independent redox reactions. The canonical transformation can be applied to the redox reactions by partitioning the original set of primary species $\{\mathcal{A}_l\}$ into two arbitrary sets $\{\mathcal{A}_j, j{=}1, \ldots, N_c\}$ and $\{\mathcal{A}_k, k{=}N_c{+}1, \ldots N_p\}$ with $N_c{=}N_p{-}N_{\rm rdx}$, such that the square submatrix ν_{kr} is nonsingular. This is always possible because the reactions are presumed to be linearly independent. The resulting set of reactions are identical to Eqn.(104).

For example, one choice for the primary species $\{\mathcal{A}_j\}$ is electron donors. Then the set $\{\mathcal{A}_k\}$ consists of electron acceptors. However, any mixed set of donors and acceptors is also possible. An example of the resulting set of reactions is illustrated in Table 2 for the simple system Fe–S–H_2O. In general multiple pathways are possible for mineral reactions depending on the redox state of the aqueous solution. Several possible mineral reactions, some involving electron transfer and some not, are listed in Table 2.

Role of the Electron in Formulating Transport Equations

Redox reactions may be expressed either as half-cell reactions or as overall oxidation/reduction reactions in which the electron does not appear explicitly. The electron can be used as a primary species only if care is exercised in how it is treated in mass conservation and mass action equations. Because the electron has zero concentration in an aqueous solution, it does not contribute to the overall charge balance of the solution, the ionic strength, or to the total mass balance. The electron does, however, occur in evaluating mass action equations, the logarithm of the fictitious electron concentration providing the pe of the aqueous solution. The purpose of this section is to explore the resulting form of the mass conservation equations for reactions formulated as half-cell or overall reactions and to demonstrate their equivalence.

Written as half-cell reactions, redox reactions can be expressed in the general form for aqueous species as

$$n_i e^- + \sum_{j=1}^{N_c-1} \nu'_{ji}\mathcal{A}'_j \rightleftharpoons \mathcal{A}'_i, \quad (i = 1, \ldots, N_{\rm sec}+1), \tag{201a}$$

Table 2. Pyrite oxidation reactions illustrating the formulation of nonequilibrium redox reactions. The list of reactions is only meant to be suggestive of the level of complexity and does not include all possible reactions relevant to pyrite oxidation.

Local Equilibrium Reactions Preserving Oxidation State	
$\mathrm{Fe^{2+}} + 2\,\mathrm{H_2O} - 2\,\mathrm{H^+}$	$\rightleftharpoons\ \mathrm{Fe(OH)_2}$
$\mathrm{Fe^{3+}} + 3\,\mathrm{H_2O} - 3\,\mathrm{H^+}$	$\rightleftharpoons\ \mathrm{Fe(OH)_3}$
$\mathrm{SO_4^{2-}} + \mathrm{H^+}$	$\rightleftharpoons\ \mathrm{HSO_4^-}$
$\mathrm{HS^-} + \mathrm{H^+}$	$\rightleftharpoons\ \mathrm{H_2S_{(aq)}}$
Kinetic Homogeneous Redox Reactions	
$\mathrm{Fe^{2+}} + \mathrm{H^+} - \frac{1}{2}\,\mathrm{H_2O} + \frac{1}{4}\,\mathrm{O_{2(aq)}}$	$\rightleftharpoons\ \mathrm{Fe^{3+}}$
$\mathrm{SO_4^{2-}} + \mathrm{H^+} - 2\,\mathrm{O_{2(aq)}}$	$\rightleftharpoons\ \mathrm{HS^-}$
Kinetic Mineral Reactions	
$\mathrm{Fe^{2+}} + 2\,\mathrm{Fe^{3+}} + 4\,\mathrm{H_2O} - 8\,\mathrm{H^+}$	$\rightleftharpoons\ \mathrm{Fe_3O_{4(s)}}$
$2\,\mathrm{Fe^{3+}} + 3\,\mathrm{H_2O} - 6\,\mathrm{H^+}$	$\rightleftharpoons\ \mathrm{Fe_2O_{3(s)}}$
$\mathrm{Fe^{3+}} + 3\,\mathrm{H_2O} - 3\,\mathrm{H^+}$	$\rightleftharpoons\ \mathrm{Fe(OH)_{3(s)}}$
$\mathrm{Fe^{2+}} + 2\,\mathrm{SO_4^{2-}} + 2\,\mathrm{H^+} - \mathrm{H_2O} - \frac{7}{2}\mathrm{O_{2(aq)}}$	$\rightleftharpoons\ \mathrm{FeS_2}$
Linearly-Dependent Reactions	
$15\,\mathrm{Fe^{2+}} - 14\,\mathrm{Fe^{3+}} + 2\,\mathrm{SO_4^{2-}} + 16\,\mathrm{H^+} - 8\,\mathrm{H_2O}$	$\rightleftharpoons\ \mathrm{FeS_2}$

and for minerals as

$$n_m e^- + \sum_{j=1}^{N_c-1} \nu'_{jm} \mathcal{A}'_j \ \rightleftharpoons\ \mathcal{M}_m, \quad (m = 1,\ \ldots, N_{\min}). \tag{201b}$$

The coefficients n_i and n_m refer to the number of electrons transferred in the reaction. Species and stoichiometric coefficients are marked with a prime to distinguish them from their counterparts appearing in half-cell reactions. Primary species consist of the set of species $\{\mathcal{A}'_j, j = 1,\ \ldots, N_c - 1\}$ and the electron e^-. This gives a total of N_c primary species, including the electron e^-. Aqueous secondary species consist of the set of species $\{\mathcal{A}'_i, i = 1,\ \ldots, N_{\rm sec}+1\}$, and are assumed to be $N_{\rm sec}+1$ in number. The reason for writing $N_{\rm sec}+1$ secondary species is so that the total number of species *not* including the electron is N, where N is equal to the sum of primary and secondary species

$$N \ = \ N_c + N_{\rm sec}. \tag{202}$$

Alternatively, it is possible to formulate redox reactions in terms of overall reactions

$$\sum_{j=1}^{N_c} \nu_{ji} \mathcal{A}_j \ \rightleftharpoons\ \mathcal{A}_i, \quad (i = 1,\ \ldots, N_{\rm sec}), \tag{203a}$$

for aqueous secondary species, and

$$\sum_{j=1}^{N_c} \nu_{jm} \mathcal{A}_j \ \rightleftharpoons\ \mathcal{A}_m, \quad (m = 1,\ \ldots, N_{\min}), \tag{203b}$$

for minerals. In this form the electron e^- does not appear explicitly in redox reactions. Primary species consist of the set $\{\mathcal{A}_j, j=1,\ \ldots, N_c\}$, and aqueous secondary species the set $\{\mathcal{A}_i, i=1,\ \ldots, N_{\rm sec}\}$. Notice that the total number of species is still N, the sum of primary and secondary species, but there is one less secondary species as a result of their being one less overall reaction compared to the number of half-cell reactions. The extra secondary species in the half-cell formulation is used to replace the electron as primary species in the overall formulation. The overall form of redox reactions written in terms of actual species in solution is preferred for most cases since the electron does not exist as a dissolved aqueous species. When written is the form of overall reactions, there is no need to distinguish redox reactions from reactions not involving transfer of electrons, and the same methods may be used for redox reactions as other reactions.

As an example, consider the oxidation of ferrous to ferric iron described by the half-cell reactions

$$\mathrm{Fe^{2+}} - e^- \ \rightleftharpoons\ \mathrm{Fe^{3+}}, \tag{204a}$$

and

$$2\,\mathrm{H_2O} - 4\,\mathrm{H^+} - 4\,e^- \ \rightleftharpoons\ \mathrm{O_2}. \tag{204b}$$

The corresponding overall reaction has the form

$$\mathrm{Fe^{2+}} + \frac{1}{4}\,\mathrm{O_2} + \mathrm{H^+} - \frac{1}{2}\,\mathrm{H_2O} \ \rightleftharpoons\ \mathrm{Fe^{3+}}. \tag{204c}$$

Primary and secondary species for the half-cell and overall formulations are listed in Table 3.

Table 3. Primary and secondary species in oxidation of ferrous to ferric iron.

Reaction	Primary species	Secondary species
half-cell	Fe^{2+}, H^+, e^-	Fe^{3+}, O_2
overall	Fe^{2+}, H^+, O_2	Fe^{3+}

An overall redox reaction is completely equivalent to its half-cell counterparts *provided* the electron is conserved in the half-cell reactions. For any half-cell reaction it is possible to write the reaction with the electron appearing on the right hand side as

$$\frac{1}{n_{i_0}}\left(\mathcal{A}'_{i_0} - \sum_{j=1}^{N_c-1}\nu'_{ji_0}\mathcal{A}'_j\right)\ \rightleftharpoons\ e^-. \tag{205}$$

Choosing $i_0 = i_{N_{\rm sec}+1}$, and using this reaction to eliminate the electron from the remaining reactions leads to the set of overall redox reactions as written in Eqns.(203a,b). This transformation amounts to exchanging the electron with the secondary species $\mathcal{A}'_{i_0}$: $e^- \leftrightarrow \mathcal{A}'_{i_0}$, and dropping the electron from the new list of secondary species. The new set of primary species consists of the species $\{\mathcal{A}_j\}=\{\mathcal{A}'_1,\ \ldots, \mathcal{A}'_{N_c-1}, \mathcal{A}'_{i_0}\}$, and secondary species $\{\mathcal{A}_i\}=\{\mathcal{A}'_1,\ \ldots, \mathcal{A}'_{N_{\rm sec}}\}$. The relation between the primed and unprimed quantities is easily found. Substituting Eqn.(205) into Eqn.(201a) for $i \neq i_0$ yields the identification

$$\mathcal{A}_j\ =\ \begin{cases} \mathcal{A}'_j, & (j=1,\ \ldots, N_c-1) \\ \mathcal{A}'_{i_0}, & (j=N_c) \end{cases}, \tag{206}$$

and

$$\nu_{ji} \;=\; \begin{cases} \nu'_{ji} - \dfrac{n_i}{n_{i_0}}\nu'_{ji_0}, & (j = 1,\, \ldots, N_c - 1) \\ \dfrac{n_i}{n_{i_0}}, & (j = N_c) \end{cases} . \tag{207}$$

In these relations the subscript i ranges from i=1, $\ldots$, $N_{\rm sec}$ representing aqueous secondary species. A similar result may be derived for mineral reactions in which the subscript i is replaced with m.

Transport Equations. The mass transport equations for redox reactions written either as half-cell reactions or as overall reactions can now be formulated. For half-cell reactions in which the electron occurs explicitly, the mass conservation equations are given formally as

$$\widehat{\mathcal{L}}C_j \;=\; -\sum_i \nu'_{ji} I'_i - \sum_m \nu'_{jm} I_m, \tag{208a}$$

for primary species other than the electron, and

$$\widehat{\mathcal{L}}C_{e^-} \;=\; -\sum_i n_i I'_i - \sum_m n_m I_m, \tag{208b}$$

for the electron, including contributions from redox reactions involving aqueous species and minerals. Transport equations for aqueous secondary species have the form

$$\widehat{\mathcal{L}}C_i \;=\; I'_i. \tag{208c}$$

The electron concentration C_{e^-} is a fictitious quantity with no direct physical meaning since there are no free electrons in solution. Because electrons are conserved in an aqueous solution, that is they are transferred from one species to another, it follows that the concentration of electrons in solution must vanish identically

$$C_{e^-} \;=\; 0. \tag{209}$$

As a consequence its derivative must also vanish

$$\widehat{\mathcal{L}}C_{e^-} \;=\; 0. \tag{210}$$

This equation implies the following relation may be written among the reaction rates of the half-cell reactions for aqueous secondary species and minerals

$$\sum_i n_i I'_i + \sum_m n_m I_m \;=\; 0, \tag{211}$$

as follows from Eqn.(208b). This relation expresses conservation of the transfer of electrons taking place in the system. Exchange of electrons takes place from one species or mineral to another. For every aqueous species or mineral which gains an electron, some other aqueous species or mineral must lose an electron.

To demonstrate the equivalence between mass transport equations based on half-cell reactions, and those based on overall redox reactions, the reaction rates I'_i are eliminated from Eqns.(208a) and (211) using Eqn.(208c), to obtain the transport equations

$$\widehat{\mathcal{L}}\left\{ C_j + \sum_i \nu'_{ji} C_i \right\} \;=\; -\sum_m \nu'_{jm} I_m, \tag{212a}$$

and

$$\widehat{\mathcal{L}} \sum_i n_i C_i \;=\; -\sum_m n_m I_m. \tag{212b}$$

The latter equation may be expressed in an alternative form by singling out some particular secondary species $\mathcal{A}'_{i_0}$ and writing the transport equation in the form

$$\widehat{\mathcal{L}} \left\{ C_{i_0} + \sum_{i \neq i_0} \frac{n_i}{n_{i_0}} C_i \right\} \;=\; -\sum_m \frac{n_m}{n_{i_0}} I_m, \tag{213}$$

obtained by dividing through by the coefficient n_{i_0}. In this form of the mass conservation equation, the former secondary species $\mathcal{A}'_{i_0}$ is treated as a primary species. It is now necessary to eliminate this species from the original set of primary species transport equations since only one primary species can occur in each transport equation. Again singling out the species $\mathcal{A}_{i_0}$ in Eqn.(212a), this equation may be written in the form

$$\widehat{\mathcal{L}} \left\{ C_j + \nu'_{ji_0} C_{i_0} + \sum_{i \neq i_0} \nu'_{ji} C_i \right\} \;=\; -\sum_m \nu'_{jm} I_m. \tag{214}$$

Multiplying Eqn.(213) by ν'_{ji_0} and subtracting from Eqn.(214) then gives

$$\widehat{\mathcal{L}} \left\{ C_j + \sum_i \left(\nu'_{ji} - \frac{\nu'_{ji_0}}{n_{i_0}} n_i \right) C_i \right\} \;=\; -\sum_m \left(\nu'_{jm} - \frac{\nu'_{ji_0}}{n_{i_0}} n_m \right) I_m. \tag{215}$$

This latter form of the transport equations is identical to that obtained from the overall formulation of oxidation/reduction reactions, similar to Eqn.(212a) with ν'_{ji} and ν'_{jm} replaced by ν_{ji} and ν_{jm}, using the transformation relations given in Eqns.(206) and (207). Consequently, it is immaterial whether half-cell reactions or overall reactions balanced on the electron are used to describe redox processes provided care is exercised to conserve electrons.

It only remains to consider the form of the mass action equations for the concentrations of aqueous secondary species. When formulated as half-cell reactions with the electron as primary species, the concentrations of aqueous secondary species are computed from the relation

$$C_i \;=\; \gamma_i^{-1} K_i \prod_j \left(\gamma_j C_j\right)^{\nu_{ji}} a_{e^-}^{n_i}. \tag{216}$$

The question arises as the the meaning of the electron activity appearing in this equation if the electron concentration is identically zero. Although, the concept of an aqueous electron concentration has no meaning when applied to the mass conservation equations, nevertheless, it is still possible and useful to define the electron activity, or pe. The electron activity is in fact provided by reaction (205). For this reaction the mass action equation reads

$$a_{e^-} \;=\; K_{e^-}^{(i_0)} \prod_j \left(\gamma_j C_j\right)^{\nu'_{ji_0}/n_{i_0}} \left(\gamma_{i_0} C_{i_0}\right)^{1/n_{i_0}}, \tag{217}$$

where $\log K_{e^-}^{(i_0)}$ denotes the corresponding equilibrium constant. It follows that the solution pe is given by

$$\mathrm{pe} \;=\; -\log a_{e^-} \;=\; -\frac{1}{n_i} \left(\log a_i - \sum_j \nu'_{ji} \log a_j \right) - \log K_{e^-}^{(i_0)}. \tag{218}$$

Physically the variable pe describes the tendency to exchange electrons, but has nothing to do with the actual concentration of electrons in the aqueous solution which is vanishingly small. Substituting this relation for the electron activity into Eqn.(216) then gives

$$C_i \;=\; \gamma_i^{-1} K_i \prod_j \left(\gamma_j C_j\right)^{\nu_{ji} - \nu'_{ji_0} n_{i_0}/n_i} \left(\gamma_{i_0} C_{i_0}\right)^{n_i/n_{i_0}} . \tag{219}$$

From the transformation relations given by Eqns.(206) and (207), this equation is just the usual mass action relation Eqn.(94). Similar considerations apply to mineral reactions.

Modeling Biomass Synthesis and Biodegradation Processes

Microbial processes are playing an increasingly important role in our understanding of the subsurface geochemical environment (Lovley and Chapelle, 1995). An excellent introduction into modeling microbially induced processes has been given by Rittmann and VanBriesen (1996). They derive overall reactions for biomass synthesis resulting from biodegradation reactions based on H_3NTA as the electron-donor primary substrate. Two different electron-acceptor substrates $O_{2(aq)}$ and NO_3^- are considered by the authors. In addition to these species, other important electron-acceptor primary substrates include SO_4^{2-}, $CO_{2(aq)}$ and Fe^{3+}.

The approach used by Rittmann and VanBriesen (1996) is somewhat cumbersome in that mass- rather than mole-based measures are used to represent organic substances. Their approach complicates the derivation of overall reactions describing biomass synthesis. The discussion presented here provides a unified treatment of organic reactions coupled to the usual aqueous acid-base, complexing, and mineral reactions employing mole-based quantities. A important feature of many biologically induced reactions is that they are strictly irreversible. As a consequence these reactions do not go to equilibrium. The reactions stop when either all donor or acceptor substrate material or biomass is completely utilized. As noted by Rittmann and vanBriesen (1996), biologically catalyzed reactions are affected by non-biological reactions and vice versa and their interaction can affect the fate of contaminants and the effectiveness of bioremediation schemes.

Rittmann and VanBriesen (1996) present a derivation of overall reactions governing biomass synthesis based on considerations of molecular biology at the cell level. Bacteria oxidize the electron-donor substrate to produce NADH (nicotinanaide adenine dinucleotide). With H_3NTA ($C_6H_9O_6N_{(aq)}$) as primary electron-donor substrate, 18 electrons are transferred according to the reaction

$$6\,CO_{2(aq)} + NH_4^+ + 17\,H^+ + 18\,e^- - 6\,H_2O \longleftarrow C_6H_9O_6N_{(aq)}. \tag{220}$$

Biomass synthesis, with biomass represented as $C_5H_7O_2N_{(s)}$, results in the transfer of 20 electrons

$$5\,CO_{2(aq)} + NH_4^+ + 19\,H^+ + 20\,e^- - 8\,H_2O \longrightarrow C_5H_7O_2N_{(s)}. \tag{221}$$

With oxygen as the electron acceptor substrate, 4 electrons are transferred

$$2\,H_2O - 4\,H^+ - 4\,e^- \;\rightleftharpoons\; O_{2(aq)}. \tag{222}$$

The overall reaction for biomass synthesis is derived by combining these reactions to balance electrons taking into account intra-cell process.

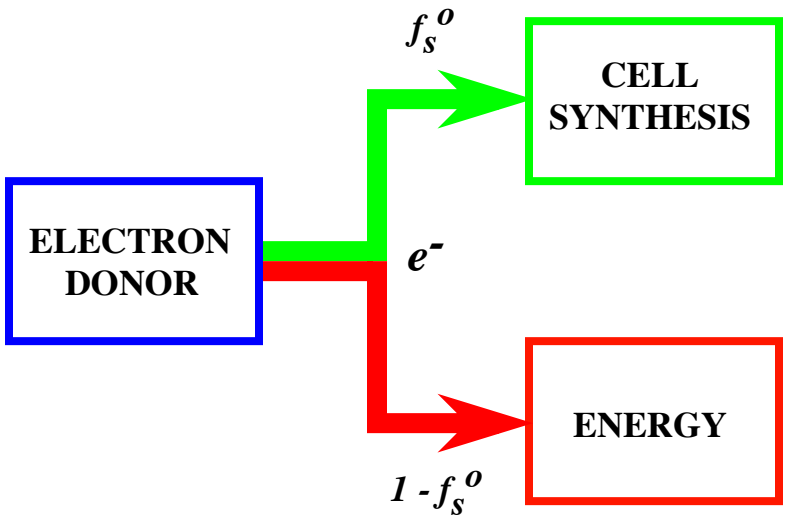

Figure 4. Schematic diagram illustrating the partitioning of electrons from the donor substrate to form biomass and create energy.

Electron acceptors other than oxygen may be involved in biomass synthesis. For example, reaction (222) may be replaced by any one of the reactions

$$2\,NO_3^- + 12\,H^+ - 10e^- - 6\,H_2O \rightleftharpoons N_2, \tag{223a}$$

$$SO_4^{2-} + 10\,H^+ + 8\,e^- - 4\,H_2O \rightleftharpoons H_2S_{(aq)}, \tag{223b}$$

$$Fe^{3+} + e^- \rightleftharpoons Fe^{2+}, \tag{223c}$$

$$CO_{2(aq)} + 8\,H^+ + 8\,e^- - 2\,H_2O \rightleftharpoons CH_{4(g)}. \tag{223d}$$

These reactions may occur simultaneously or individually depending on the nature of the geochemical system. Within a flow column they may occur in different, possibly overlapping, regions along the flow path.

In terms of a given set of primary species $\{\mathcal{A}_j\}$ excluding electron donor $\mathcal{A}_d$ and acceptor $\mathcal{A}_a$ species, the reactions for oxidation of the primary electron-donor substrate, reduction of the primary electron-acceptor substrate, and biomass synthesis can be written as half-cell reactions in the general form

$$\sum_j \nu_{jd}\mathcal{A}_j + n_d^e e^- \longleftarrow \mathcal{A}_d, \quad \text{(donor)}, \tag{224a}$$

$$\sum_j \nu_{ja}\mathcal{A}_j + n_a^e e^- \rightleftharpoons \mathcal{A}_a, \quad \text{(acceptor)}, \tag{224b}$$

$$\sum_j \nu_{jc}^{\mathcal{S}}\mathcal{A}_j + n_c^e e^- \longrightarrow \mathcal{A}_c, \quad \text{(cell synthesis)}, \tag{224c}$$

where $\mathcal{A}_c$ represents biomass. A fourth reaction describes biomass decay expressed as the overall reaction

$$\nu_{ac}^{\mathcal{D}}\mathcal{A}_a + \sum_j \nu_{jc}^{\mathcal{D}}\mathcal{A}_j \longleftarrow \mathcal{A}_c, \quad \text{(decay)}. \tag{224d}$$

Note that the electron donor primary substrate does not appear in this reaction.

The transfer of electrons from the electron donor substrate must be conserved by cell processes of synthesis and respiration generating more biomass and energy. If the quantity

f_s° represents the fraction of electrons going to biomass synthesis, then the fraction of electrons for respiration providing energy is

$$f_e^\circ \;=\; 1 - f_s^\circ. \tag{225}$$

The flow of electrons from the donor substrate and their partitioning between biomass synthesis and energy production is illustrated in Figure 4. The overall reaction for biomass systhesis is constructed from a linear combination of reactions (224a), (224b) and (224c) with weighting factors f_s° and f_e° (Christensen and McCarty, 1975; Pavlostathis and Giraldo-Gomez, 1991). This may be accomplished by first writing these reactions in terms of a single electron brought to the right-hand side

$$\frac{1}{n_d^e}\mathcal{A}_d - \frac{1}{n_d^e}\sum_j \nu_{jd}\mathcal{A}_j \longrightarrow e^-, \tag{226}$$

$$\frac{1}{n_a^e}\mathcal{A}_a - \frac{1}{n_a^e}\sum_j \nu_{ja}\mathcal{A}_j \;\rightleftharpoons\; e^-, \tag{227}$$

$$\frac{1}{n_c^e}\mathcal{A}_c - \frac{1}{n_c^e}\sum_j \nu_{jc}^{\mathcal{S}}\mathcal{A}_j \longleftarrow e^-. \tag{228}$$

Combining these reactions with weighting factors f_s° and $1 - f_s^\circ$ according to

$$\mathcal{R}_{(226)} - (1 - f_s^\circ)\mathcal{R}_{(227)} - f_s^\circ\mathcal{R}_{(228)}, \tag{229}$$

yields the following overall reaction for biomass synthesis

$$\frac{1}{n_d^e}\mathcal{A}_d - \frac{1 - f_s^\circ}{n_a^e}\mathcal{A}_a + \sum_j \left[\frac{f_s^\circ}{n_c^e}\nu_{jc}^{\mathcal{S}} + \frac{1 - f_s^\circ}{n_a^e}\nu_{ja} - \frac{1}{n_d^e}\nu_{jd}\right]\mathcal{A}_j \longrightarrow \frac{f_s^\circ}{n_c^e}\mathcal{A}_c. \tag{230}$$

From this reaction an expression for the yield $\mathcal{Y}_c^d$ for biomass synthesis is obtained as the ratio of the rate of cell production to the rate of donor substrate utilization

$$\mathcal{Y}_c^d \;=\; f_s^\circ\frac{n_d^e}{n_c^e}. \tag{231}$$

The yield is proportional to the electron synthesis factor f_s° and the ratio of electrons transferred in the donor and biomass systhesis reactions. The biomass yield may be different for different electron acceptor substrates as well.

With oxygen as the electron acceptor substrate, and taking f_s°=0.64, n_c^e=20, n_d^e=18, and n_a^e=-4, reaction (230) becomes

$$\begin{aligned}&0.0555556\,\mathrm{C_6H_9O_6N} - 0.173333\,\mathrm{CO_{2(aq)}} + 0.0235556\,\mathrm{H^+} - 0.102667\,\mathrm{H_2O}\\ &- 0.0235556\,\mathrm{NH_4^+} + 0.09\,\mathrm{O_{2(aq)}} \longrightarrow 0.032\,\mathrm{C_5H_7O_2N}.\end{aligned} \tag{232}$$

The yield $\mathcal{Y}$ has the value $\mathcal{Y}$=0.576. Using as electron acceptor $\mathrm{NO_3^-}$ with f_s°=0.62 gives

$$\begin{aligned}&0.0555556\,\mathrm{C_6H_9O_6N} - 0.178333\,\mathrm{CO_{2(aq)}} + 0.100556\,\mathrm{H^+} - 0.142667\,\mathrm{H_2O}\\ &- 0.038\,\mathrm{N_2} - 0.0245556\,\mathrm{NH_4^+} + 0.076\,\mathrm{NO_3^-} \longrightarrow 0.031\mathrm{C_5H_7O_2N}.\end{aligned} \tag{233}$$

For this reaction the yield $\mathcal{Y}$ has the value $\mathcal{Y}$=0.558.

Reactions (232) and (233) are linearly independent provided the intra-cell electron synthesis factor f_s° is different for different electron acceptors. Otherwise the reactions are linearly dependent. Provided local equilibrium prevails within the aqueous phase between different redox couples, catalyzed by bacteria, reactions based on different electron-acceptor substrates with equal intra-cell electron factors f_s° are linearly dependent and as a consequence the stoichiometry of the linearly-dependent reactions does not play a role in the transport equations, their rates being additive [see Eqn.(187)]. Only if disequilibrium of redox couples persists does the stoichiometry of the overall reaction come into play according to Eqn.(188).

Kinetic Rate Law. Introducing the yield, reaction (230) can be written as

$$\frac{1}{\mathcal{Y}_c^d}\,\mathcal{A}_d - \frac{1-f_s^\circ}{f_s^\circ}\,\frac{n_c^e}{n_a^e}\,\mathcal{A}_a + \sum_j \left[\nu_{jc}^{\mathcal{S}} + \frac{1-f_s^\circ}{f_s^\circ}\,\frac{n_c^e}{n_a^e}\,\nu_{ja} - \frac{1}{\mathcal{Y}_c^d}\,\nu_{jd}\right]\mathcal{A}_j \longrightarrow \mathcal{A}_c, \tag{234}$$

in which the stoichiometric coefficient multiplying biomass is normalized to unity. The kinetic rate law for biomass synthesis is presumed to be adequately described by the Monod rate law

$$I_c \;=\; k_c\,\chi_c\,\frac{C_d}{K_d + C_d}\,\frac{C_a}{K_a + C_a}, \tag{235}$$

for single acceptor and donor substrates with concentrations C_a and C_d, respectively, and where k_c represents the rate constant and χ_c denotes the concentration of cells. Note that an affinity factor, present in mineral precipitation and dissolution reactions, is absent from the Monod rate law. The rate law describing biomass decay is assumed to be first order of the form

$$I_c^{\mathcal{D}} \;=\; -\lambda_c \chi_c, \tag{236}$$

where λ_c denotes the decay constant.

Mass Transport Equations. To set up the mass transport equations the first step is to identify an appropriate set of primary and secondary species to represent the reactions taking place in the particular system at hand. The primary electron donor substrate must be chosen as primary species as well as at least one on the primary electron acceptor substrates. If redox reactions are described through kinetic rate laws then all electron acceptors become primary species. On the other hand if redox reactions are represented by local equilibrium constraints, catalyzed by the presence of bacteria, then only one electron acceptor can be chosen as primary species, with the remaining electron acceptors included as aqueous secondary species. In addition to the biomass synthesis reaction (234) and decay reaction (224d), and possibly electron acceptor equilibria, additional reactions including homogeneous reactions

$$\nu_{di}^{aq}\mathcal{A}_d + \nu_{ai}^{aq}\mathcal{A}_a + \sum_j \nu_{ji}^{aq}\mathcal{A}_j \;\rightleftharpoons\; \mathcal{A}_i, \tag{237}$$

and mineral precipitation and dissolution reactions

$$\nu_{di}^{min}\mathcal{A}_d + \nu_{ai}^{min}\mathcal{A}_a + \sum_j \nu_{jm}^{min}\mathcal{A}_j \;\rightleftharpoons\; \mathcal{M}_m, \tag{238}$$

must also be accounted for in a geochemical system. In these reactions allowance is made for participation by both the electron donor and acceptor substrates. For the set of primary

species $\{\mathcal{A}_d,\ \mathcal{A}_a,\ \mathcal{A}_j\}$, the mass transport equations have the following form for primary species

$$\widehat{\mathcal{L}}C_d \ = \ -\frac{1}{\mathcal{Y}_c^d}\, I_c^{\mathcal{S}} - \sum_i \nu_{di}^{aq} I_i^{aq} - \sum_m \nu_{dm}^{min} I_m^{min}, \tag{239}$$

$$\widehat{\mathcal{L}}C_a \ = \ \frac{1-f_s^\circ}{f_s^\circ}\,\frac{n_c^e}{n_a^e}\, I_c^{\mathcal{S}} + \nu_{ac}^{\mathcal{D}}\,\lambda_c\,\chi_c - \sum_i \nu_{ai}^{aq} I_i^{aq} - \sum_m \nu_{am}^{min} I_m^{min}, \tag{240}$$

$$\begin{aligned}\widehat{\mathcal{L}}C_j \ = \ & -\left[\nu_{jc}^{\mathcal{S}} + \frac{1-f_s^\circ}{f_s^\circ}\,\frac{n_c^e}{n_a^e}\,\nu_{ja} - \frac{1}{\mathcal{Y}_c^d}\,\nu_{jd}\right] I_c^{\mathcal{S}} + \nu_{jc}^{\mathcal{D}}\,\lambda_c\,\chi_c \\ & - \sum_i \nu_{ji}^{aq} I_i^{aq} - \sum_m \nu_{jm}^{min} I_m^{min},\end{aligned} \tag{241}$$

secondary species

$$\widehat{\mathcal{L}}C_i \ = \ I_i^{aq}, \tag{242}$$

biomass

$$\frac{\partial \chi_c}{\partial t} \ = \ I_c^{\mathcal{S}} - \lambda_c \chi_c, \tag{243}$$

and finally for minerals

$$\frac{\partial \phi_m}{\partial t} \ = \ \overline{V}_m I_m^{min}. \tag{244}$$

Mineral reaction rates are denoted by I_m^{min}, and homogeneous aqueous reaction rates by I_i^{aq}.

For the case in which the rates I_i^{aq} for homogeneous reactions are in local equilibrium, their rates may be eliminated by replacing the corresponding transport equations with mass action equations. This results in the primary species transport equations

$$\widehat{\mathcal{L}}\Psi_d \ = \ -\frac{1}{\mathcal{Y}_c^d}\, I_c^{\mathcal{S}} - \sum_m \nu_{dm}^{min} I_m^{min}, \tag{245a}$$

$$\widehat{\mathcal{L}}\Psi_a \ = \ \frac{1-f_s^\circ}{f_s^\circ}\,\frac{n_c^e}{n_a^e}\, I_c^{\mathcal{S}} + \nu_{ac}^{\mathcal{D}}\,\lambda_c\,\chi_c - \sum_m \nu_{am}^{min} I_m^{min}, \tag{245b}$$

$$\widehat{\mathcal{L}}\Psi_j \ = \ -\left[\nu_{jc}^{\mathcal{S}} + \frac{1-f_s^\circ}{f_s^\circ}\,\frac{n_c^e}{n_a^e}\,\nu_{ja} - \frac{1}{\mathcal{Y}_c^d}\,\nu_{jd}\right] I_c^{\mathcal{S}} + \nu_{jc}^{\mathcal{D}}\,\lambda_c\,\chi_c - \sum_m \nu_{jm}^{min} I_m^{min}, \tag{245c}$$

where

$$\Psi_d \ = \ C_d + \sum_i \nu_{di}^{aq} C_i, \tag{246a}$$

$$\Psi_a \ = \ C_a + \sum_i \nu_{ai}^{aq} C_i, \tag{246b}$$

$$\Psi_j \ = \ C_j + \sum_i \nu_{ji}^{aq} C_i. \tag{246c}$$

Parallel Reactions. So far the discussion has focused on the presence a single electron donor and acceptor substrate. However, in natural systems it is common for a number of different electron donor and acceptor substrates to be present at any one time. In such cases several parallel reactions representing biosynthesis may take place simultaneously. For the case of multiple electron acceptors indexed by β, these reactions may be written collectively in the general form

$$\sum_j \nu_{jc}^{\beta} \mathcal{A}_j \longrightarrow \mathcal{A}_c, \tag{247}$$

where the sum over the index j includes electron donor and acceptor substrates in addition to the other primary species. The reaction rate is given by the Monod rate law

$$I_c^{\beta} \;=\; k_c^{\beta} \chi_c \frac{C_{a_\beta}}{K_{a_\beta} + C_{a_\beta}} \frac{C_d}{K_d + C_d}, \tag{248}$$

with electron acceptor concentration C_{a_β}. The total rate for biomass synthesis is given by the sum over all parallel reactions related to different electron acceptors

$$\begin{aligned} I_c &= \sum_\beta I_c^{\beta}, \\ &= \chi_c \frac{C_d}{K_d + C_d} \sum_\beta \frac{k_c^{\beta} C_{a_\beta}}{K_{a_\beta} + C_{a_\beta}} \end{aligned} \tag{249}$$

For example, for parallel reactions based on $O_{2(aq)}$ and NO_3^- as electron acceptors the total rate for biomass synthesis is equal to the sum of the individual rates

$$\begin{aligned} I_c &= I_{\mathrm{O_{2(aq)}}} + I_{\mathrm{NO_3^-}}, \\ &= \chi_c \frac{C_d}{K_d + C_d} \left[\frac{k_{\mathrm{O_{2(aq)}}} C_{\mathrm{O_{2(aq)}}}}{K_{\mathrm{O_{2(aq)}}} + C_{\mathrm{O_{2(aq)}}}} + \frac{k_{\mathrm{NO_3^-}} C_{\mathrm{NO_3^-}}}{K_{\mathrm{NO_3^-}} + C_{\mathrm{NO_3^-}}} \right]. \end{aligned} \tag{250}$$

The primary species mass transport equations can be written in the form

$$\widehat{\mathcal{L}} \Psi_j \;=\; -\sum_{c\beta} \nu_{jc}^{\beta} I_c^{\beta} - \sum_{jm} \nu_{jm} I_m^{min}, \tag{251}$$

and for biomass synthesis as

$$\frac{\partial \chi_c}{\partial t} \;=\; \sum_\beta I_c^{\beta} \;=\; I_c. \tag{252}$$

The equations may be further generalized to more than one electron donor substrate if desired.

NUMERICAL MODELING USING THE COMPUTER CODE MULTIFLO

Setting Up a Reactive Transport Problem

Posed in its most general form, the reactive transport problem attempts to answer the question: What is the time–space evolution of a geochemical system given prescribed initial

and boundary conditions? Part of the problem is to predict which secondary mineral alteration products will form. Because it is not usually possible to predict this in advance of the calculation, it is necessary to allow for as many potential alteration products as possible. To some extent this becomes more of an art than a science and some experience is usually required in selecting potential candidate minerals. This section describes how to set up a reactive transport problem and presents two examples: *in situ* leaching of copper ore and acid mine drainage.

The parameters required for modeling a geochemical system include both physical and chemical properties. Physical properties include quantities such as porosity, permeability and tortuosity. Chemical properties include the initial and boundary fluid compositions. The initial fluid composition may be constrained to be in equilibrium with minerals which make up the host rock. The pH, Eh, pCO_2, and other parameters must be specified, as well as the concentrations of major and minor cations and anions as required by the system being investigated. It is important to know the actual minerals which make up the host rock, their abundances, and an estimate of their surface areas. The latter is perhaps the most difficult information to obtain. Ideally the numerical model should first be calibrated to the system being investigated if quantitative, meaningful results are to be obtained. Fortunately, the possible variation in surface area is not as arbitrary as might be expected and in some cases scaling relations can be used to estimate its sensitivity on the predicted results (Lichtner, 1993). As the surface area is taken to be larger and larger, the corresponding reaction rate approaches the condition of local equilibrium. Another factor of uncertainty is caused by highly fractured rock. The same mineral may need to be described by different rate mechanisms depending whether the mineral is contained in the matrix or on fracture surfaces that are more accessible to the infiltrating fluid.

The computer code MULTIFLO accounts for any number of homogeneous equilibrium reactions within the aqueous phase and kinetic reactions of minerals (Lichtner and Seth, 1997). Flow equations describing aqueous and gaseous phases are sequentially coupled to reactive solute transport equations. The code enables coupling changes in porosity and permeability resulting from mineral precipitation and dissolution to the flow field (Lichtner, 1996). Calculations can be carried out in 1, 2 or 3 spatial dimensions using a variety of numerical solution techniques including fully implicit, operator splitting, and explicit finite difference with an option to use the Leonard-TVD algorithm to describe high Peclet number flows (Gupta et al., 1991).

Determining Initial and Boundary Conditions

To set up a reactive transport problem one of the first steps is to determine the initial solution composition of the pore fluid occupying the porous medium and the composition of the fluid at the boundaries of the system. Several different types of boundary conditions are possible such as specifying the solution composition, a free flowing boundary condition usually specified through a zero concentration gradient, specifying the solute flux, and simply zero flux corresponding to a system closed with respect to mass transfer.

Calculating the initial and boundary fluid compositions generally requires solving a distribution of species problem for some specified set of conditions or constraints. These include some combination of the following.

Total Concentration: The "total" concentration $\mathcal{W}_j^0$ is expressed relative to the set of pri-

mary species used to describe the system as

$$m_j + \sum_i \nu_{ji} m_i \;=\; \mathcal{W}_j^0(\boldsymbol{r}), \tag{253}$$

where m_j, m_i denote the molalities of the primary and secondary species, respectively. The definition of $\mathcal{W}_j^0$ is similar to the definition of the generalized concentration Ψ_j in the transport problem, but without the density factor to convert to molarity units. As noted previously in connection with the definition of Ψ_j, $\mathcal{W}_j^0$ may in general take on both positive or negative values depending on the sign of the stoichiometric coefficients ν_{ji}. To have the true physical meaning of "total" concentration the coefficients ν_{ji} must be positive definite.

Given a set of reactants $\mathcal{A}_r$ with specified amounts N_r^0 in units of moles (kg H_2O)$^{-1}$ which are to be reacted with a fluid of initial composition $\mathcal{W}_j^{00}$, the resulting equilibrium concentration of the solution may be obtained by specifying as constraints on the system the total concentrations $\mathcal{W}_j^0$ defined as

$$\mathcal{W}_j^0 \;=\; \mathcal{W}_j^{00} + \sum_r \nu_{jr} N_r^0. \tag{254}$$

The stoichiometric coefficients ν_{jr} refer to the reaction coefficients of $\mathcal{A}_r$ expressed in terms of the basis $\mathcal{A}_j$

$$\sum_j \nu_{jr} \mathcal{A}_j \;\rightleftharpoons\; \mathcal{A}_r. \tag{255}$$

For example, if it is desired to find the equilibrium concentration resulting from adding a specified number of moles of pyrite $N_{\mathrm{FeS_2}}^0$ to an aqueous solution consisting of pure water in some initial redox state, then in terms of the set of basis species $\{\mathrm{Fe^{3+}}, \mathrm{SO_4^{2-}}, \mathrm{H^+}, \mathrm{O_{2(aq)}}\}$ the "total" concentrations are specified as

$$\mathcal{W}_{\mathrm{Fe^{3+}}}^0 \;=\; \mathcal{W}_{\mathrm{Fe^{3+}}}^{00} + N_{\mathrm{FeS_2}}^0, \tag{256a}$$

$$\mathcal{W}_{\mathrm{SO_4^{2-}}}^0 \;=\; \mathcal{W}_{\mathrm{SO_4^{2-}}}^{00} + 2\, N_{\mathrm{FeS_2}}^0, \tag{256b}$$

$$\mathcal{W}_{\mathrm{H^+}}^0 \;=\; \mathcal{W}_{\mathrm{H^+}}^{00} + N_{\mathrm{FeS_2}}^0, \tag{256c}$$

$$\mathcal{W}_{\mathrm{O_{2(aq)}}}^0 \;=\; \mathcal{W}_{\mathrm{O_{2(aq)}}}^{00} - \frac{15}{4}\, N_{\mathrm{FeS_2}}^0. \tag{256d}$$

These relations correspond to the pyrite reaction

$$\mathrm{Fe^{3+}} + 2\,\mathrm{SO_4^{2-}} + \mathrm{H^+} - \frac{15}{4}\,\mathrm{O_{2(aq)}} - \frac{1}{2}\mathrm{H_2O} \;\rightleftharpoons\; \mathrm{FeS_2}. \tag{257}$$

Note that the "total" oxygen concentration may be negative according to Eqn.(256d).

Individual Species Concentration: This is the simplest constraint of all in which the concentration of a particular primary species is specified by a possibly time-dependent value

$$m_j \;=\; m_j^0(\boldsymbol{r},\, t). \tag{258}$$

The pH of the solution is specified by a constraint of the form

$$m_{\mathrm{H^+}} \;=\; \frac{10^{-\mathrm{pH_0}}}{\gamma_{\mathrm{H^+}}}, \tag{259}$$

for some specified value $\mathrm{pH_0}$.

Gas Constraint: The partial pressure of a gaseous species such as O_2 or CO_2 may be specified leading to the constraint

$$P_l^g \;=\; K_l^g \prod_j \left(\gamma_j m_j\right)^{\nu_{ji}^g}. \tag{260}$$

This constraint provides a linear relation among the logarithms of the primary species concentrations.

Mineral Equilibria: Equilibrium with minerals leads to the constraint equation

$$K_m \prod_j \left(\gamma_j m_j\right)^{\nu_{jm}} \;=\; 1. \tag{261}$$

This constraint also provides a linear relation among the logarithms of the primary species concentrations.

Charge Balance: Charge balance implies the constraint

$$\sum_j z_j \Psi_j \;=\; 0. \tag{262}$$

In Situ Copper Leaching

In situ leaching of ore offers a promising alternative to conventional mining techniques which require removal of large quantities of rock followed by crushing and milling operations. Solution mining typically involves introduction of an acidic leach solution, referred to as the lixiviant, into the ore zone through injection wells. The leach solution reacts with ore and gangue minerals and is extracted from one or more wells surrounding the injection well. The extracted solution is referred to as the pregnant leach solution. Solvent extraction methods are then used to recover the ore. Under the proper conditions the process results in an efficient, low cost method for ore production. Low grade ore bodies that are uneconomical by conventional means may become economically viable using *in situ* leach methods.

There are, however, several complicating factors that need to be considered during *in situ* leaching. One is the possible contamination of groundwater surrounding the ore deposit. The groundwater composition must be carefully monitored during the leaching process to ensure that none of the lixiviant escapes. After the leaching operation is complete it is usually necessary to restore the groundwater close to its original condition. Such environmental considerations can add to the cost of the solution mining operation, and in unfavorable circumstances even render the process uneconomic.

Reactive transport modeling of the *in situ* leach operation can provide insight into the processes taking place inside the leaching zone. Precipitation of secondary minerals as the lixiviant reacts with ore and gangue minerals can adversely affect the leach operation by consuming acid as well as clogging the pore spaces and halting flow through the ore body. In addition, secondary minerals may armor the surfaces of ore-bearing minerals thereby limiting the ability of the lixiviant to leach out the ore. Modeling may also be useful in reclamation of the site by, for example, providing an estimate of the number of pore volumes of ambient groundwater necessary to flush through the leach zone to restore the groundwater composition close to its original condition.

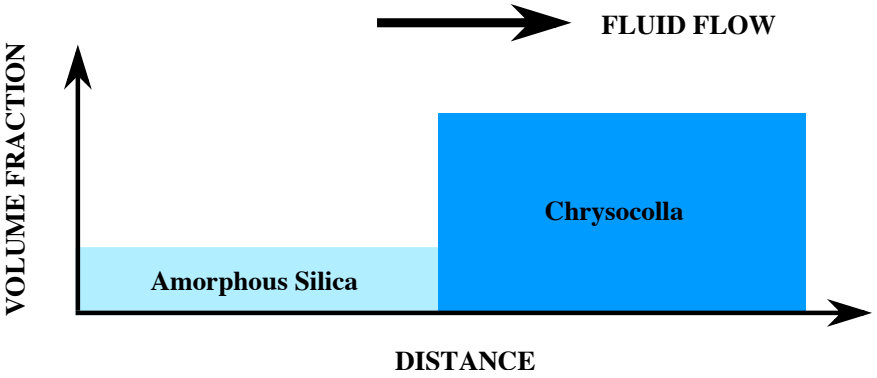

Figure 5. Schematic diagram at an instant in time of copper leaching from chrysocolla to produce amorphous silica and release copper into solution.

The process of leaching chrysocolla by a sulfuric acid solution leads to consumption of acid with a consequent increase in pH according to a reaction of the form

$$\mathrm{CuSiO_3 \cdot H_2O + 2\,H^+ \longrightarrow Cu^{2+} + SiO_{2(am)} + 2\,H_2O}. \tag{263}$$

Typically a sulfuric acid solution with pH values in the range of 1–2 is injected into the ore body. At this low pH, because most of the sulfur in solution occurs in the form of the bisulfate ion $\mathrm{HSO_4^-}$ rather than as $\mathrm{SO_4^{2-}}$, the ionic strength of the injected solution is lower than might be expected—on the order of 1/2 molal. The silica released during the leaching process is assumed to precipitate as amorphous silica $\mathrm{SiO_{2(am)}}$. A schematic diagram of this process is shown in Figure 5. The rate constant for the dissolution of chrysocolla is pH-dependent of the form

$$k_{\mathrm{chry}} \;=\; k_0 a_{\mathrm{H^+}}^n, \tag{264}$$

with n=0.39 (Terry and Monhemius, 1983). As a consequence, increasing the pH from 1 to 4 results in a decrease in the rate constant by a factor of approximately 15.

Local Equilibrium Calculation of Chemical Shock Fronts. A pure advective transport calculation of the leaching process in a one-dimensional column, for conditions of local chemical equilibrium of solids with an aqueous solution, provides a simplified calculation for determining the leaching efficiency of the column. Given the inlet fluid composition and the initial composition of the host rock, the resulting mineral alteration pattern, reaction front velocities, and fluid composition within each alteration zone is determined by solving a set of algebraic equations (Walsh et al., 1989; Lichtner, 1991). The host rock is treated as a homogeneous porous medium with a uniform distribution of chrysocolla. No distinction is made between chrysocolla located in fracture fillings and that disseminated in the rock matrix. The pure advective local equilibrium calculation can be thought of as the asymptotic solution of a kinetic calculation for an infinitely long flow column (Lichtner, 1993).

For the simple system Cu–Si–$\mathrm{H_2O}$, the change in pH, effluent copper concentration, and the amount of amorphous silica precipitated may be estimated by combining mass conservation equations with local chemical equilibrium mass action equations at the chrysocolla dissolution front. Mass conservation implies that the jumps in total copper concentration and pH across the chrysocolla dissolution front, representing a chemical shock wave, satisfy the equation

$$[\mathrm{Cu^{2+}}] + \frac{1}{2}\,[\mathrm{H^+}] \;=\; 0, \tag{265}$$

where $[\mathrm{Cu}^{2+}]$ and $[\mathrm{H}^{+}]$ represent the difference between the effluent ($C_{\mathrm{Cu}^{2+}}$, $C_{\mathrm{H}^{+}}$) and inlet ($C^0_{\mathrm{Cu}^{2+}}$, $C^0_{\mathrm{H}^{+}}$) concentrations of copper and hydrogen ions defined by

$$[\mathrm{Cu}^{2+}] \;=\; C_{\mathrm{Cu}^{2+}} - C^0_{\mathrm{Cu}^{2+}}, \tag{266}$$

and

$$[\mathrm{H}^{+}] \;=\; C_{\mathrm{H}^{+}} - C^0_{\mathrm{H}^{+}}. \tag{267}$$

The concentration of silica is continuous across the front, buffered by equilibrium with amorphous silica, in accordance with the downstream equilibrium condition (Walsh et al., 1989). Simultaneous equilibrium of chrysocolla and amorphous silica implies the mass action relation

$$\frac{K_{\mathrm{chry}}}{K_{\mathrm{SiO}_{2(\mathrm{am})}}} \;=\; \frac{\gamma_{\mathrm{Cu}^{2+}} C_{\mathrm{Cu}^{2+}}}{\left(\gamma_{\mathrm{H}^{+}} C_{\mathrm{H}^{+}}\right)^2}, \tag{268}$$

with activity coefficients $\gamma_{\mathrm{Cu}^{2+}}$ and $\gamma_{\mathrm{H}^{+}}$. Combining the mass action equation with the mass conservation relation Eqn.(265) yields a quadratic equation for the pH:

$$\frac{\gamma^2_{\mathrm{H}^{+}}}{\gamma_{\mathrm{Cu}^{2+}}} \frac{K_{\mathrm{chry}}}{K_{\mathrm{SiO}_{2(\mathrm{am})}}} C^2_{\mathrm{H}^{+}} + \frac{1}{2} C_{\mathrm{H}^{+}} - \left(C^0_{\mathrm{Cu}^{2+}} + \frac{1}{2} C^0_{\mathrm{H}^{+}} \right) \;=\; 0. \tag{269}$$

Solving this equation for an inlet pH_0=1, and initial copper concentration $C^0_{\mathrm{Cu}^{2+}} = 0$, gives pH = 4.22, with $\log K_{\mathrm{chry}} = 3.9279$, $\log K_{\mathrm{SiO}_{2(\mathrm{am})}} = -2.7136$, and unit activity coefficients. The effluent total copper concentration is equal to 1.58×10^{-2}M. The volume fraction of amorphous silica produced is given approximately by the relation

$$\phi_{\mathrm{SiO}_{2(\mathrm{am})}} \;=\; \frac{\overline{V}_{\mathrm{SiO}_{2(\mathrm{am})}}}{\overline{V}_{\mathrm{chry}}} \phi^0_{\mathrm{chry}} \;=\; 5.94 \times 10^{-4}, \tag{270}$$

for an initial chrysocolla volume fraction $\phi^0_{\mathrm{chry}} = 0.0015$, with $\overline{V}_{\mathrm{chry}} = 73.19$ and $\overline{V}_{\mathrm{SiO}_{2(\mathrm{am})}} = 29$ cm^3/mol.

To obtain the efficiency of copper leaching, the number of pore volumes of lixiviant necessary to remove all copper from the column, which is equivalent to the retardation of the chrysocolla dissolution front, must be calculated. The front velocity v is given by the expression

$$v \;=\; v_0 \frac{\phi[\mathrm{Cu}^{2+}]}{\phi[\mathrm{Cu}^{2+}] + \overline{\mathrm{V}}^{-1}_{\mathrm{chry}} \phi^0_{\mathrm{chry}}}, \tag{271}$$

where v_0 represent the average pore velocity. For a constant Darcy flow rate of 20 m/y and a porosity of 0.02, approximately 8 days are required to flush out a 22 m long column. The time to completely remove all copper from the system takes approximately 1.4 years according to the value of $v_0/v \simeq 66$ given by Eqn.(271).

For a more complicated example consider the system Cu–Ca–Si–S–$\mathrm{H_2O}$ in which gypsum is also allowed to form. The stability fields of various copper-bearing phases which may form in this system are shown in a pe-pH diagram displayed in Figure 6. The brochantite field is present only for sufficiently low concentrations of silica. At silica concentrations below saturation with chalcedony, the chrysocolla field is replaced by tenorite. According to the diagram dissolution of chrysocolla occurs if the pH remains below approximately 4. For an oxidizing inlet fluid with pH 1, in equilibrium with gypsum and amorphous silica, reacting with chrysocolla, secondary products gypsum and amorphous silica form with a

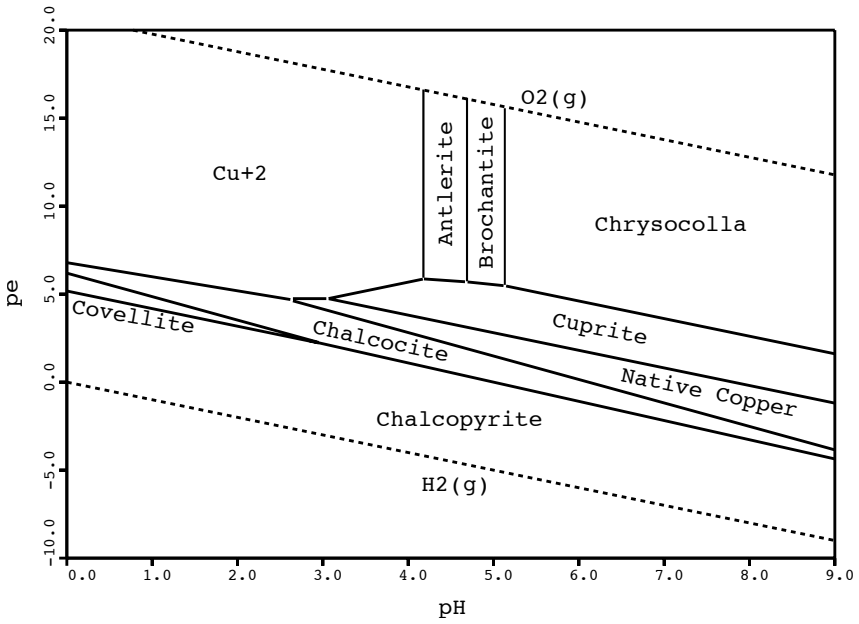

Figure 6. Activity diagram for the copper–sulfate–silica–iron system. The diagram is constructed with fixed activities of silica ($\log a_{\mathrm{SiO}_{2(\mathrm{aq})}} = -3$), sulfate ($\log a_{\mathrm{SO}_4^{2-}} = -2$), and iron ($\log a_{\mathrm{Fe}^{2+}} = -4$). The Cu^{2+} field is determined for $\log a_{\mathrm{Cu}^{2+}} = -2$.

consequent increase in pH. The resulting solution composition is listed in Table 4. The reaction zone sequence:

$$\underbrace{\mathrm{SiO}_{2(\mathrm{am})} + \mathrm{gypsum}}_{\mathrm{zone1}} \mid \underbrace{\mathrm{chrysocolla}}_{\mathrm{zone2}}, \tag{272}$$

is obtained in which gypsum and amorphous silica precipitate from solution as chrysocolla dissolves. These results can be expected to hold approximately for a kinetic description of mineral reaction rates given sufficiently long travel times and thus provides a simple interpretation of the much more complicated kinetic results.

Table 4. Local equilibrium reaction for the system Cu–Ca–Si–S–H_2O describing the dissolution of chrysocolla to form alteration products gypsum and amorphous silica. Concentration is in units of molality.

	inlet	zone 1	zone 2
pH	1.00	1.00	4.20
	primary species		
Cu^{2+}	6.61E-09	6.61E-09	5.48E-02
Ca^{2+}	1.31E-02	1.31E-02	6.78E-03
$SiO_{2(aq)}$	1.93E-03	1.93E-03	1.93E-03
SO_4^{2-}	2.66E-02	2.66E-02	6.16E-02
	aqueous complexes		
OH^-	1.42E-13	1.42E-13	2.32E-10
HSO_4^-	9.58E-02	9.58E-02	1.28E-04
$H_2SO_{4(aq)}$	7.07E-06	7.07E-06	5.81E-12
$HSiO_3^-$	2.93E-12	2.93E-12	4.77E-09
$CuOH^+$	1.57E-15	1.57E-15	1.97E-05
$CuSO_{4(aq)}$	3.39E-09	3.39E-09	5.44E-02
$CaOH^+$	8.54E-15	8.54E-15	6.68E-12
$CaSO_{4(aq)}$	4.25E-03	4.25E-03	4.25E-03
		mineral volume fraction(s)	
$\phi_{\text{ chrysocolla}}$	—	0.	5.00E-03
$\phi_{\text{ SiO}_{2(\text{am})}}$	—	1.98E-03	0.
$\phi_{\text{ gypsum}}$	—	2.96E-04	0.
ϕ	—	5.27E-02	5.00E-02
v/v_0	—	0.	7.401E-02

MULTIFLO Calculations. In this section the computer code MULTIFLO, a multiphase, multicomponent, nonisothermal reactive transport model (Lichtner and Seth, 1997), is used to simulate the leaching process of copper ore in a five-spot well pattern. The ore is assumed to be in the form of chrysocolla located primarily on fractures in a porphyry copper deposit. Gangue minerals are assumed to consist of quartz, kaolinite, muscovite and goethite representing a weathered zone in the ore deposit. Initial volume fractions and effective reaction rates are given in Table 5. A two-dimensional horizontal slice through the ore deposit is modelled.

The porosity of the oxide-ore zone is assumed to 0.1 with a permeability of 1.5×10^{-13} m^2. An injection and extraction rate of 40 gpm (2.52 liter/s) distributed over a depth of 120 m corresponding to the ore zone is used in the simulation. Hydraulic conductivity is assumed to be homogeneous and isotropic. Symmetry is imposed on the flow field requiring simulation of only one quarter of the five-spot pattern with no-flow boundary conditions imposed along the edges of the quarter flow field. The quarter-section of the five-spot pattern consists of a square domain 15 m on a side with quarter-strength injection and extraction wells located at the lower left and upper right corners, respectively. A spatial grid of 30×30 equally spaced nodes of 0.5 m was used in the simulation. A steady-state flow field is computed first which is then used in the reactive transport calculation. Calculations are carried out for a period of 5 years.

The initial and injection fluid compositions used in the calculations are presented in Tables 6 and 7 along with thermodynamic data used in the calculations. With the exception

Table 5. Mineral abundances and effective rate constants used for the five-spot copper leaching calculations.

mineral	volume fraction —	effective rate constant [moles cm^{-3} s^{-1}]
primary minerals		
chrysocolla	0.005	2×10^{-10}
goethite	0.025	1×10^{-11}
kaolinite	0.05	1×10^{-13}
muscovite	0.05	1×10^{-13}
quartz	0.82	1×10^{-14}
secondary minerals		
amorphous silica	0.	1×10^{-11}
gypsum	0.	1×10^{-10}
jarosite	0.	1×10^{-10}
jurbanite	0.	1×10^{-10}
alunite	0.	1×10^{-10}
antlerite	0.	1×10^{-10}
porosity	0.05	—

of the aqueous complex $CuSO_{4(aq)}$ and the minerals chrysocolla ($CuSiO_3 \cdot H_2O$) and jurbanite ($AlOHSO_4 \cdot 5H_2O$), all thermodynamic data were taken from the EQ3/6 database `data0.com.R16` at 25°C (Wolery, 1992). The equilibrium constants for $CuSO_{4(aq)}$ and jurbanite were taken from the MINTEQ database, version 3.0 (Allison et al., 1991). The molar volume for jurbanite was derived from data provided in Phillips and Griffin (1981) who reported a specific density of 1.78–1.83 g/cm^3. The equilibrium constant for chrysocolla was determined by assuming equilibrium between the assemblage chrysocolla–tenorite–chalcedony, with equilibrium constants for tenorite and chalcedony taken from the EQ3/6 database.

The initial fluid composition was computed assuming a pH of 8 and equilibrium with minerals calcite, muscovite, kaolinite, goethite, chalcedony, and chrysocolla. The total concentration of sodium was fixed at 5×10^{-3} M, sulfate at 5×10^{-4} M, and the chloride concentration was determined by charge balance. A partial pressure of $CO_{2(g)}$ of 10^{-3} bars was assumed. The composition of the raffinate was assumed to be constant during the course of the simulation. The raffinate was in equilibrium with minerals jarosite, gypsum, amorphous silica, and goethite at a pH of 1. Total sulfate was determined by charge balance.

Table 6. Initial aqueous solution composition in equilibrium with gangue minerals.

```
ionic strength =  7.4758E-03
pH =  8.0000     pe =  12.601     eh =  0.7454
species    molality      psi   act. coef.  act. ratio/H+  constraint
na+       5.0000E-03  5.0000E-03  0.9133       5.664     1 total
k+        2.5768E-05  2.5768E-05  0.9111       3.376     3 muscovite
ca+2      6.5026E-04  6.8569E-04  0.7067       12.74     3 calcite
h+        1.0837E-08  1.5399E-05  0.9228          0.     8 pH
cu+2      6.4090E-09  3.2342E-08  0.7067       7.737     3 chrysocolla
al+3      2.8166E-17  2.0413E-08  0.4824       7.345     3 kaolinite
fe+2      1.2435E-23  3.5980E-12  0.7067      -6.975     3 goethite
sio2(aq)  1.8703E-04  1.8703E-04   1.000      -3.728     3 chalcedony
hco3-     1.6819E-03  1.7418E-03  0.9133      -10.74     4 co2(g)
so4-2     4.8021E-04  5.0000E-04  0.6942      -19.25     1 total
cl-       3.6709E-03  3.6709E-03  0.9111      -10.40    -1 chrg
o2(aq)    2.5277E-04  2.5277E-04   1.000      -3.597     4 o2(g)

complex      molality     act. coef.  act/H+     log K
co2(aq)      3.39703E-05  1.0000     -4.4689     6.3447
caso4(aq)    1.97849E-05  1.0000     -4.7037     2.1111
co3-2        1.03300E-05 0.69743     -20.916    -10.329
cahco3+      8.60589E-06 0.91328      2.8999     1.0467
caco3(aq)    7.03072E-06  1.0000     -5.1530    -7.0017
oh-          1.10869E-06 0.91220     -13.920    -13.995
cuoh+        2.55797E-08 0.91328     0.37299    -7.2875
al(oh)4-     1.94646E-08 0.91328     -15.676    -22.883
caoh+        7.10715E-09 0.91328    -0.18321    -12.850
al(oh)3(aq)  9.45040E-10  1.0000     -9.0245    -16.158
hso4-        3.47879E-10 0.91328     -17.424     1.9791
cuso4(aq)    3.08271E-10  1.0000     -9.5111     2.3100
cucl+        4.53657E-11 0.91328     -2.3782    0.43700
al(oh)2+     3.78482E-12 0.91328     -3.4569    -10.595
fe(oh)3(aq)  3.42373E-12  1.0000     -11.465    -3.5100

                    mineral saturation indices
 mineral         log S.I.   log K     mineral        log S.I.     log K
chrysocolla    0.          -3.928     cuprite       -18.53     -35.64
quartz         0.2712       3.999     gypsum         -2.332      4.482
chalcedony     0.           3.728     alunite       -13.84       0.3479
sio2(am)      -1.015        2.714     alohso4        -9.114      3.230
kaolinite      0.          -6.810     calcite         0.         -1.849
gibbsite      -0.6229      -7.756     anorthite      -7.106     -26.58
k-feldspar    -0.4052       0.2753    albite         -1.156      -2.764
muscovite      0.         -13.59      tenorite        0.         -7.656
goethite       0.           7.955     chalcanthite   -9.200      2.622
jarosite     -24.61        34.84      brochantite    -4.289     -15.44
aragonite     -0.1444      -1.993     antlerite      -5.239      -8.730
malachite     -1.442       -5.940

gas   log partial pressure   pressure
o2(g)         -0.6990        0.2000
co2(g)        -3.000         1.0000E-03

charge balance - q =  -1.0307E-16

solution density =   1.0005     g/cm^3
```

Table 7. Aqueous solution composition of the lixiviant.

```
ionic strength =  0.4995
pH =  1.0000     pe =  19.601     eh =   1.160
species    molality      psi   act. coef.  act. ratio/H+  constraint
na+       5.0000E-03  5.0000E-03  0.6810      -1.397     1 total
k+        1.2647E-04  1.2647E-04  0.6420      -2.994     3 jarosite
ca+2      1.1037E-02  1.5291E-02  0.2610     -0.1500     3 gypsum
h+        0.1249      0.3293      0.8009          0.     8 pH
cu+2      6.2008E-09  1.0000E-08  0.2610      -6.400     1 total
al+3      6.2276E-03  2.5000E-02  9.2949E-02  0.5050     1 total
fe+2      3.3666E-09  4.3435E-02  0.2610      -6.666     3 goethite
sio2(aq)  1.9337E-03  1.9337E-03   1.000      -2.714     3 sio2(am)
hco3-     2.2555E-09  3.3971E-04  0.6810      -9.550     4 co2(g)
so4-2     6.1235E-02  0.2608      0.1867      -3.020    -1 chrg
cl-       5.0000E-03  5.0000E-03  0.6420      -3.205     1 total
o2(aq)    2.5277E-04  1.1112E-02   1.000      -3.597     4 o2(g)

complex      molality     act. coef.  act/H+     log K
hso4-        0.16001     0.68102     -1.6994     1.9791
fe+3         3.68344E-02 9.29493E-02  1.2769     8.4900
also4+       9.94509E-03 0.68102     -1.0988     3.0100
al(so4)2-    8.82703E-03 0.68102     -2.9577     4.9000
feso4+       4.86569E-03 0.68102     -1.4093     10.418
caso4(aq)    4.25402E-03  1.0000     -2.3712     2.1111
fe(so4)2-    1.07510E-03 0.68102     -3.8721     11.704
fehso4+2     6.59083E-04 0.20595     -1.3739     10.030
co2(aq)      3.39703E-04  1.0000     -3.4689     6.3447
h2so4(aq)    1.08970E-05  1.0000     -4.9627    -1.0209
fe(oh)2+     1.07483E-06 0.68102     -5.0651     2.8200
aloh+2       3.10241E-07 0.20595     -4.7012    -4.9571
cuso4(aq)    3.77836E-09  1.0000     -8.4227     2.3100
feso4(aq)    1.59239E-09  1.0000     -8.7980     2.2000
cahco3+      7.23489E-11 0.68102     -9.2370     1.0467
cucl+        2.08650E-11 0.68102     -9.7770    0.43700
fe(oh)3(aq)  3.42373E-12  1.0000     -11.465    -3.5100
al(oh)2+     2.16223E-12 0.68102     -10.762    -10.595

                  mineral saturation indices
 mineral        log S.I.    log K     mineral        log S.I.    log K
chrysocolla   -13.43       -3.928     cuprite        -47.42    -35.64
quartz          1.286       3.999     gypsum           0.        4.482
chalcedony      1.015       3.728     alunite        -11.34      0.3479
sio2(am)        0.          2.714     alohso4         -0.9492    3.230
kaolinite     -12.71       -6.810     calcite        -12.20     -1.849
gibbsite       -7.993      -7.756     anorthite      -33.02    -26.58
k-feldspar    -11.19        0.2753    albite         -12.61     -2.764
muscovite     -25.53      -13.59      tenorite       -14.45     -7.656
goethite        0.          7.955     chalcanthite    -8.111     2.622
jarosite        0.         34.84      brochantite    -46.54    -15.44
aragonite     -12.35       -1.993     antlerite      -33.04     -8.730
malachite     -29.34       -5.940

gas   log partial pressure   pressure
o2(g)         -0.6990        0.2000
co2(g)        -2.000         1.0000E-02

charge balance - q =   2.3027E-12

solution density =   1.0520     g/cm^3
```

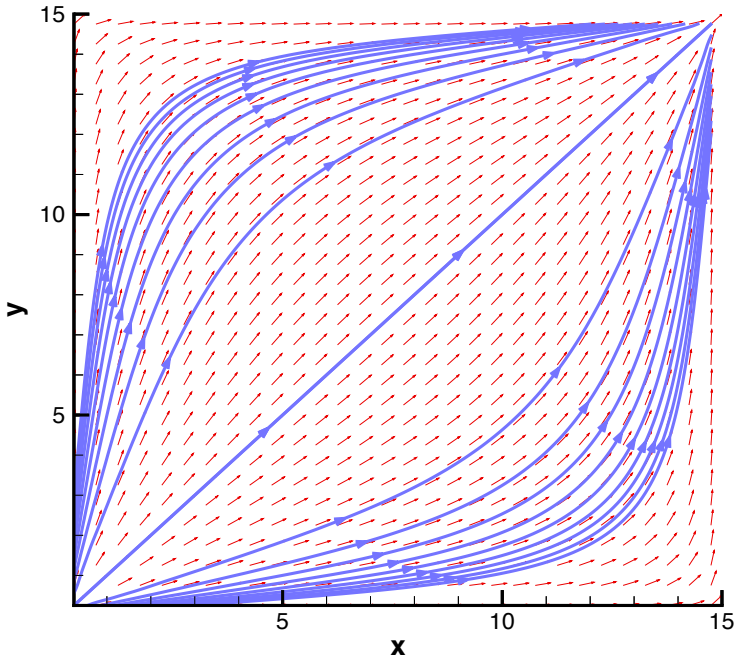

Figure 7. Steady-state velocity field showing streamlines from the injection well to the extraction well in a quarter section of a five-spot well pattern.

Results. A two-dimensional horizontal slice through the ore deposit is modelled. The steady-state velocity profile is shown in Figure 7. The flow velocity varies spatially throughout the symmetry element. It is largest at the injection and extraction wells, and smallest in the opposite corners of the leach field.

The copper recovery is shown in Figure 8 plotted as a function of time. This corresponds to the copper concentration of the solution at the extraction well referred to as the pregnant leach solution (PLS). The copper recovery begins to decline after an elapsed time of approximately 0.4 years. The gradual decline from 0.4 to approximately 1.1 years is caused by the reduction in surface area of the remaining chrysocolla. A steeper drop occurs after 1.1 years as all of the chrysocolla is leached from the formation, but at a much lower copper recovery compared to the earlier stages of the leach operation.

The pH of the PLS is shown in Figure 9 plotted as a function of time. The pH reaches a plateau of approximately 4.2 and then drops to the inlet pH as all chrysocolla is leached. The plateau value agrees with the value obtained from the pure advection local equilibrium model at the chrysocolla dissolution front (see Table 4).

Spatial profiles after an elapsed time of one quarter year are shown for chrysocolla (Figure 10), porosity (Figure 11), gypsum (Figure 12), amorphous silica (Figure 13), jurbanite (Figure 14), jarosite (Figure 15) and alunite (Figure 16). Precipitation of amorphous silica and gypsum occur near the injection well. Precipitation of jurbanite results in a reduction in porosity across the flow field which could be detrimental to the leach operation if complete sealing of the pore spaces were to occur. It should be noted, however, that considerable uncertainty exists in thermodynamic properties and stable mineral phases at high aluminum concentrations in acidified groundwater (Nordstrom, 1982; Nordstrom and Ball, 1986; Filipek et al., 1987; Glynn and Brown, 1996).

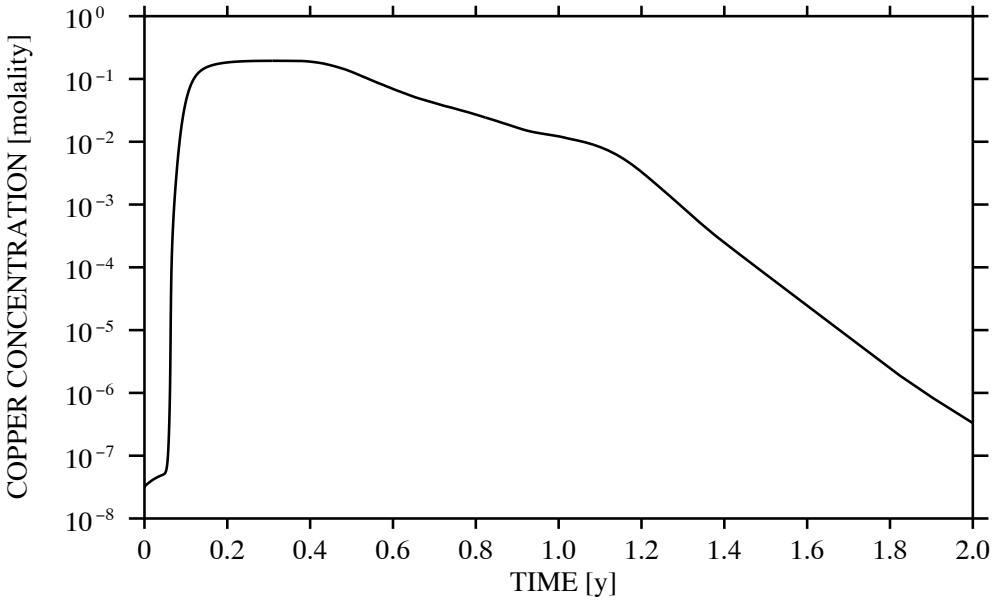

Figure 8. Copper recovery plotted as a function of time

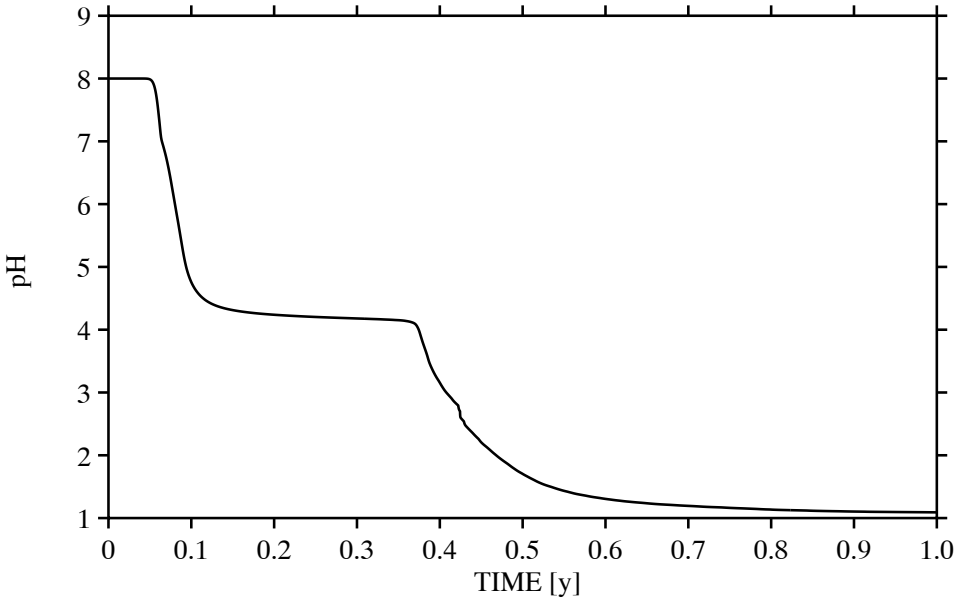

Figure 9. The pH of the PLS plotted as a function of time

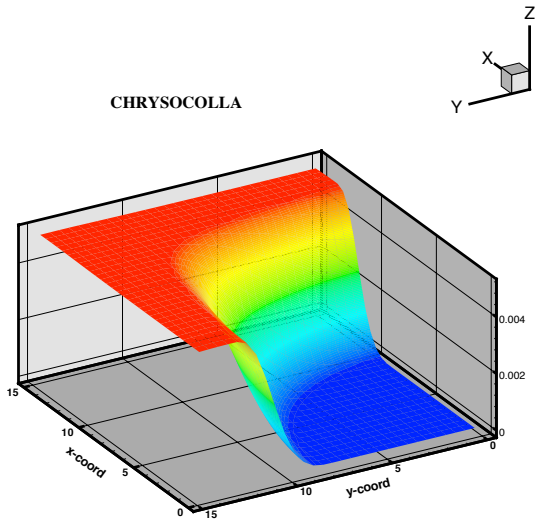

Figure 10. Chrysocolla profile at 0.25 year

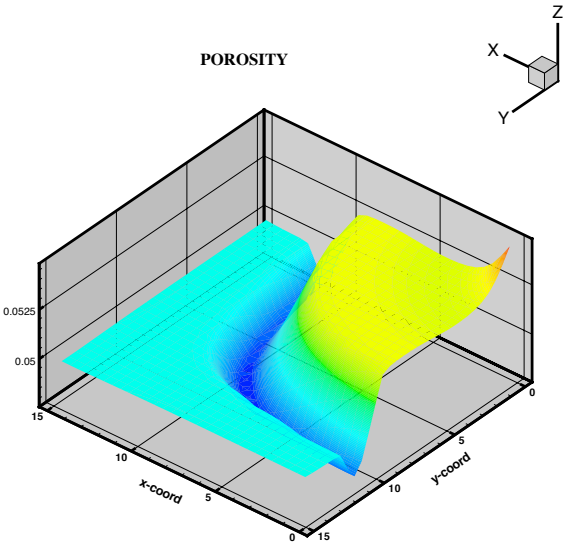

Figure 11. Porosity profile at 0.25 year

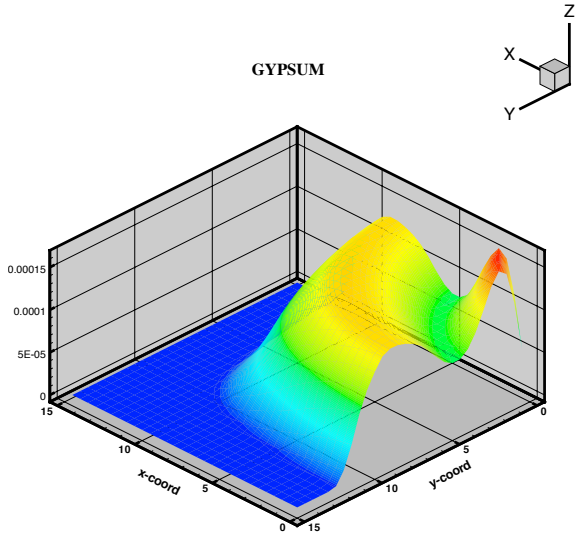

Figure 12. Gypsum profile at 0.25 year

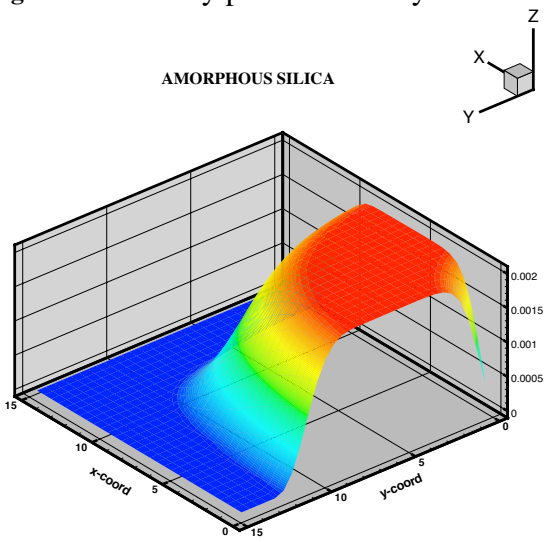

Figure 13. Amorphous silica profile at 0.25 year

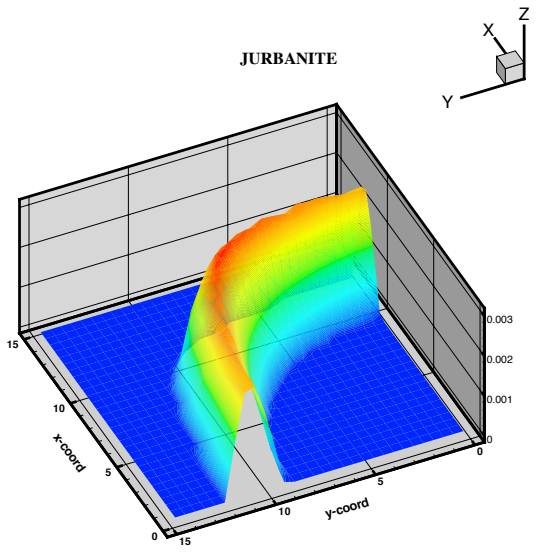

Figure 14. Jurbanite profile at 0.25 year

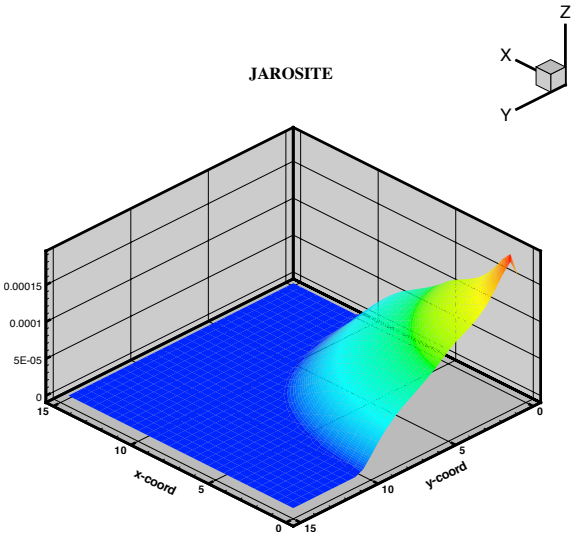

Figure 15. Jarosite profile at 0.25 year

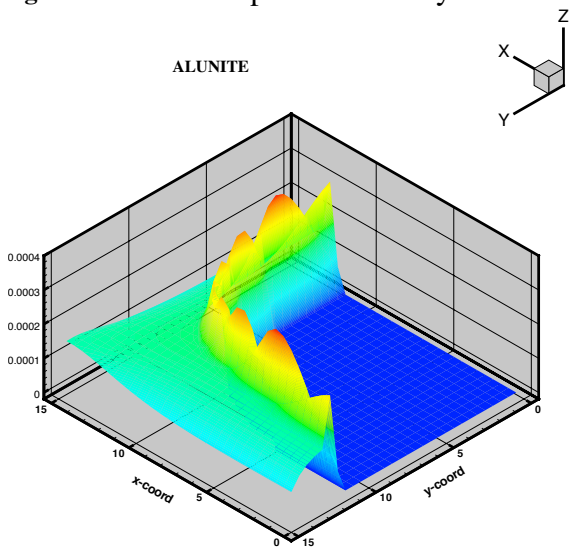

Figure 16. Alunite profile at 0.25 year

Acid Mine Drainage

Pyrite oxidation in abandoned mines and mine tailings causes the production of acid which in turn leads to mobilization of heavy metals with consequent pollution of the environment. As oxidizing water infiltrates through a column of rock containing pyrite, oxygen is consumed by the pyrite resulting in the precipitation of iron oxide and formation of acid. A partially saturated environment provides a continuous source of oxygen limited only by its rate of diffusion through the gas phase. The net amount of acid produced depends on the neutralization capacity of the gangue minerals in the host rock, the rate of consumption of oxygen by pyrite, and the rate of diffusion of oxygen through the partially saturated zone. This example also provides an interesting case of parallel linearly-dependent reactions to describe the oxidation rate of pyrite.

To illustrate the production of acid resulting from pyrite oxidation a hypothetical situation is considered in which local equilibrium is assumed for all aqueous reactions including the Fe(III)–Fe(II) redox couple and sulfate reduction. The effects of bacteria *Thiobacillus* and *Ferrobacillus ferrooxidans* on pyrite oxidation are not directly considered; however, the assumption of local equilibrium of redox species provides an endmember case of their catalytic effect. It should be emphasized that the values of parameters for various physical properties used in the calculation may not be representative of an actual field situation.

In this example pyrite is assumed to be oxidized by downward percolating water initially in equilibrium with the atmosphere. The host rock is represented by weathered material composed of gangue minerals quartz, K-feldspar and kaolinite with minor amounts of pyrite. The rock composition used in the calculation is 4% pyrite, 20% K-feldspar and kaolinite, and 40% quartz providing a weak neutralizing capacity of the acid produced by pyrite oxidation. The porosity of the rock is 16%. The minerals are assumed to be distributed uniformly throughout a one-dimensional vertical column with the exception of pyrite which is absent from the first 1 m of the profile where the porosity becomes 20%. A column of height 20 m with the water table located at a depth of 10 m is modelled. The spatial grid used in the calculation consists of 200 equally spaced nodes with a grid spacing of 0.1 m. A steady-state liquid saturation profile is assumed consistent with an infiltration rate of 0.1 m y^{-1} as shown in Figure 17. Gaseous diffusion coefficients used in the calculation for oxygen and carbon dioxide are assumed to be equal with the value 2.13×10^{-5} m^2 s^{-1}. Aqueous diffusion is assumed to be species-independent with the value of 10^{-9} m^2 s^{-1}. Dispersion is not considered. Tortuosity coefficients are set to unity for both aqueous and gaseous diffusion. Effects of changes in porosity on transport are not taken into account in the calculations.

Eight primary species are used to represent the chemical system consisting of the species K^+, Fe2+, Al^{3+}, H^+, $Sio_{2(aq)}$, SO_4^{2-}, HCO_3^-, and $O_{2(aq)}$. The composition of the infiltrating fluid is assumed to be in equilibrium with quartz and ferrihydrite with a pH of 5 and with a partial pressure of oxygen of 0.2 bars and CO_2 of 10^{-2} bars. Total concentrations of K^+ and Al^{3+} are assumed to have the values 1×10^{-4} and 1×10^{-8} molal, respectively. Sulfate is determined by charge balance. The resulting solution composition is listed in Table 8.

The initial fluid in the column is assumed to be in equilibrium with primary host rock minerals quartz, kaolinite, K-feldspar, and pyrite, in addition to muscovite with a pH of 7 and with a partial pressure of oxygen of 0.2 bars and CO_2 of 10^{-3} bars. Total Fe^{2+} is set at 1×10^{-4} molal. The resulting solution composition is listed in Table 9.

Oxidation of pyrite is represented by two parallel linearly-dependent rate laws. The

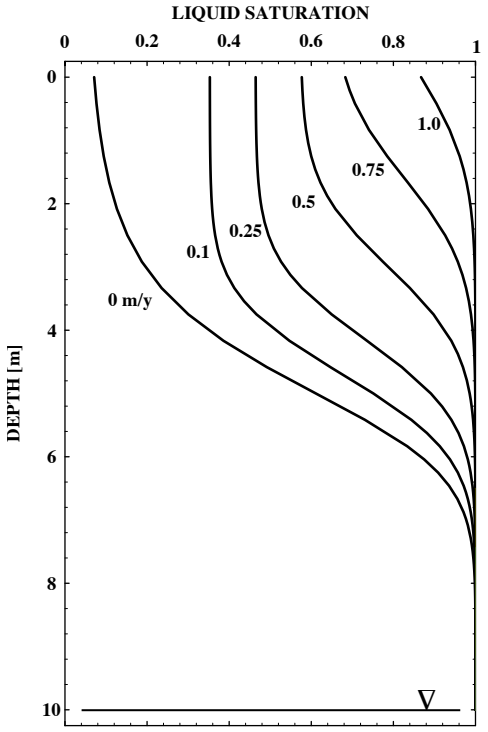

Figure 17. Liquid saturation above the water table plotted as a function of depth for different infiltration rates based the van Genuchten equation for relative permeability [See Lichtner (1996)].

first is based on the work of Williamson and Rimstidt (1994) valid for the pH range 2–10 in the presence of dissolved oxygen given by

$$k \;=\; k_1\, m_{\mathrm{O_{2(aq)}}}^{0.5}\, m_{\mathrm{H^+}}^{-0.11}. \tag{273}$$

with $k_1{=}10^{-12}$ moles cm^{-2} s^{-1}. This rate law requires the presence of dissolved oxygen for pyrite oxidation to occur. The second form is the usual transition state rate law, but with a smaller rate constant equal to $k{=}2.5 \times 10^{-14}$ moles cm^{-2} s^{-1}. For both rates the rate constant is multiplied by the usual affinity factor so that the rate goes to zero when the fluid composition is in equilibrium with pyrite. A specific pyrite surface area of 10 cm^{-1} is used in the calculations. The surface areas of primary minerals are allowed to vary according to the the two thirds power of the mineral volume fraction.

Effective rate constants ($k_m s_m$) of 10^{-15} moles cm^{-3} s^{-1} for quartz, 10^{-14} moles cm^{-3} s^{-1} for K-feldspar, and $10^{-13.5}$ moles cm^{-3} s^{-1} for kaolinite are used in the calculation. For the secondary products ferrihydrite, alunite, jarosite, and $KAlSO_4$ (jubanite) a rate constant of 10^{-11} moles cm^{-3} s^{-1} was used in the calculation representing close to local equilibrium rates.

A number of different cases may considered. One is to study the effect of oxygen consumption by pyrite oxidation and the supply of oxygen by diffusion from the atmosphere. A second case is to investigate the effect of the pyrite rate law on acid production. And a third to study the effect of acid neutralization by gangue minerals in the host rock by varying the kaolinite rate constant, for example. Results are presented for the base case with the parameters described above. The calculation was carried out to 50 years. Variable time-stepping was used with a maximum time step of 2 years. A fully implicit finite difference algorithm was used in the calculation.

Results for Base Case

Shown in Figure 18 is the pH at a depth of 20 m plotted as a function of time. With increasing time the pH reaches a minimum of approximately 1.5 and then begins to slowly increase. Approximately 30 y are required before the acid plume reaches a depth of 20 m. The spatial pH profile is shown in Figure 19. With increasing time the pH approaches a stationary state with a minimum pH of approximately 0.5 at a depth of 6 m. The corresponding $O_{2(g)}$ concentration plotted for different times is shown in Figure 20 which decreases with depth as pyrite is oxidized. These results differ from those presented in Lichtner (1996) in which a gaseous diffusion coefficient one order of magnitude larger was used in the calculation.

The pyrite dissolution rate for each linearly-dependent parallel reaction is shown in Figure 21. The transition state dissolution rate is approximately constant with depth with a slight increase in magnitude as pyrite comes to equilibrium at a depth of approximately 6 m. The increase in rate is caused by a larger surface area due to less dissolution of pyrite compared to that nearer to the ground surface. By contrast the rate law proportional to the square root of the oxygen partial pressure goes to zero higher in the column as oxygen is depleted. Comparing the rates with the corresponding pH profile, it is clear that the transition state rate law generates more acid compared to oxygen limited rate law. Presumably the pyrite oxidation mechanisms correspond to reactions of the form Eqns.(198a) and (198b) for oxidation by dissolved oxygen and Fe^{3+}, respectively. Clearly the latter reaction leads to a greater production of acid. Ideally the transition state rate law would come into play only in regions of high Fe^{3+} concentration. The transition state rate law does not depend on the details of the reaction, i.e. whether reaction (198a) or (198b) is applicable. It is always in a far-from-equilibrium state regardless of whether dissolved oxygen is present or not, until finally equilibrium with pyrite is approached and the affinity factor begins to play a role.

Finally mineral volume fractions shown in Figures 22 and 23 for elapsed times of 25 and 50 years. Pyrite is oxidized over a depth of approximately 6 m with precipitation of secondary products ferrihydrite, jarosite and jurbanite. The secondary products form essentially constant alteration zones which increase in concentration while remaining fixed in position with increasing time.

It must be emphasized that the results presented here are only meant to be qualitative, at best, because of the high ionic strength solutions which are generated, the uncertainty in rate laws and surface areas, and the uncertainty in the alteration products which form and in their thermodynamic properties.

Table 8. Aqueous solution composition of the infiltrating fluid.

```
ionic strength =  1.6000E-04
pH =  5.0000     pe =  15.601     eh =   .9229
species    molality      psi   act. coef.  act. ratio/H+  constraint
k+        9.9964E-05  1.0000E-04   1.000       .9998     1 total
fe+2      2.0200E-13  1.8123E-06   1.000      -2.695     3 ferrihydrite
al+3      4.1168E-09  1.0000E-08   1.000       6.615     1 total
h+        1.0000E-05  3.4790E-04   1.000       .0000     8 pH
sio2(aq)  1.0016E-04  1.0016E-04   1.000      -3.999     3 quartz
so4-2     4.8163E-05  4.8245E-05   1.000      -14.32    -1 chrg
hco3-     1.5360E-05  3.5506E-04   1.000      -9.814     4 co2(g)
o2(aq)    2.5277E-04  2.5323E-04   1.000      -3.597     4 o2(g)

complex      molality     act. coef.  act/H+     log K
co2(aq)      3.39703E-04  1.0000     -3.4689     6.3447
fe(oh)2+     1.68267E-06  1.0000     -.77400     2.8200
fe(oh)3(aq)  7.87046E-08  1.0000     -7.1040    -3.5100
feoh+2       5.08159E-08  1.0000      2.7060     6.3000
hso4-        4.58999E-08  1.0000     -12.338     1.9791
kso4-        3.64883E-08  1.0000     -12.438     .87960
aloh+2       4.54422E-09  1.0000      1.6575    -4.9571
h3sio4-      1.11738E-09  1.0000     -13.952    -9.9525
al(oh)2+     1.04727E-09  1.0000     -3.9799    -10.595
oh-          1.01135E-09  1.0000     -13.995    -13.995
al(oh)3(aq)  2.86325E-10  1.0000     -9.5431    -16.158
fe+3         7.87046E-11  1.0000      4.8960     8.4900
co3-2        7.20444E-11  1.0000     -20.142    -10.329
al(oh)4-     5.38591E-12  1.0000     -16.269    -22.883
fe(oh)4-     1.97697E-12  1.0000     -16.704    -13.110

                  mineral saturation indices
mineral         log S.I.    log K     mineral        log S.I.     log K
ferrihydrite   1.3501E-15   3.594     k-feldspar     -4.108       .2753
pyrite         -236.1      -217.4     muscovite      -4.740      -13.59
siderite       -12.32       .1920     alohso4        -4.473       3.230
melanterite    -14.66       2.349     jurbanite      -3.898       3.805
gibbsite       -1.141      -7.756     alunite        -7.443       .3479
kaolinite      -1.580      -6.810     jarosite       -3.576       34.84
quartz          .0000       3.999

gas   log partial pressure   pressure
o2(g)         -.6990            .2000
co2(g)        -2.000          1.0000E-02
h2(g)         -41.20          6.2659E-42
h2s(g)        -137.5          3.4376-138

charge balance - q =   1.8955E-21

solution density =   1.0001     g/cm^3
```

Table 9. Initial aqueous solution composition of the initial fluid.

```
ionic strength =  9.4157E-03
pH =  7.0000     pe = -2.6863     eh =  -.1589
species    molality      psi   act. coef.  act. ratio/H+  constraint
k+        6.1951E-03  6.3368E-03   1.000       4.792     3 k-feldspar
fe+2      6.7648E-05  1.0000E-04   1.000       9.830     1 total
al+3      8.5222E-15  1.7303E-09   1.000       6.931     3 muscovite
h+        1.0000E-07  3.3808E-05   1.000       .0000     8 pH
sio2(aq)  1.0016E-04  1.0027E-04   1.000      -3.999     3 quartz
so4-2     3.0174E-03  3.1915E-03   1.000      -16.52    -1 chrg
hco3-     1.5360E-04  1.8765E-04   1.000      -10.81     4 co2(g)
o2(aq)    1.7939E-69 -1.7507E-10   1.000      -68.75     3 pyrite

complex      molality     act. coef.  act/H+     log K
kso4-        1.41673E-04  1.0000     -10.849     .87960
co2(aq)      3.39703E-05  1.0000     -4.4689     6.3447
feso4(aq)    3.23515E-05  1.0000     -4.4901     2.2000
h3sio4-      1.11738E-07  1.0000     -13.952    -9.9525
oh-          1.01135E-07  1.0000     -13.995    -13.995
co3-2        7.20444E-08  1.0000     -21.142    -10.329
hso4-        2.87566E-08  1.0000     -14.541     1.9791
al(oh)4-     1.11494E-09  1.0000     -15.953    -22.883
al(oh)3(aq)  5.92721E-10  1.0000     -9.2271    -16.158
hs-          4.52009E-11  1.0000     -17.345    -138.32
h2s(aq)      4.39387E-11  1.0000     -10.357    -131.33
al(oh)2+     2.16795E-11  1.0000     -3.6639    -10.595
fe(oh)3(aq)  1.36045E-11  1.0000     -10.866    -3.5100
khso4(aq)    1.21699E-11  1.0000     -10.915     .81360
fe(oh)2+     2.90858E-12  1.0000     -4.5363     2.8200
h2(aq)       1.84694E-12  1.0000     -11.734    -46.107
aloh+2       9.40698E-13  1.0000      1.9734    -4.9571
h2sio4-2     1.09825E-13  1.0000     -26.959    -22.960
fe(oh)4-     3.41729E-14  1.0000     -20.466    -13.110
feoh+2       8.78378E-16  1.0000     -1.0563     6.3000
h2so4(aq)    2.87566E-18  1.0000     -17.541    -1.0209
fe+3         1.36045E-20  1.0000      1.1337     8.4900

                  mineral saturation indices
mineral         log S.I.    log K     mineral        log S.I.     log K
ferrihydrite    -3.762       3.594    k-feldspar     1.5429E-15    .2753
pyrite         -4.9374E-14  -217.4    muscovite      1.0800E-14  -13.59
siderite        -.7913       .1920    alohso4        -6.360       3.230
melanterite     -4.341       2.349    jurbanite      -5.785       3.805
gibbsite        -.8254      -7.756    alunite        -7.109       .3479
kaolinite       -.9476      -6.810    jarosite       -15.48       34.84
quartz           .0000       3.999

gas   log partial pressure   pressure
o2(g)          -65.85          1.4194E-66
co2(g)         -3.000          1.0000E-03
h2(g)          -8.629          2.3521E-09
h2s(g)         -9.369          4.2761E-10

charge balance - q =  -7.8493E-19

solution density =   1.0006     g/cm^3
```

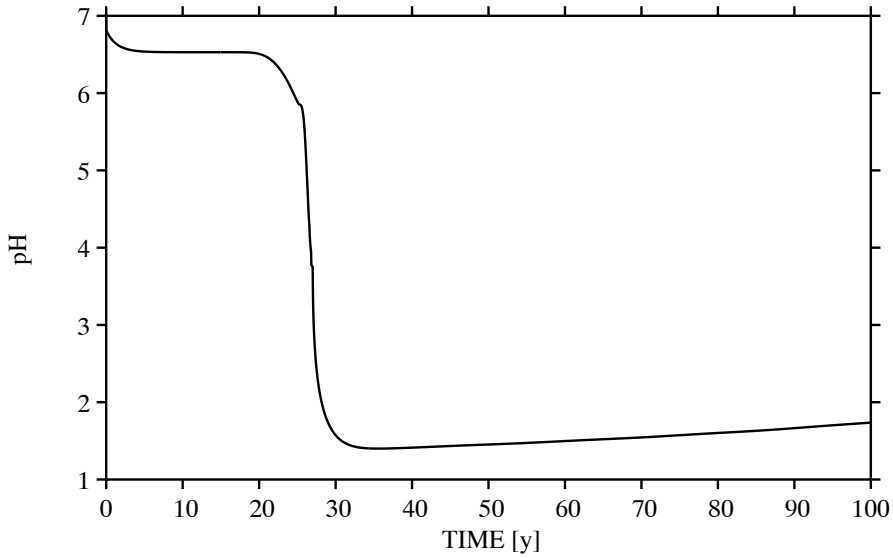

Figure 18. The pH plotted as a function of time at a depth of 20 m.

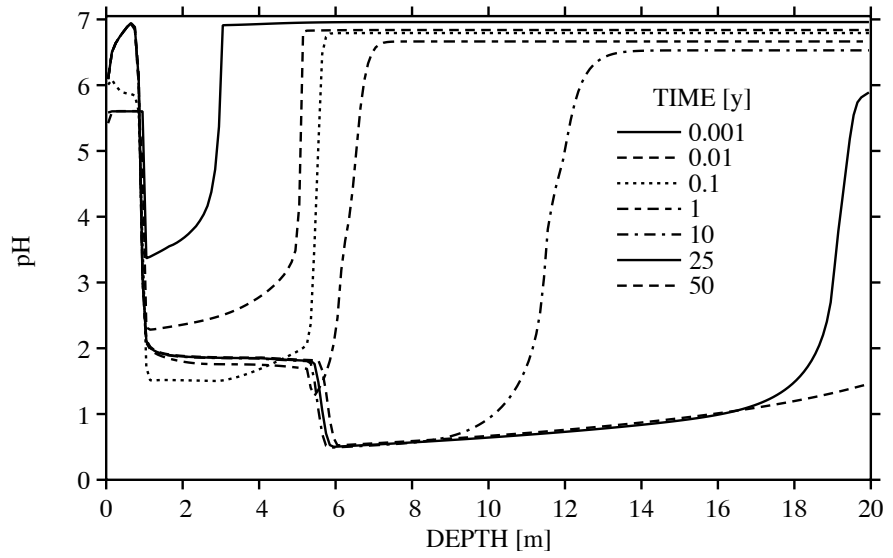

Figure 19. The pH plotted as a function of depth for elapsed times indicated in the figure.

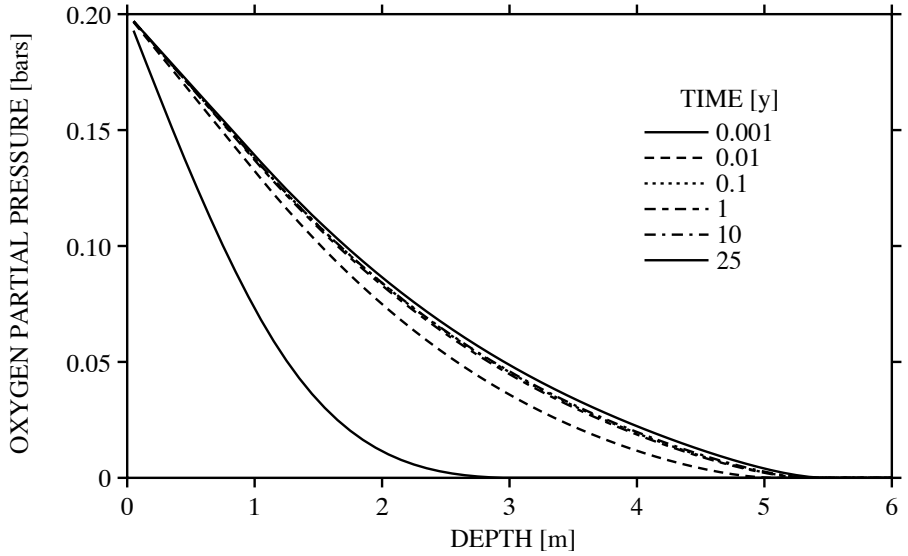

Figure 20. The concentration of gaseous oxygen plotted as a function of depth for an elapsed time of 25 y.

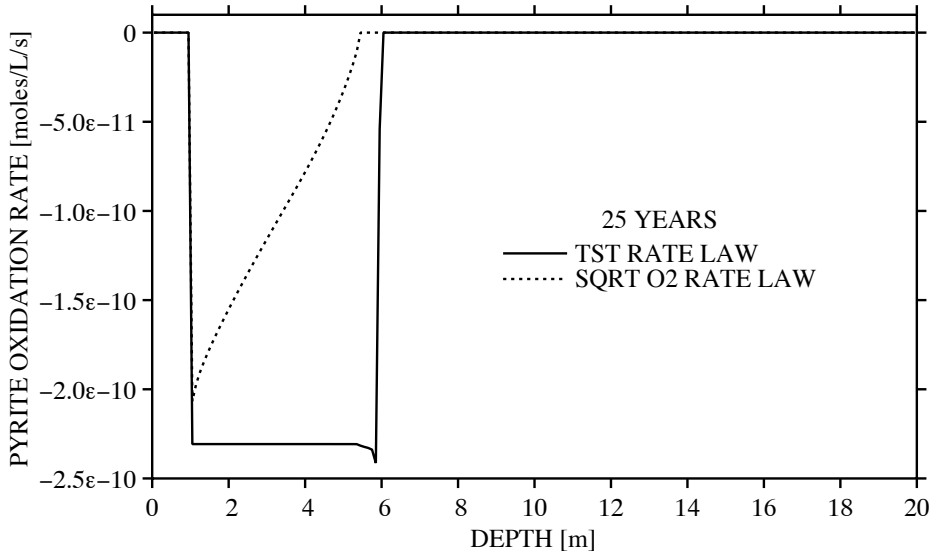

Figure 21. Pyrite reaction rates plotted as a function of depth for an elapsed time of 25 y.

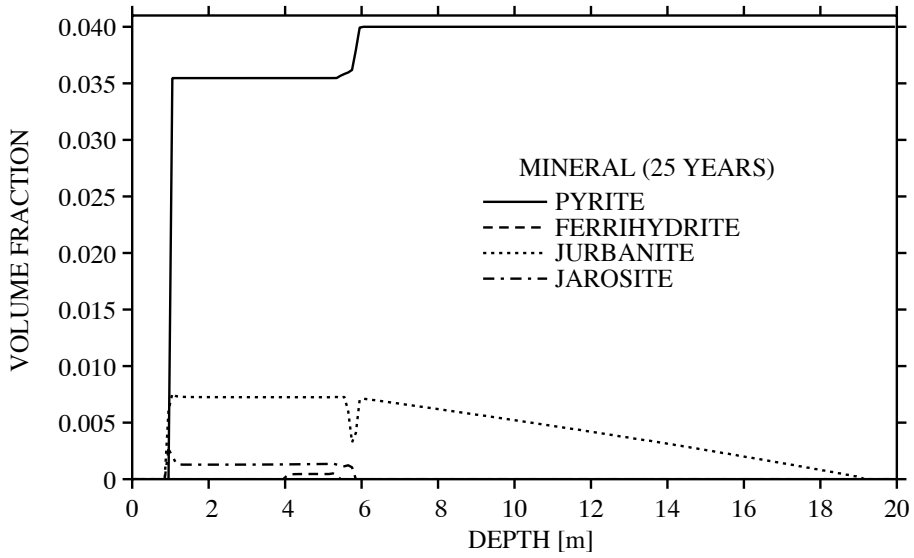

Figure 22. Mineral volume fractions plotted as a function of depth for an elapsed time of 25 y.

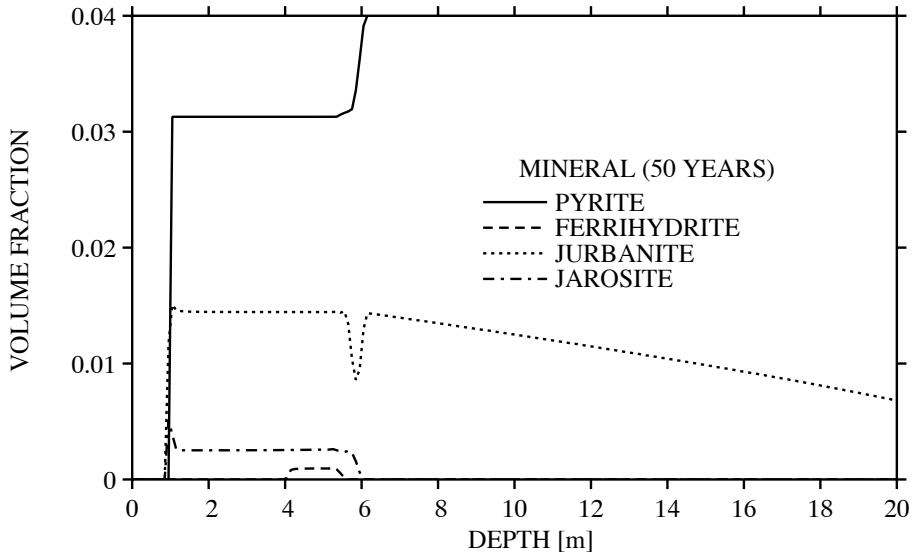

Figure 23. Mineral volume fractions plotted as a function of depth for an elapsed time of 50 y.

SUMMARY

A general formulation of reactive transport equations in a porous medium has been presented including homogeneous reactions of aqueous species, heterogeneous reactions of minerals, and microbiological processes. The canonical form of chemical reactions was introduced and the transformation between primary or basis species derived. The use of parallel linearly-dependent reactions was discussed for incorporating different reaction rate mechanisms. It was demonstrated how the electron may be used in reactive transport equations with redox reactions formulated in terms of half-cell reactions. A single component system was investigated for both a one-dimensional porous medium and a two-dimensional geometry incorporating fracture-matrix interaction. Finally two multicomponent examples were considered using the computer code MULTIFLO of *in situ* leaching of copper ore and acid mine drainage.

REFERENCES

Aagaard P., and Helgeson, H.C. (1982) Thermodynamic and kinetic constraints on reaction rates among minerals and aqueous solutions. I. Theoretical considerations. American Journal of Science 282:237–285.

Allison J.D., Brown D.S. and Novo-Gradac K.J. (1991) MINTEQA2/PRODEFA2, A geochemical assessment model for environmental systems: Version 3.0 user's manual. EPA/600/3-91/021. Athens, GA. Environmental Protection Agency.

Aris, R. and Mah, R.H.S. (1963) Independence of chemical reactions. I & EC Fundamentals 2:90–94.

Bear, J. (1972) Dynamics of fluids in porous media. Elsevier. 764 pp.

Blum, A.E., and Stillings, L.L. (1995) Feldspar dissolution kinetics. (eds. White, A.F. and Brantley, S.L.) Chapter 7, Reviews in Mineralogy 34:291–351.

Boudart, M. and Djéga-Mariadassou (1984) Kinetics of Heterogeneous catalytic reactions, Princeton University Press. 222 pp.

Christensen, D.R., and McCarty, P.L. (1975) Multiprocess biological treatment model. J. Water Pollution Control Federation 47:2652–2664.

Damköhler, Von G. (1936) Einflüsse der strömung, diffusion und des wärmeüberganges auf die leistung von reactionsöfen. Zeitschrift Elektrochem. 42:846–862.

Denbigh, K. (1981) The Principles of Chemical Equilibrium. Cambridge University Press, Fourth Edition, 494 pp.

Filipek, L.H., Nordstrom, D.K., and Ficklin, W.H. (1987) Interaction of acid mine drainage with waters and sediments of west squaw creek in the west Shasta mining district, California. Environment and Science and Technology, 21:388–396.

Glynn, P., and Brown, J. (1996) Reactive transport modeling of acidic metal-contaminated groundwater at a site with sparse spatial information. Eds. Lichtner, P.C., Steefel, C.I., and Oelkers, E.H. Reviews in Mineralogy 34:377–438.

Gupta, A.D., Lake, L.W., Pope, G.A., Sephernoori, K., and King, M.J. (1991) High–resolution monotonic schemes for reservoir fluid flow simulation. In Situ., 15:289–317.

Helgeson, H.C., Murphy, W.M., and Aagaard P. (1984) Thermodynamic and kinetic constraints on reaction rates among minerals and aqueous solutions. II. Rate constants, effective surface area, and the hydrolysis of feldspar. Geochimica et Cosmochimica Acta, 51:3137–3153.

Horiuti, J. (1957) Stoichiometrische Zahlen und die Kinetik der chemischen Reaktionen. Catalysis Jour. 5:1–26.

Langmuir, D. (1997) Aqueous environment geochemistry. Prentice Hall. 600 pp.

Lasaga, A.C. (1981) Rate laws in chemical reactions. In Kinetics of Geochemical Processes, Reviews in Mineralogy (A.C. Lasaga and R.J. Kirkpatrick, eds.), Mineral. Soc. Am., 8:135–169.

Lasaga, A.C. (1995) Fundamental approaches in describing mineral dissolution and precipitation rates. In Chemical Weathering Rates of Silicate Minerals, (eds. White, A.F. and Brantley, S.L.), Chapter 2, Reviews in Mineralogy Volume 31, 23–86.

Lichtner P.C. (1985) Continuum model for simultaneous chemical reactions and mass transport in hydrothermal systems, Geochimica et Cosmochimica Acta, 49, 779–800.

Lichtner, P.C. (1988) The quasi-stationary state approximation to coupled mass transport and fluid-rock interaction in a porous media. Geochimica et Cosmochimica Acta, 52:143–165.

Lichtner P.C. (1991) The quasi-stationary state approximation to fluid/rock reaction: local equilibrium revisited, *in* Ganguly, J., editor, Diffusion, atomic ordering and mass transport. Advances in Physical Geochemistry, New York, Springer Verlag, 8:454–562.

Lichtner, P.C. (1992) Time-space continuum description of fluid/rock interaction in permeable media. Water Resources Research, 28:3135–3155.

Lichtner, P.C. (1993) Scaling properties of time-space kinetic mass transport equations and the local equilibrium limit. American Journal of Science, 293:257–296.

Lichtner, P.C. (1995) Principles and practice of reactive transport modeling. Mat. Res. Soc. Symp. Proc., Kyoto, Japan, 353:117–130.

Lichtner, P.C. (1996) Continuum formulation of multicomponent-multiphase reactive transport. Eds. Lichtner, P.C., Steefel, C.I., and Oelkers, E.H. Reviews in Mineralogy 34:1–81.

Lichtner, P.C., and Seth, M. S. (1997) User's manual for MULTIFLO: Multicomponent-multiphase reactive transport model. CNWRA, San Antonio, TX.

Lichtner, P.C., Steefel, C.I., and Oelkers, E.H. (1996) Reactive Transport in Porous Media. Reviews in Mineralogy. **34**, 438 pp.

Lindberg, R.D. and Runnells, D.D. (1984) Ground water redox reactions: An analysis of equilibrium state applied to Eh measurements and geochemical modeling. Science, 225:925–927.

Marsily, de G. (1986) Quantitative hydrology. Academic Press. 440 pp.

Murphy, W.M., Oelkers, E.H., and Lichtner, P.C. (1989) Surface reaction versus diffusion control of mineral dissolution and growth rates in geochemical processes. Chemical Geology, 78:357–380.

Nordstrom, D.K. (1982) The effect of sulfate on aluminum concentrations in natural waters: some stability relations in the system Al_2O_3–SO_3–H_2O at 298 K. Geochim. Cosmochim. Acta 46:681–692.

Nordstrom, D.K., and Ball, J.W. (1986) The geochemical behavior of aluminum in acidified surface waters. Science, 232:54–56.

Oelkers, E.H., Schott, J., Devidal, J.L. (1994) The effect of aluminum, pH, and chemical affinity on the rates of aluminosilicate dissolution reactions. Geochim. Cosmochim. Acta 58:2011–2024.

Pavlostathis, S.G., and Giraldo-Gomez, E. (1991) Kinetics of anaerobic treatment: a critical review. Critical Reviews in Environmental Control 21:411–490.

Phillips, W.R., and Griffin, D.T. (1981) Optical Mineralogy: The nonopaque minerals. W.H. Freeman and Company, 677 pp.

Rimstidt, J.D., and Barnes, H.L. (1980) The kinetics of silica-water interactions. Geochim. Cosmochim. Acta 44:1683–1700.

Rittmann, B.E., and VanBriesen, J.M. 1996. Microbiological processes in reactive modeling. Eds. Lichtner, P.C., Steefel, C.I., and Oelkers, E.H., Reviews in Mineralogy 34:311–334.

Steefel, C.I. and Lichtner, P.C. 1997. Multicomponent Reactive Transport in Single Fractures: Application to Water–Rock Interaction Adjacent to Cement-Bearing Nuclear Waste Repositories, Submitted to J. Hydrology.

Steefel, C.I., and MacQuarrie, K.T.B. 1996. Approaches to modeling of reactive transport in porous media. Eds. Lichtner, P.C., Steefel, C.I., and Oelkers, E.H. Reviews in Mineralogy 34:1–81.

Steefel, C.I., and Van Cappellen, P. (1990) A new kinetic approach to modeling water–rock interaction. The role of nucleation, precursors, and Ostwald ripening. Geochimica et Cosmochimica Acta 54:2657–2677.

Steefel, C.I., and Lasaga, A.C. (1994) A coupled model for transport of multiple chemical species and kinetic precipitation/dissolution reactions with application to reactive flow in single phase hydrothermal systems. American Journal of Science, 294:529–592.

Tang, D.H., Frind, E.O., and Sudicky, E.A. (1981) Contaminant transport in fractured porous media: analytical solution for a single fracture. Water Resources Research 17:555–564.

Tempkin, M.I. (1963) The kinetics of stationary reactions. Akad. Nauk SSSR Doklady. 152:782–785.

Terry, B., and Monhemius, A.J. (1983) Acid dissolution of willemite ($(Zn, Mn)_2 SiO_4$) and hemimorphite ($Zn_4Si_2O_7 (OH)_2 H_2O$). Metallurgical Transactions 14B:335–346.

Van Cappellen, P., and Gaillard J.F. 1996. Biochemical dynamics in aquatic sediments. Eds. Lichtner, P.C., Steefel, C.I., and Oelkers, E.H. Reviews in Mineralogy 34:335–376.

Walsh, M.P., Bryant, S.L., Schechter, R.S., and Lake, L.W. (1984) Precipitation and dissolution of solids attending flow through porous media. American Institut of Chemical Engineering Journal, 30, 317–327.

Williamson, M.A., and Rimstidt, J.D. (1994) The kinetics and electrochemical rate-determining step of aqueous pyrite oxidation. Geochimica Cosmochimica Acta 58:3867–3880.

Wolery, T.J. (1992) EQ3NR, a computer program for geochemical aqueous speciation–solubility calculations: Theoretical manual, users's guide, and related documentation (Version 7.0) UCRL-MA-110662. Lawrence Livermore National Laboratory, Livermore, CA.